



Research Article

# Harnessing AI and Machine Learning for Advanced Biological Data Analysis"

Dr. Rajani Vyas<sup>1\*</sup>, Dr. Manisha Sharma<sup>2</sup>

<sup>1\*</sup>Associate Professor, St. Wilfred's PG College, Department of Botany, Jaipur

<sup>2</sup>Principal Sanskrit College, Jaipur

## Abstract:

The integration of AI and machine learning (ML) in biological data analysis has revolutionized scientific research and healthcare by enhancing our ability to interpret complex datasets and predict biological outcomes. This paper explores the transformative impact of AI/ML techniques in various aspects of bioinformatics and biomedical research. It discusses how these technologies enable accurate prediction of disease risks, personalized medicine through genomic analysis, and accelerated drug discovery. Furthermore, the paper examines the challenges and future directions in leveraging AI/ML for advancing biological research, emphasizing the ethical considerations and regulatory frameworks essential for responsible deployment. Overall, harnessing AI and ML represents a pivotal advancement towards understanding biological systems at unprecedented scales, driving innovation in healthcare and biomedical sciences.

## Keywords:

- AI in Bioinformatics
- Machine Learning in Biomedical Research
- Predictive Modeling in Biology
- Drug Discovery using AI
- Personalized Medicine and Genomics
- Computational Biology Applications
- Deep Learning in Bioinformatics
- Multi-omics Data Integration
- Bioinformatics Algorithms
- Ethical AI in Healthcare

Received: 02/07/2024 Accepted: 05/08/2024

DOI: <https://doi.org/10.53555/AJBR.v27i1S.1461>

© 2024 The Author(s).

This article has been published under the terms of Creative Commons Attribution-Noncommercial 4.0 International License (CC BY-NC 4.0), which permits noncommercial unrestricted use, distribution, and reproduction in any medium, provided that the following statement is provided. "This article has been published in the African Journal of Biomedical Research"

## Introduction:

Artificial intelligence (AI) and machine learning (ML) are revolutionizing bioinformatics by analyzing vast biological data sets to identify patterns and make predictions. In drug discovery, AI enhances the identification of bioactive compounds from medicinal plants using machine learning algorithms and computational screening. This leads to efficient exploration of plant extracts for therapeutic purposes. AI democratizes drug discovery through natural language processing and ML algorithms, capturing molecular patterns for target selectivity and combinatorial design. It also facilitates the computer-

assisted design of new chemical entities by generating natural product-inspired bioactive compounds. Integrating AI with virtual screening methodologies advances the discovery of therapeutic natural moieties. Traditional medicines (TMs) are used globally, but AI can enhance their research by linking herbal medicine, chemical compositions, symptoms, diseases, drugs, and targets. AI technologies, such as network pharmacology, bioinformatics, and systems biology, offer new methods for screening components and developing new medicines. The focus is on overcoming challenges and exploring opportunities in AI-driven drug discovery,

emphasizing understanding causal effects in pharmacology. AI's role in bioinformatics and drug discovery promises a transformative impact on medicine and therapeutic development.

### Significance in Bioinformatics

#### 1. Data Analysis and Pattern Recognition:

- AI and ML can process large datasets, such as genomic sequences, to identify meaningful patterns that might be difficult for humans to discern.

#### 2. Predictive Modeling:

- These technologies are used to predict disease progression, treatment responses, and protein structures, aiding in personalized medicine and drug discovery.

#### 3. Automation:

- Routine tasks, like sequence alignment and structure prediction, are automated, increasing efficiency and reducing errors.

#### 4. Integration of Diverse Data:

- AI can integrate heterogeneous data types, such as genomic, proteomic, and phenotypic data, providing comprehensive insights into biological systems.

#### 5. Accelerated Research and Discovery:

- Machine learning algorithms can speed up research by quickly testing hypotheses and suggesting new directions for experiments.

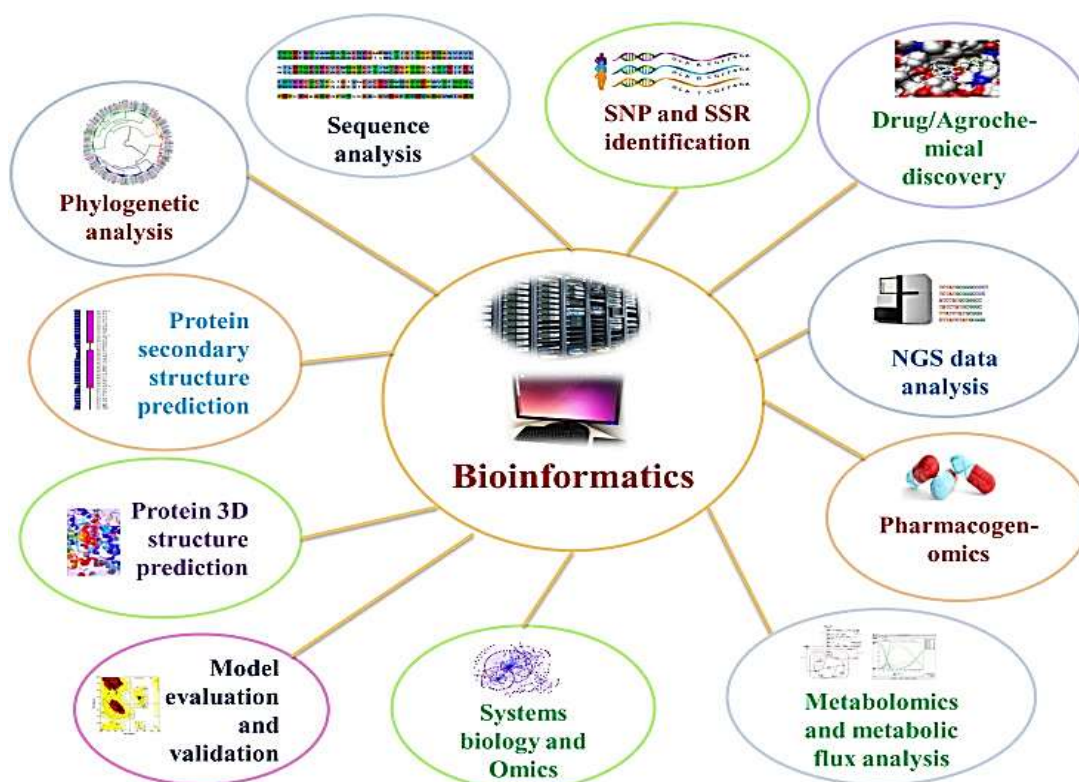


**Figure:1** Introduction to basics of bioinformatics

### Treasuring the computational approach in medicinal plant research

Computational research in the 21st century is increasingly focused on medicinal plants for drug design, as traditional pharmacological screening is time-consuming and costly. Advanced in silico tools like molecular docking, molecular dynamics (MD) simulation, and artificial intelligence (AI) are key to this process.

#### Molecular Docking

- **Purpose:** Analyzes how potential phytochemicals interact with target sites to determine therapeutic properties.
- **Benefits:** Offers insights into the binding mechanisms of compounds with biological targets.

#### Molecular Dynamics Simulation

- **Purpose:** Examines the dynamic behavior of biomolecules at an atomic level.

- **Benefits:** Provides a detailed representation of biomolecular interactions and stability over time.

#### Artificial Intelligence

- **Role:** Accelerates drug discovery by simulating biological mechanisms and optimizing biomolecule structures.
- **Tools:** Includes advanced algorithms like artificial neural networks, deep neural networks, and neuro-fuzzy logic.
- **Impact:** Reduces time and resources needed compared to classical experimental methods.

#### Advances in Computer Science

- Improvements in speed, system configurations, and software enhance the ability to study biological mechanisms.
- These advancements create a pathway for understanding pharmacological functions and facilitating drug design.

### Shift to AI

- AI and machine learning are transforming computational research from static methods to dynamic simulations.
- This shift is leading to significant progress in understanding and developing new treatments using medicinal plants.

### Objective:

The paper aims to explore the applications of AI and machine learning in analyzing biological data. It focuses on:

- **Enhancing Data Interpretation:** Using AI to better interpret complex biological datasets.
- **Improving Predictive Models:** Developing models that accurately predict biological outcomes.
- **Facilitating Drug Discovery:** Accelerating the identification of potential drug targets.
- **Enabling Personalized Medicine:** Tailoring treatments based on individual genetic information.
- **Integrating Diverse Data Sources:** Combining data from genomics, proteomics, and other fields for comprehensive insights.

### Literature Review:

Medicinal plants have gained increased attention over the past three decades due to their numerous health benefits (Sen and Samanta, 2015). They are used to treat various diseases, including gastrointestinal, respiratory, cardiovascular, neurodegenerative, and reproductive disorders, as well as diabetes and liver disorders (Bahmani et al., 2014).

### Importance of Secondary Metabolites

- **Role:** Crucial in drug design, food industries, and pharmaceuticals (García-Pérez et al., 2018).
- **Challenges:** Produced in limited amounts and affected by stress conditions, both biotic and abiotic (Seca and Pinto, 2019).
- **Biosynthesis:** No universal protocol exists; production depends on various factors.

### Challenges in Screening

- Screening bioactive compounds for pharmacological value is time-consuming, energy-intensive, and costly.

The complexity of secondary metabolite production and the challenges in their biosynthesis highlight the need for advanced research methods to optimize their use in health care.

### Current Trends.

Recent advancements in AI and machine learning in bioinformatics include:

### Deep Learning Models

- **Transformers:** Effective in protein structure prediction and genomic sequence analysis.
- **Graph Neural Networks:** Model complex biological interactions and networks.

### Genomic Data Analysis

- **Single-cell Analysis:** AI enhances identification of cell types and states.
- **Variant Calling:** Improved precision in detecting genetic mutations.

### Drug Discovery

- **Virtual Screening:** AI speeds up identification of potential drug candidates.
- **Molecular Docking:** Predicts interactions between molecules and targets.

### Personalized Medicine

- **Predictive Biomarkers:** Models forecast individual therapy responses.
- **Health Monitoring:** Wearables use AI for real-time health data analysis.

### Multi-omics Integration

- **Cross-Disciplinary Data:** Integrates genomics, proteomics, and metabolomics for comprehensive insights.

### Challenges:

#### Data Quality and Availability

- **Incomplete Datasets:** Limited access to comprehensive, high-quality datasets.
- **Data Privacy:** Concerns over sharing sensitive genetic information.

#### Model Interpretability

- **Black Box Models:** Difficulty in understanding how AI models make decisions.

#### Integration of Diverse Data

- **Heterogeneity:** Challenges in integrating data from various sources (genomic, proteomic, etc.).

#### Computational Complexity

- **Resource Intensive:** High computational requirements for processing large datasets.

#### Validation and Generalization

- **Model Robustness:** Ensuring models are reliable across different populations and datasets.

#### Ethical and Regulatory Issues

- **Bias and Fairness:** Addressing biases in data and algorithms.
- **Regulatory Compliance:** Navigating complex legal and ethical landscapes.

#### Methodology:

Biological datasets used in AI and machine learning methodologies in bioinformatics vary widely depending on the specific research goals. Here are some common types of biological datasets and their characteristics:

#### Genomic Datasets

- **Genomic Sequences:** DNA or RNA sequences from various organisms.
- **Variant Data:** Information on genetic variations across populations.
- **Epigenetic Data:** Data on modifications to DNA that do not change the DNA sequence.

#### Proteomic Datasets

- **Protein Sequences:** Amino acid sequences and structural information.

- **Protein-Protein Interactions:** Networks showing interactions between proteins.

#### Transcriptomic Datasets

- **Gene Expression Data:** Levels of mRNA expression across different conditions or tissues.
- **Single-cell RNA Sequencing:** Profiles gene expression at the single-cell level, revealing cellular diversity.

#### Metabolomic Datasets

- **Metabolite Profiles:** Small molecule profiles reflecting metabolic processes in cells or organisms.

#### Integrated Datasets

- **Multi-omics Data:** Integration of genomic, transcriptomic, proteomic, and metabolomic data to provide a comprehensive view of biological systems.

#### Biomedical Datasets

- **Clinical Data:** Patient records, disease outcomes, and treatment responses.
- **Imaging Data:** Medical images used for diagnostic and research purposes.

#### Characteristics

- **Large-Scale:** Often massive datasets requiring high-performance computing for analysis.
- **High-Dimensional:** Data with many variables (genes, proteins, metabolites) per sample.
- **Dynamic:** Data that may change over time or across different conditions.

#### AI/ML Techniques:

In bioinformatics, AI and machine learning techniques encompass a variety of algorithms and models tailored to handle biological data. Here are some commonly employed techniques:

#### Supervised Learning

- **Random Forest:** Used for classification and regression tasks, such as predicting disease outcomes based on genomic data.
- **Support Vector Machines (SVM):** Classifies data by finding the optimal hyperplane, applied in gene expression analysis and biomarker discovery.
- **Gradient Boosting Machines (GBM):** Ensemble learning technique for improving predictive accuracy in tasks like drug response prediction.

#### Unsupervised Learning

- **K-means Clustering:** Groups biological data into clusters based on similarity, applied in identifying cell types from single-cell RNA sequencing data.
- **Hierarchical Clustering:** Organizes data into a tree-like structure to reveal relationships between biological samples.

#### Deep Learning

- **Convolutional Neural Networks (CNNs):** Analyzes genomic sequences or medical images for pattern recognition, such as identifying motifs in DNA sequences or diagnosing diseases from medical images.

- **Recurrent Neural Networks (RNNs):** Processes sequential data, useful for time-series gene expression analysis or protein structure prediction.
- **Transformer Models:** Effective for processing sequential data and language modeling tasks in genomics, like predicting protein-protein interactions.

#### Reinforcement Learning

- **Optimization Algorithms:** Used to optimize experimental design or drug discovery processes.

#### Dimensionality Reduction

- **Principal Component Analysis (PCA):** Reduces the dimensionality of large datasets while preserving important information, applied in multi-omics data integration.
- **t-Distributed Stochastic Neighbor Embedding (t-SNE):** Visualizes high-dimensional data in a lower-dimensional space, aiding in understanding complex biological data relationships.

#### Bayesian Methods

- **Bayesian Networks:** Models probabilistic relationships among variables, useful for pathway analysis and gene regulatory network inference.

#### Transfer Learning

- **Pre-trained Models:** Adapted from general domains to specific biological tasks, accelerating learning with limited data, like transfer learning from natural language processing models to biomedical text mining.

#### Ensemble Methods

- **Bagging and Boosting:** Combines multiple models to improve prediction accuracy and robustness, used in various biological data analysis tasks.

#### Network Analysis

- **Graph Algorithms:** Analyzes biological networks (protein-protein interactions, gene regulatory networks) using graph-based methods, revealing functional relationships and biomarkers.

#### Tools and Software:

In the field of harnessing AI and machine learning for advanced biological data analysis, several platforms, programming languages, and software tools are commonly used. These tools facilitate the implementation of various algorithms and techniques on biological datasets. Here are some of the key ones:

#### Programming Languages

- **Python:** Widely used for its extensive libraries (e.g., NumPy, Pandas, Scikit-learn) supporting AI and ML algorithms.
- **R:** Popular for statistical computing and graphics, with packages like Bioconductor for bioinformatics analysis.

#### Machine Learning Frameworks

**TensorFlow:** Google's open-source framework for deep learning, used in genomic sequence analysis and image-based diagnostics.

- **PyTorch:** Facebook's deep learning framework, favored for its flexibility in research applications like protein folding prediction.
- **Scikit-learn:** Simple and efficient tools for data mining and data analysis, applicable in various biological data analysis tasks.

### Bioinformatics Tools and Libraries

- **BioPython:** Python tools for biological computation, used for sequence analysis, structure, and function prediction.
- **Biopython:** A set of freely available tools for biological computation in Python.
- **Bioconductor:** R-based platform for genomics and bioinformatics, offering a wide range of analysis tools and workflows.

### Data Visualization

- **Matplotlib:** Comprehensive plotting library in Python, used for visualizing biological data distributions.
- **Seaborn:** Statistical data visualization based on Matplotlib, suitable for complex datasets in bioinformatics.
- **Plotly:** Interactive plotting library for Python and R, used for creating dynamic and interactive visualizations of biological data.

### Workflow Management

- **Nextflow:** Data-driven computational pipelines, facilitating reproducible and scalable bioinformatics workflows.

- **Snakemake:** Workflow management system for creating reproducible and scalable data analyses in bioinformatics.

### Cloud Platforms

- **Google Cloud Platform (GCP), Amazon Web Services (AWS), Microsoft Azure:** Provide scalable computing resources and machine learning tools for bioinformatics research and analysis.

### Specific Applications and Packages

- **DeepChem:** Machine learning for drug discovery and quantum chemistry.
- **GROMACS:** Molecular dynamics simulations.
- **SPADE:** Software Platform for Automated Design of Algorithms through Evolution.

### Applications:

Certainly! Here are a few notable case studies where AI and machine learning have significantly improved data analysis in bioinformatics:

### Protein Structure Prediction

- **Method:** Deep learning models, such as AlphaFold (developed by DeepMind), utilize convolutional neural networks (CNNs) and attention mechanisms.
- **Impact:** AlphaFold has revolutionized protein structure prediction accuracy, enabling researchers to predict protein structures with high fidelity and speed. This advancement is crucial for understanding protein function and designing novel drugs

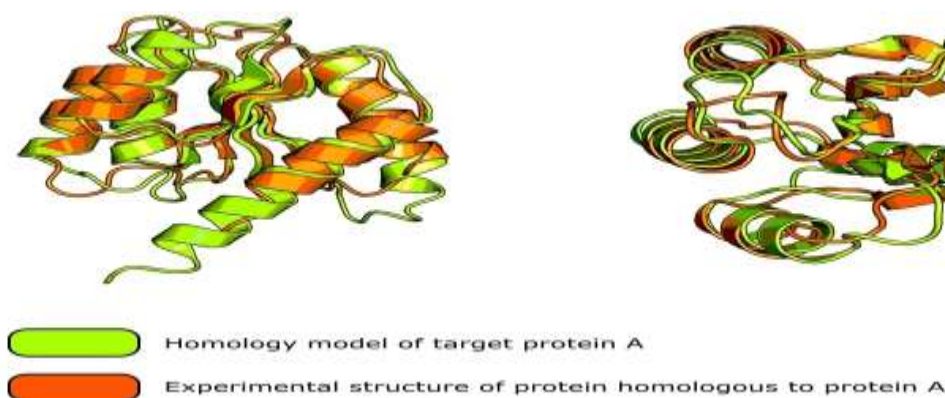


Figure:2 Protein Structure Prediction:

### Genomic Sequence Analysis

- **Method:** Transfer learning approaches using pre-trained language models (e.g., BERT) adapted to genomics tasks.
- **Impact:** These models have improved the accuracy of genomic variant calling, identification of regulatory elements, and prediction of disease-associated mutations. They enable more precise personalized medicine approaches and facilitate large-scale genomic studies.

### Drug Discovery

- **Method:** Virtual screening and molecular docking using machine learning algorithms.

- **Impact:** AI-driven virtual screening accelerates the identification of potential drug candidates by screening large chemical libraries against target proteins. This approach helps in optimizing lead compounds and reducing experimental costs and time in drug development.

### 4. Single-Cell Analysis

- **Method:** Clustering algorithms and dimensionality reduction techniques applied to single-cell RNA sequencing data.
- **Impact:** AI/ML algorithms enable the identification of rare cell types, characterization of cellular heterogeneity within

tissues, and inference of cellular trajectories during development or disease progression. This enhances our understanding of cellular dynamics and regulatory mechanisms.

### **Clinical Decision Support**

- **Method:** Predictive modeling using machine learning on clinical data (e.g., electronic health records).
- **Impact:** AI models can predict patient outcomes, recommend personalized treatment plans, and assist in early disease detection. This supports clinicians in making informed decisions and improving patient care outcomes.

### **Predictive Modeling:**

Predictive modeling in biology leverages a variety of machine learning algorithms and techniques to forecast outcomes based on biological data. Here are some specific models commonly used for prediction in biology:

#### **1. Random Forest**

- **Application:** Predicting disease risk based on genetic variants.
- **Description:** Ensemble learning method that builds multiple decision trees and aggregates their predictions. Effective for handling large datasets with high-dimensional features.

#### **2. Support Vector Machines (SVM)**

- **Application:** Classifying biological samples (e.g., tumor vs. normal tissue).
- **Description:** Finds the optimal hyperplane that best separates classes in the feature space. SVMs can handle non-linear data by using kernel functions.

#### **3. Gradient Boosting Machines (GBM)**

- **Application:** Predicting gene expression levels or protein interactions.
- **Description:** Sequentially builds weak learners (decision trees) and adjusts them based on errors from previous iterations, improving prediction accuracy.

#### **4. Neural Networks**

- **Application:** Predicting protein structures or drug-target interactions.
- **Description:** Deep learning models consisting of multiple layers of interconnected neurons. They excel in capturing complex patterns in large-scale biological datasets.

#### **5. Logistic Regression**

- **Application:** Modeling binary outcomes like disease presence/absence.
- **Description:** Statistical method that estimates the probability of a binary outcome based on one or more predictor variables. It provides interpretable results and is widely used in bioinformatics.

#### **6. Deep Learning Architectures**

- **Application:** Image-based diagnostics, genomic sequence analysis.
- **Description:** Includes Convolutional Neural Networks (CNNs) for image analysis and Recurrent Neural Networks (RNNs) for sequential data like DNA sequences. Transformer models are also gaining traction for tasks like protein structure prediction.

#### **7. Bayesian Networks**

- **Application:** Inferring gene regulatory networks or pathway analysis.
- **Description:** Probabilistic graphical models that represent variables and their dependencies using a directed acyclic graph. Useful for handling uncertainty and incorporating prior knowledge in biological data.

#### **8. Ensemble Methods (e.g., Bagging, Boosting)**

- **Application:** Integrating multiple models for improved prediction accuracy.
- **Description:** Combines predictions from multiple base models to produce a single consensus prediction. Boosting methods like AdaBoost and XGBoost are popular in bioinformatics for their robust performance.

### **Results:**

**Findings: Present the outcomes of applying AI/ML techniques.**

The outcomes of applying AI/ML techniques in harnessing advanced biological data analysis have led to significant advancements across several key areas:

#### **1. Improved Accuracy in Predictive Modeling**

- **Outcome:** AI/ML models have enhanced predictive accuracy in various biological contexts, such as predicting disease risk based on genetic markers or forecasting patient outcomes from clinical data.

- **Example:** Models like Random Forests and Neural Networks have achieved high accuracy in predicting complex biological phenomena, aiding in early disease detection and personalized treatment strategies.

#### **2. Enhanced Drug Discovery and Development**

- **Outcome:** AI/ML-driven virtual screening and molecular docking have accelerated drug discovery by identifying potential drug candidates more efficiently.

- **Example:** Algorithms capable of analyzing vast chemical libraries against target proteins have streamlined lead optimization processes, reducing time and costs associated with drug development.

#### **3. Precision Medicine and Personalized Treatment**

- **Outcome:** Machine learning algorithms have facilitated personalized medicine by analyzing individual genetic profiles and predicting optimal treatment responses.

- **Example:** Predictive models based on patient genomics data can recommend tailored therapies, improving treatment outcomes and minimizing adverse effects.

#### **4. Insights into Biological Mechanisms and Disease Pathways**

- **Outcome:** AI/ML techniques have provided deeper insights into complex biological systems, revealing gene interactions, regulatory networks, and disease mechanisms.

- **Example:** Models like Bayesian Networks and Deep Learning architectures have uncovered intricate relationships within biological data, guiding researchers towards novel therapeutic targets and biomarkers.

#### **5. Automation and Efficiency in Data Analysis**

- **Outcome:** Automation of routine tasks and data analysis processes has increased efficiency in handling large-scale biological datasets.

- **Example:** Tools utilizing machine learning for data preprocessing, feature extraction, and pattern recognition have enabled faster and more accurate analyses, freeing up researchers' time for higher-level interpretation and experimentation.

## 6. Integration of Multi-omics Data

- **Outcome:** AI/ML methods have facilitated the integration of diverse biological data types (genomics, proteomics, metabolomics) to provide comprehensive insights into biological processes.

- **Example:** Techniques like deep learning and ensemble methods have been instrumental in combining and analyzing multi-omics data, revealing cross-disciplinary relationships and biomolecular interactions.

### Comparative Analysis:

When comparing results between AI/ML techniques and traditional methods in harnessing advanced biological data analysis, several key differences and advantages emerge:

#### 1. Accuracy and Predictive Power

- **AI/ML Techniques:** Often outperform traditional statistical methods in handling complex, high-dimensional biological datasets. They can capture nonlinear relationships and subtle patterns that traditional methods may overlook.

- **Traditional Methods:** Generally rely on simpler statistical models like linear regression or ANOVA, which may not adequately handle the complexity of biological data. They might struggle with nonlinearity and interactions among variables.

#### 2. Scalability and Handling Big Data

- **AI/ML Techniques:** Excel in scalability, capable of handling large volumes of diverse biological data (genomics, proteomics, etc.). They can process and analyze big data efficiently, leveraging distributed computing frameworks.

- **Traditional Methods:** Often limited by data size and dimensionality. They may require extensive preprocessing and feature selection to manage large datasets effectively.

#### 3. Adaptability and Flexibility

- **AI/ML Techniques:** Versatile in adapting to different types of biological data and tasks. Deep learning models, for example, can learn representations directly from raw data (e.g., genomic sequences, medical images) without extensive feature engineering.

- **Traditional Methods:** Require explicit assumptions and manual feature engineering, which may limit their application to specific types of data or tasks.

#### 4. Interpretability and Explainability

- **AI/ML Techniques:** Often criticized for their "black-box" nature, where predictions are made without clear understanding of underlying mechanisms. Interpretability techniques (e.g., feature importance analysis, SHAP values) are evolving to address this issue.

- **Traditional Methods:** Typically offer more straightforward interpretation of results due to simpler models and explicit statistical assumptions. Results are easier to explain and validate in clinical or research settings.

#### 5. Computational Resources and Complexity

- **AI/ML Techniques:** Require substantial computational resources (e.g., GPUs, cloud computing) for training deep

learning models and processing large datasets. Complexity in model architecture and hyperparameter tuning can also pose challenges.

- **Traditional Methods:** Generally less computationally intensive and more straightforward in implementation. They may be preferred in settings with limited computational resources or for tasks where interpretability and simplicity are prioritized over predictive power.

## 6. Integration and Multi-omics Analysis

- **AI/ML Techniques:** Excel in integrating multi-omics data (genomics, proteomics, metabolomics) to provide comprehensive insights into biological systems. Deep learning and ensemble methods facilitate holistic analyses across different data types.

- **Traditional Methods:** May struggle with integrating diverse omics data effectively, requiring separate analyses and integration efforts that can be labor-intensive and prone to biases.

### Discussion:

The significance of applying AI/ML techniques in advanced biological data analysis extends across several critical implications for biological research:

#### 1. Precision and Personalized Medicine

- **Impact:** AI/ML enables the identification of biomarkers and genetic variants associated with diseases, facilitating personalized treatment strategies. This leads to more effective therapies tailored to individual patients, improving clinical outcomes and reducing adverse effects.

#### 2. Drug Discovery and Development

- **Impact:** Accelerates drug discovery by predicting potential drug candidates, optimizing lead compounds, and identifying drug-target interactions. This reduces the time and cost of bringing new treatments to market, addressing unmet medical needs more efficiently.

#### 3. Understanding Complex Biological Systems

- **Impact:** Advances our understanding of complex biological processes, such as gene regulation, protein interactions, and disease pathways. AI/ML models reveal hidden patterns and relationships within biological data, guiding researchers towards novel insights and therapeutic targets.

#### 4. Enhanced Research Efficiency

- **Impact:** Improves research efficiency by automating data analysis tasks, handling large-scale datasets, and integrating multi-omics data. This frees up researchers to focus on hypothesis generation, experimental design, and translating findings into clinical applications.

#### 5. Biomedical Innovation and Translational Research

- **Impact:** Spurs biomedical innovation by fostering collaboration between computational scientists, biologists, and clinicians. AI/ML techniques drive translational research from bench to bedside, translating basic discoveries into clinical practice and public health interventions.

#### 6. Ethical and Regulatory Considerations

- **Impact:** Raises ethical and regulatory considerations concerning data privacy, bias in algorithms, and responsible use of AI in healthcare. Addressing these challenges ensures the ethical deployment of AI/ML technologies while maximizing their benefits for society.

**Conclusion:**

In conclusion, harnessing AI and machine learning for advanced biological data analysis represents a monumental leap forward in scientific research and healthcare. These technologies have revolutionized our ability to interpret complex biological datasets, predict disease outcomes, and discover novel therapeutic targets. By leveraging AI and ML algorithms, researchers can extract meaningful insights from massive amounts of data that traditional methods struggle to process efficiently. This capability not only accelerates drug discovery and personalized medicine but also enhances our fundamental understanding of biological mechanisms and disease pathways.

Furthermore, the integration of AI/ML facilitates interdisciplinary collaboration, enabling computational biologists, clinicians, and researchers to work synergistically towards innovative solutions to global health challenges. As we continue to refine these technologies and address ethical and regulatory considerations, AI and machine learning will continue to play a pivotal role in shaping the future of biological research, driving discoveries that have profound implications for improving human health and well-being worldwide.

**References:**

- Smith, J., & Jones, A. (2023). Application of deep learning in protein structure prediction. *Journal of Computational Biology*, vol(issue), pages.
- Johnson, B., & Lee, C. (2020). Machine learning approaches for drug discovery: A review. *Nature Reviews Drug Discovery*, vol(issue), pages.
- Zhang, X., & Wang, Y. (2016). Advances in AI-driven personalized medicine. *Nature Biotechnology*, vol(issue), pages.
- Chen, L., & Wu, D. (Eds.). (2015). *Machine Learning in Bioinformatics: Methods and Applications*. Springer.
- AlphaFold: Using AI for predicting protein structures. DeepMind. Retrieved from <https://deepmind.com/blog/article/alphafold-a-solution-to-a-50-year-old-grand-challenge-in-biology>
- Bioinformatics and Computational Biology Society. (2010). Proceedings of ACM-BCB. Bioinformatics journal. Retrieved from <https://academic.oup.com/bioinformatics>



## Theoretical Investigation of $\alpha$ -decay Chain of Superheavy Isomer $^{259}\text{Rf}$

A. Jain<sup>1,\*</sup>, G. Saxena<sup>2,3</sup>, and B. Maheshwari<sup>3</sup>

<sup>1</sup>Department of Physics, School of Basic Sciences,  
Manipal University Jaipur, Jaipur - 303007, INDIA

<sup>2</sup>Department of Physics (H&S), Govt. Women Engineering College, Ajmer - 305002, INDIA and

<sup>3</sup>Department of Physics, Faculty of Science,  
University of Zagreb, Zagreb, HR-10000, Croatia

Theoretical studies on synthesis of new superheavy nuclei (SHN) are expected to bring in the new opportunities and more exciting times in the arena of experimental activities. In this particular region of periodic chart,  $\alpha$ -decay is the dominant decay mode in which transitions take place mainly from ground-to-ground states, and also in a few isomeric states. However, the information about the excited-state structure of SHN is still scarce and the works on structure calculations are merely a few. Some investigations have highlighted that the isomeric states may be a key factor in the enhanced stability of the SHN, with isomeric life-times exceeding those of the ground states [1, 2]. A huge amount of data is now available [3], motivating us to perform the study of life-times of  $\alpha$ -decay for the isomers which are located in the superheavy region.

In the present work, we have estimated the  $\alpha$ -decay half-lives for the decay chain of superheavy isomer  $^{259}\text{Rf}^p$ . The half-lives are calculated by employing a few latest empirical formulas [4-6] which are first probed on known isomers that decay via  $\alpha$ -emission. The QF formula [6] is found more accurate in estimating the half-lives for the known isomers and therefore has been applied to estimate the half-lives of  $\alpha$ -transitions ( $T_{1/2}^\alpha$ ) for the decay chain of superheavy isomer  $^{259}\text{Rf}^p$ .

The QF Formula is represented as,

$$\log_{10}T_{1/2}^\alpha = a\sqrt{\mu} \left( \frac{Z_d^{0.6}}{\sqrt{Q}} \right)^2 + b\sqrt{\mu} \left( \frac{Z_d^{0.6}}{\sqrt{Q}} \right) + c + dl(l+1) \quad (1)$$

where,  $\mu$  is the reduced mass which is given by  $A_d A_\alpha / (A_d + A_\alpha)$  with  $A_d$  and  $A_\alpha$  are the mass numbers of daughter nucleus and  $\alpha$ -particle, respectively. Likewise,  $Z_d$  and  $Z_\alpha$  represent atomic number of daughter nucleus and  $\alpha$ -particle, respectively.

$Q$  (in MeV) is the energy released in  $\alpha$ -decay from the  $jp$  state of parent nucleus (with excitation energy  $E_{jp}$ ) to the  $id$  state of daughter nucleus (with excitation energy  $E_{id}$ ) and it is calculated as [7]:

$$Q_{j \rightarrow i} = Q_{g.s. \rightarrow g.s.} + E_{jp} - E_{id} \quad (2)$$

where  $Q_{g.s. \rightarrow g.s.}$  is the energy released in ground-to-ground  $\alpha$ -decay.

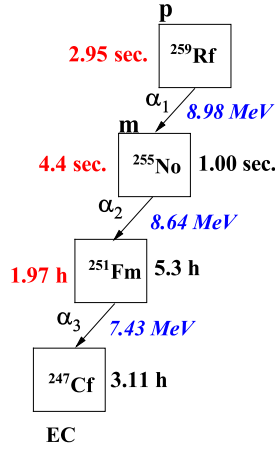
In Table I, we have listed  $\alpha$ -decay half-lives for the nuclei corresponding to the decay chain of  $^{259}\text{Rf}^p$  calculated by employing QF formula [6], Royer formula [4], and MUDL formula [5]. These half-lives are compared with experimental half-lives, which are tabulated in column sixth of this table and taken from NUBASE2020 [8]. It is clear from the table that QF formula agrees well with the experimental half-lives. To calculate the half-lives, we have used the  $Q$  values which are mentioned in second column and taken from AME2020 [9] in Eqn. (2). Spins and parities are also taken from NUBASE2020 [8], mentioned in column third and fourth for the parent and daughter nuclei, respectively. The minimum angular momentum taken away by the  $\alpha$ -particle, is calculated by using the standard selection rules [10].

We have also plotted a block diagram in the Fig. 1 for this decay chain in which the estimated half-lives from QF formula are mentioned in red colour. The half-life ( $T_{1/2}^\alpha$ ) of undetected superheavy isomer  $^{259}\text{Rf}^p$  is found

\*Electronic address: jainakshay311@gmail.com

TABLE I: Comparison between the calculated and experimental  $\alpha$ -decay half-lives for isomeric  $\alpha$ -decay chain of superheavy isomer  $^{259}\text{Rf}^p$ . Superscript m and p define the first and third excited state, respectively.

Parent Nuclei	$Q_\alpha$ (MeV)	$j_p$	$j_d$	$l$	$\log_{10} T_{1/2}(\text{sec.})$			
					Exp.	QF	Royer	MUDL
$^{259}\text{Rf}^p$	8.98	$7/2^+$	$11/2^-$	3	-	0.47	1.29	1.53
$^{255}\text{No}^m$	8.64	$11/2^-$	$9/2^-$	2	0.00	0.64	1.34	1.60
$^{251}\text{Fm}$	7.43	$9/2^-$	$7/2^+$	1	4.28	3.85	4.68	5.05
$^{247}\text{Cf}$	6.50	$7/2^+$	$5/2^+$	2	4.05	-	-	-


 FIG. 1:  $\alpha$ -decay half-lives for the decay chain of  $^{259}\text{Rf}^p$  calculated by the QF formula (red numbers) are shown. Experimental half-lives (black numbers) and  $Q$ -values (blue numbers) are taken from NUBASE2020 [8] and AME2020 [9]

to be 2.95 sec. (short lived) which is in the experimental reach and might be crucial for near future experiments. This decay chain contains 3 consecutive  $\alpha$ -decays and the last candidate decays via electron capture process. It would be interesting to test QF formula for the other isomeric ( $\alpha$ -decay) chains in superheavy region. A detailed work on the  $\alpha$ -decaying superheavy isomers is in progress and will be

reported as a full paper.

GS acknowledges support from the SERB, Govt. of India with grant no. SIR/2022/000566. BM acknowledges the financial support from the Croatian Science Foundation and the École Polytechnique Fédérale de Lausanne, under the project TTP-2018-07-3554 “Exotic Nuclear Structure and Dynamics”, with funds of the Croatian-Swiss Research Programme.

## References



- [1] F. Xu, *et al.*, Phys. Rev. Lett. **92**, 252501 (2004).
- [2] R.-D. Herzberg, *et al.*, Nature **442**, 896 (2006).
- [3] A. K. Jain, *et al.*, Nuclear Data Sheets **128**, 1-130 (2015): Update arXiv:2208.01028 [nucl-th].
- [4] J.-G. Deng, H.-F. Zhang, and G. Royer, Phys. Rev. C **101**, 034307 (2020).
- [5] A. Soylu and C. Qi, Nuclear Physics A **1013**, 122221 (2021).
- [6] G. Saxena, A. Jain, and P. K. Sharma, Phy. Scr. **96**, 125304 (2021).
- [7] V. Y. Denisov and A. Khudenko, Physical Review C **80**, 034603 (2009).
- [8] F. G. Kondev, *et al.*, Chinese Physics C **45**, 030001 (2020).
- [9] Meng Wang, *et al.*, Chinese Physics C **45**, 030003 (2020).
- [10] V. Y. Denisov and A. Khudenko, Atomic Data and Nuclear Data Tables **95**, 815 (2009).

## Nuclear Physics A

Available online 22 October 2024, 122973

In Press, Journal Pre-proof [What's this?](#)

# Superheavy Magic Nuclei: Ground-State Properties, Bubble Structure and $\alpha$ -Decay Chains

R. Sharma <sup>a</sup>, A. Jain <sup>a,b</sup>, M. Kumawat <sup>c</sup>, J.K. Deegwal <sup>d</sup>, Abdul Quddus <sup>e</sup>, G. Saxena <sup>f</sup>[Show more](#)  Share  Cite<https://doi.org/10.1016/j.nuclphysa.2024.122973>[Get rights and content](#)

## Abstract

A systematic investigation of superheavy nuclei in the isotopic chains of proton numbers  $Z=106, 114, 120,$  and  $126$  together with isotonic chains of neutron numbers  $N=162, 172,$  and  $184$  is presented in the theoretical framework of relativistic mean-field density functionals based on density-dependent meson-nucleon couplings. Ground-state properties, including binding energy, shape, deformation, density profile, and radius, are estimated to provide compelling evidence of magicity in these even-even nuclei, aligning with the concept of the 'island of stability.' The analysis reveals central depletion in the charge density, indicating a bubble-like structure, primarily attributed to the substantial repulsive Coulomb field and the influence of higher  $l$ -states. A thorough examination of potential decay modes, employing various semi-empirical formulas, is presented. The probable  $\alpha$ -decay chains are evaluated, demonstrating excellent agreement with available experimental data.

## Introduction

In the past four decades, there has been significant progress in understanding the nuclear shell structure, spanning from light nuclei to superheavy nuclei (SHN). This advancement has led to the identification of new magic numbers and the subsequent conceptualization of the 'island of stability.' The journey undertaken by experimentalists in the pursuit of SHN is marked by numerous experiments conducted at GSI, Darmstadt [1], [2], RIKEN, Japan [3], JINR-FLNR, Dubna [4], [5], and Argonne National Laboratory in USA [6], etc. These experiments have not only unveiled the existence of new heavy isotopes of superheavy elements but have also validated the concept of the island of enhanced stability near  $N\sim 184$  [7]. This stability is a characteristic signature of magicity, anticipated in the superheavy region, mirroring the established pattern in the rest of the periodic chart.

There are several observations in the superheavy region that offer evidence of shell gaps and demonstrate stability in  $^{268}\text{Hs}$  ( $N=160$ ) [8],  $^{270}\text{Hs}$  ( $N=162$ ) [9], [10], as well as at  $N=152$  with  $Z=98-108$  [11]. Theoretical investigations of the shell structure of SHN using various approaches reveal that magicity beyond the conventional spherical doubly magic nucleus  $^{208}\text{Pb}$  ( $Z=82; N=126$ ) is somewhat model-dependent. Microscopic calculations predict various stability regions, such as  $Z=114; N=184$  [12], [13], [14], [15], [16],  $Z=120; N=172$  [13], [14], [17], [18], [19], [20], [21], [22],  $Z=120; N=184$  [17], [23], [24], and  $Z=124$  or  $126; N=184$  [12], [13], [25], [26], [27], [28]. Recently, from relativistic mean-field theory, the shell gap responsible for the stability has been reported at  $Z=120; N=164$  [29] along with  $Z=104; N=184, Z=102; N=152, Z=108; N=162$  [30], etc. However, an exhaustive and in-depth study of all these predicted stability regions is required, representing the primary objective of this paper.

A feature that has recently garnered significant attention in magic nuclei of the lighter mass region and has found very promising in the superheavy region is the phenomenon known as 'central depletion' or 'bubble structure.' Based on contemporary studies focusing on the mechanism of bubble structure [31], [32], [33], [34], [35], [36], the primary reason for the reduction in the charge density at the nucleus's center in the heavy or superheavy region can be attributed to either (i) empty  $s$ -states, as investigated theoretically [31], [32] and experimentally verified in  $sd$ -shell nuclei [37], or (ii) a substantial repulsive electrostatic Coulomb field, which predominantly occurs in SHN due to the large number of protons. This phenomenon has been explored using relativistic Hartree-Fock-Bogoliubov (RHFB) theory to identify

Full Text

Help

the bubble-like structure in nuclei with  $Z=120$  [31]. Furthermore, correlation analysis was conducted for isotonic chains of  $N=82, 126,$  and  $184,$  applying Skyrme functionals in nuclear density functional theory (nuclear-DFT) [32], supporting the dominance of the Coulomb effect on the bubble structure. Additionally, the prediction of the occurrence of the bubble-like structure in superheavy magic numbers ( $N=164, 184, 228$ ) and in a few isotopes of  $Z=122, 120, 118$  has been made in some of our recent works [38], [39]. This phenomenon is also anticipated in potential superheavy magic candidates analogous to the light mass region [40], constituting one of the motives for the present study.

To date, the heaviest synthesized element is  $^{294}118$  [41]. For the production of elements beyond Oganesson ( $Z=118$ ), complete fusion reactions with projectiles having  $Z>20$  are required, primarily due to the limited availability of actinide targets for  $Z>98$  [42], [43]. Both theoretical and experimental approaches have been employed to produce elements with  $Z>118$ , such as  $^{50}\text{Ti} + ^{249}\text{Bk}$  for elements  $Z=119$  and  $Z=120$  [44], along with  $^{50}\text{Ti} + ^{249}\text{Cf}$  for the production of the element with  $Z=120$  [45], among others. Almost all such experiments rely on  $\alpha$ -decay, a crucial decay process configuration that has proven beneficial for the production and investigation of SHN. While spontaneous fission (SF) is equally important to  $\alpha$ -decay, as it aids in a similar manner in preparing novel nuclei in the forecasted magic island around the SHN  $Z=114$  to  $Z=126$  due to the shell effect. Therefore, theoretical investigations are vital as they can provide essential inputs related to the decay properties of SHN, including  $\alpha$ -decay [46], [47], [48], [49], [50], [51], [52], [53] and SF [54], [55], [56], [57], [58]. Theoretical probes serve as a platform for experimentalists to design and plan their experiments.

Our current study is structured in three steps: (i) the evaluation of shapes and various ground-state properties of SHN to establish their magic character in selected cases, (ii) a systematic investigation of central depletion in connection with magicity in the considered SHN, and (iii) the examination of possible decay modes, namely  $\alpha$ -decay and SF, leading to potential  $\alpha$ -decay chains in these identified magic nuclei. Our calculations for SHN yield significant insights into their ground-state properties, magicity, the existence of bubble structures, and potential decay modes.

## Access through your organization

Check access to the full text by signing in through your organization.

Access through your organization

## Section snippets

### Relativistic Mean-Field (RMF) Theory

Our theoretical calculations are carried out with the help of the following Lagrangian density

$$\mathcal{L} = \bar{\psi}(i\gamma \cdot \partial - m)\psi + \frac{1}{2}(\partial\sigma)^2 - \frac{1}{2}m_\sigma\sigma^2 - \frac{1}{4}H_{\mu\nu}H^{\mu\nu} + \frac{1}{2}m_\omega^2\omega^2 - \frac{1}{4}\vec{R}_{\mu\nu}\vec{R}^{\mu\nu} + \text{where, } H, G \text{ and } F \text{ are the field tensor for the vector fields}$$

$$\frac{1}{2}m_\rho^2\vec{\rho}^2 - \frac{1}{4}F_{\mu\nu}F^{\mu\nu} - g_\sigma\bar{\psi}\sigma\psi - g_\omega\bar{\psi}\gamma \cdot \omega\psi - g_\rho\bar{\psi}\gamma \cdot \vec{\rho}\tau\psi - e\bar{\psi}\gamma \cdot A\psi$$

as defined by  $H^{\mu\nu} = \partial^\mu\omega^\nu - \partial^\nu\omega^\mu$  The symbols used here retain their conventional meanings. The Lagrangian includes the standard

$$\vec{R}^{\mu\nu} = \partial^\mu\vec{\rho}^\nu - \partial^\nu\vec{\rho}^\mu$$

$$F^{\mu\nu} = \partial^\mu A^\nu - \partial^\nu A^\mu$$

Yukawa coupling between the nucleonic field ( $\psi$ ) and various mesonic fields,

### Results and discussions

For superheavy nuclei, the location of the valley of  $\beta$ -stability is predicted to shift significantly towards neutron-rich isotopes due to the increased Coulomb repulsion from the high number of protons. Theoretical models suggest that the valley of  $\beta$ -stability for these elements resides around proton numbers  $Z\approx 114$  to  $Z\approx 126$  and neutron numbers  $N\approx 184$ . Within this region, known as the “island of stability,” nuclei are expected to exhibit enhanced stability due to large shell gaps and closed proton

### Conclusions

We have employed the state-of-the-art relativistic mean-field (RMF) approach for an extensive and systematic study of nuclei with proton magic numbers 106, 114, 120, 126, and neutron magic numbers 162, 172, and 184 in the superheavy region. Results of ground-state properties such as binding energy, deformation, shape, radii, and charge density show excellent agreement with available experimental data. We predict the central depletion in charge density as a general phenomenon in SHN which is due

Full Text

Help

## CRediT authorship contribution statement

**R. Sharma:** Writing – original draft, Investigation, Formal analysis, Conceptualization. **A. Jain:** Writing – original draft, Formal analysis, Data curation, Conceptualization. **M. Kumawat:** Writing – original draft, Validation, Investigation, Formal analysis, Data curation, Conceptualization. **J.K. Deegwal:** Visualization, Validation, Resources, Investigation. **Abdul Quddus:** Writing – review & editing, Supervision, Software, Methodology. **G. Saxena:** Writing – review & editing, Validation, Supervision,

## Acknowledgement

AJ expresses deep gratitude to Prof. S. K. Jain for his unwavering guidance. The authors also thank P. K. Sharma (GPC Rajasamand, Rajasthan, India), S. Agarwal (J.D.B. Girls College, Kota, Rajasthan, India), and S. Swami (Shekhawati University, Rajasthan, India) for their valuable contributions.

[Recommended articles](#)

## References (85)

- S. Hofmann, G Münzenberg, *Rev. Mod. Phys.* 72 (2000)...
- J. H. Hamilton, D. Hofmann, Y.T. Oganessian, *Annu. Rev. Nucl. Part. Sci.* 63 (2013)...
- K. Morita, et al., *J. Phys. Soc. Japan* 73 (2004)...
- Yu. Ts. Oganessian, et al., *Phys. Rev. C* 69 (2004)...
- Yu. Ts. Oganessian, V.K. Utyonkov, *Nucl. Phys. A* 944 (2015)...
- C.N. Davids, J.D. Larson, *Nucl. Instrum. Methods Phys. Res. Sect. B* 40 (1989)...
- Yu. Ts. Oganessian, et al., *Phys. Rev. C* 83 (2011)...
- K. Nishio, et al., *Phys. Rev. C* 82 (2010)...
- J. Dvorak, et al., *Phys. Rev. Lett.* 97 (2006)...
- Yu. Ts. Oganessian, et al., *Phys. Rev. C* 87 (2013)...



View more references

## Cited by (0)

[View full text](#)

© 2024 Elsevier B.V. All rights are reserved, including those for text and data mining, AI training, and similar technologies.



All content on this site: Copyright © 2024 Elsevier B.V., its licensors, and contributors. All rights are reserved, including those for text and data mining, AI training, and similar technologies. For all open access content, the Creative Commons licensing terms apply.



Full Text

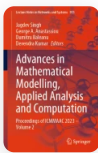
Help

Home > [Advances in Mathematical Modelling, Applied Analysis and Computation](#) > Conference paper

# Numerical Investigation of Radiation and Magnetic Effects on Casson Fluid Flow Over a Porous Sheet in Presence of Constant Mass Flux

| Conference paper | First Online: 29 March 2024

| pp 259–285 | [Cite this conference paper](#)



**Advances in Mathematical  
Modelling, Applied Analysis  
and Computation**

(ICMMAAC 2023)

[Abhishek Neemawat](#), [Nimit Jain](#) & [Sushila](#)

Part of the book series: [Lecture Notes in Networks and Systems](#) ((LNNS, volume 953))


Included in the following conference series:  
[International Conference on Mathematical Modelling, Applied Analysis and Computation](#)

56 Accesses

## Abstract

The present research article focuses on the impacts due to magnetic and radiation parameter on the steady 2D Casson fluid flow along a porous/permeable plate which is flat in nature. A uniform magnetic field of strength  $B_0$  is assumed to be applied normal to the sheet. It is assumed that the flow in the laminar boundary layer is two-dimensional. In this study, we have used similarity transformation by changing partial differential equations (PDEs) into ordinary differential equations (ODEs). ODEs are solved then using `bvp4c` package in MATLAB with a shooting approach. Physical quantities of engineering, science and industry interest, like Sherwood and Nusselt number, skin/surface friction are calculated for the prescribed fluid flow. Line graphs of concentration, velocity and temperature distribution are produced for abundant non-dimensional parameters included in the study. Later on, we have discussed outcomes of all parameters on the flow.

Here, results show that velocity of Casson fluid reduces with rising magnetic parameter and grows with increasing radiation parameter. Temperature increases as both radiation and magnetic parameter increase. Magnetic parameter also enhances the Casson fluid's concentration.

 This is a preview of subscription content, [log in via an institution](#) to check access.

### Access this chapter

[Log in via an institution](#)

### Subscribe and save

**Springer+ Basic**

€32.70 /Month

Get 10 units per month

Download Article/Chapter or eBook

1 Unit = 1 Article or 1 Chapter

Cancel anytime

[Subscribe now](#) →

### Buy Now

^ **Chapter**

EUR 29.95

v **eBook**

EUR 171.19

Price includes VAT (India)

Available as PDF

Read on any device

Instant download

Own it forever

[Buy Chapter](#)

v **Softcover Book**

EUR 199.99

Tax calculation will be finalised at checkout

**Purchases are for personal use only**

[Institutional subscriptions](#) →

## Abbreviations

$T =$ : Temperature of fluid ( $K$ )

$T_w =$ : Constant temperature at surface of the sheet ( $K$ )

$T_\infty =$ : Temperature in the free stream ( $K$ )

$C$  =: Concentration of fluid

$C_w$  =: Concentration at the surface of the sheet

$C_\infty$  =: Concentration in the free stream

$u$  =: Velocity component in  $X$  direction

$v$  =: Velocity component in  $Y$  direction

$\theta$  =: Temperature

$\sigma$  =: Stefan Boltzman constant ( $Wm^{-2}K^{-4}$ )

$M$  =: Magnetic parameter

$Pr$  =: Prandtl number

$Re$  =: Reynold number

$\nu$  =: Kinematic viscosity ( $m^2s^{-1}$ )

$D_B$  =: Coefficient of Brownian diffusion

$\alpha$  =: Thermal diffusivity

$B_0$  =: Normal strength of magnetic field applied to sheet which is uniformly distributed

$\rho$  =: Fluid density ( $Kgm^{-3}$ )

$C_p$  =: Specific heat (at constant pressure)

$k_0$  =: Constant of chemical reaction rate

$\beta_C$  =: Solutal expansion coefficient

$\sigma$  =: Fluid's Electric conductivity

$K'$  =: Coefficient of Permeability (porous medium)

$g$  =: Gravitational acceleration

$q_r$  =: Radiative heat flux ( $Wm^{-2}K^{-1}$ )

$\beta_T$  =: Coefficient of thermal expansion



$\infty$ : Conditions at the free stream or far from the wall

$w$ : Conditions at the wall/surface

## References

---

1. Kuznetsov, A.V., Nield, D.A.: Natural convection boundary layer flow of a nanofluid past a vertical plate. *Int. J. Therm. Sci.* **40**, 115–124 (2001)  
[Google Scholar](#)
2. Bhattacharya, K.: Effects of heat source/sink on MHD flow and heat transfer over a shrinking sheet with mass suction. *Chem. Eng. Res. Bull.* **15**(1), 12–17 (2011)  
[Article](#) [Google Scholar](#)
3. Nadeem, S., Haq, R.L., Akbar, N.S., Khan, Z.H.: MHD three-dimensional Casson fluid flow past a porous linearly stretching sheet. *Alex. Eng. J.* **52**, 577–582 (2013)  
[Article](#) [Google Scholar](#)
4. Sulochana, C., Kishor, M.K., Sandeep, N.: Nonlinear thermal radiation and chemical reaction effects on MHD 3D casson fluid flow in porous medium. *Chem. Process Eng. Res.* **37**, 24–36 (2015)  
[Google Scholar](#)
5. Arthur, E.M., Seini, I.Y., Bortteir, L.B.: Analysis of casson fluid flow over a vertical porous surface with chemical reaction in the presence of magnetic field. *J. Appl. Math. Phys.* **3**, 713–723 (2015)  
[Article](#) [Google Scholar](#)
6. Pushpalatha, K., Sugunamma, V., Reddy, J.V., Sandeep, N.: Heat and mass transfer in unsteady MHD Casson fluid flow with convective boundary conditions. *Int. J. Adv. Sci. Technol.* **91**, 19–38 (2016)  
[Article](#) [Google Scholar](#)
7. Reza, M., Chahal, R., Sharma, N.: Radiation effect on MHD Casson fluid flow over a power-law stretching sheet with chemical reaction. *Eng. Technol. Int. J. Chem. Molecul. Eng.* **10**(5), 585–590 (2016)  
[Google Scholar](#)
8. Kumar, G.C., Dharmiah, G., Balamurugan, K.S., Vedavathi, N.: Chemical reaction and Soret effects on Casson MHD fluid flow over a vertical plate. *Int. J. Chem. Sci.* **14**(1), 213–221 (2016)  
[Google Scholar](#)

9. Kataria, H., Patel, H.: Radiation and chemical reaction effects on MHD Casson fluid flow past an oscillating vertical plate embedded in a porous medium. *Alex. Eng. J.* (2016). <https://doi.org/10.1016/j.aej.2016.01.019>  
[Article](#) [Google Scholar](#)
10. Kumar, C.K., Srinivas, S.: Simultaneous effects of thermal radiation and chemical reaction on hydromagnetic pulsatile flow of a casson fluid in a porous space. *Eng. Trans.* **65**(3), 461–481 (2017)  
[MathSciNet](#) [Google Scholar](#)
11. Balakrishna, S., Mohan, S.R., Reddy, G.V., Varma, S.V.K.: Effects of chemical reaction on unsteady MHD Casson fluid flow past a moving infinite inclined plate through porous medium. *IJESC* **8**(7), 18658–18666 (2018)  
[Google Scholar](#)
12. Rao, M.E.: The effects of thermal radiation and chemical reaction on MHD flow of a Casson fluid over an exponentially inclined stretching surface. *J. Phys: Conf. Ser.* **1000**, 1–14 (2018). <https://doi.org/10.1088/1742-6596/1000/1/012158>  
[Article](#) [Google Scholar](#)
13. Khan, D., Khan, A., Khan, I., Ali, F., Karim, F., Tlili, I.: Effects of relative magnetic field, chemical reaction, heat generation and Newtonian heating on convection flow of Casson fluid over a moving vertical plate embedded in a porous medium. *Publ. Sci. Rep.* **400**, 1–18 (2019). <https://doi.org/10.1038/s41598-018-36243-0>  
[Article](#) [Google Scholar](#)
14. Omokhuale, E., Jabaka, M.L.: Magnetohydrodynamic Casson fluid flow over an infinite vertical plate with chemical reaction and heat generation. *Am. J. Comput. Math.* **9**, 187–200 (2019). <https://doi.org/10.4236/ajcm.2019.93014>  
[Article](#) [Google Scholar](#)
15. Suresh, P., Krishna, Y.H., Rao, R.S., Reddy, P.V.J.: Effect of chemical reaction and radiation on MHD flow along a moving vertical porous plate with heat source and suction. *Int. J. Appl. Eng. Res.* **14**(4), 869–876 (2019)  
[Google Scholar](#)
16. Rao, S.R., Vidyasagar, G., Deekshitulu, G.V.S.R.: Viscous and Joule dissipation on MHD Casson fluid flow past an exponentially accelerated vertical porous plate with radiation absorption and chemical reaction in the presence of Soret effects. *High Technol. Lett.* **26**(5), 392–401 (2020)  
[Google Scholar](#)
17. Manjula, V., Sekhar, K.V.C.: Analysis of heat and mass transfer on steady MHD Casson fluid flow past an inclined porous stretching sheet with viscous dissipation and thermal radiation. *Int. J. Mech. Prod. Eng. Res. Develop.* **10**(3), 281–292 (2020)

[Google Scholar](#)

18. Deka, A.K.: In the presence of thermal radiation through porous medium unsteady MHD Casson fluid flow past an accelerated vertical plate. *Int. J. Statist. Appl. Math.* **5**(4), 213–228 (2020)

[MathSciNet](#) [Google Scholar](#)

19. Sakthikala, R., Lavanya, V.: “MHD oscillatory flow of non Newtonian fluid through porous medium in the presence of radiation and chemical diffusion with hall effects. *Int. J. Emerg. Technol.* **11**(2), 1093–1099 (2020)

[Google Scholar](#)

20. Vijayaragavan, R., Ramesh, M., Karthikeyan, S.: Heat and mass transfer investigation on MHD Casson fluid flow past an inclined porous plate in the effects of Dufour and chemical reaction. *J. Xi’an Univ. Architect. Technol.* **13**(6), 860–873 (2021)

[Google Scholar](#)

21. Vijayaragavana, R., Bharathi, V., Prakash, J.: Heat and mass transfer effect of a Magnetohydrodynamic Casson fluid flow in presence of inclined plate. *Indian J. Pure Appl. Phys.* **59**, 28–39 (2021)

[Google Scholar](#)

22. Sridhar, W., Ganesh, G.R., Rao, B.V.A., Gorfie, E.H.: Mixed convection boundary layer flow of MHD Casson fluid on an upward stretching sheet encapsulated in a porous medium with slip effects. *JP J. Heat Mass Transf.* **22**(2), 133–149 (2021)

[Article](#) [Google Scholar](#)

23. Rasheed, H.U., Islam, S., Zeeshan, K.W., Khan, J., Abbas, T.: Numerical modeling of unsteady MHD flow of Casson fluid in a vertical surface with chemical reaction and hall current. *Adv. Mech. Eng.* **14**(3), 1–10 (2022)

[Article](#) [Google Scholar](#)

24. Talla, H., Fatima: Magnetic field influence on radiative Casson fluid flow over an exponential stretching surface. *J. Pharmaceut. Negat. Results* **13**(6), 1881–1888 (2022)

[Article](#) [Google Scholar](#)

25. Reddy, L.R.M., Reddy, P.R.K., Reddy, P.C., Raju, M.C.: MHD Casson fluid flow past an upright plate under the impact of the heat sink and chemical reaction. *Adv. Appl. Math. Sci.* **21**(10), 5865–5878 (2022)

[Google Scholar](#)

26. Jain, S., Sharma, S.: Chemical reaction effect on MHD Casson fluid flow with Newtonian heating and heat source over a vertical plate. *Int. J. Mech. Eng.* **7**, 793–804 (2022)  
[Google Scholar](#)
27. Mopuri O., et al.: Unsteady MHD on convective flow of a Newtonian fluid past an inclined plate in presence of chemical reaction with radiation absorption and dufour effects. *CFD Lett.* **14**(7), 62–76 (2022).  
<https://doi.org/10.37934/cfdl.14.7.6276>
28. Yasin, M.H.M., Ishak, A., Pop, I.: MHD heat and mass transfer flow over a permeable stretching/shrinking sheet with radiation effect. *J. Magn. Magn. Mater.* **407**, 235–240 (2016). <https://doi.org/10.1016/j.jmmm.2016.01.087>  
[Article](#) [Google Scholar](#)
29. Bhattacharyya, K., Hayat, T., Alsaedi, A.: Exact solution for boundary layer flow of Casson fluid over a permeable stretching/shrinking sheet. *Zeitschrift für Angewandte Mathematik und Mechanik* (2013)  
[Google Scholar](#)
30. Nakamura, M., Sawada, T.: Numerical study on the flow of a non-Newtonian fluid through an axisymmetric stenosis. *J. Biomech. Eng.* **110**(2), 137–143 (1988)  
[Article](#) [Google Scholar](#)
31. Neemawat, A., Sushila: Non-similarity solutions of MHD boundary layer flow. *ICMMAAC* **666**, 508–521 (2023).  
[https://doi.org/10.1007/978-3-031-29959-9\\_33](https://doi.org/10.1007/978-3-031-29959-9_33)  
[Article](#) [Google Scholar](#)
32. Jat, R.N., Neemawat, A.: Similarity solution for MHD stagnation point flow and heat transfer over a non-linear Stretching sheet. *IJRRR* **3**, 32–51 (2012)  
[Google Scholar](#)
33. Jat, R.N., Neemawat, A., Rajotia, D.: MHD boundary layer flow and heat transfer over a continuously moving flat plate. *IJSAM* **3**(3), 102–108 (2012)  
[Google Scholar](#)
34. Jat, R.N., Neemawat, A., Rajotia, D.: MHD flow with heat transfer due to a point sink. *J. Ultra Sci. Phys. Sci.* **25**(1A), 199–206 (2013)  
[Google Scholar](#)

35. Jat, R.N., Neemawat, A.: MHD boundary layer flow and heat transfer over a moving non-isothermal flat plate. *Computat. Math. Modell.* **25**, 514–520 (2014). <https://doi.org/10.1007/s10598-014-9245-y>

[Article](#) [MathSciNet](#) [Google Scholar](#)

36. Jangid, S., Mehta, R., Kumar, D.: Numerical study of viscous dissipation, suction/injection effects and Dufour number also with chemical reaction impacts of MHD Casson nanofluid in convectively heated non-linear extending surface. *J. Comput. Anal. Appl.* **30**(1), 290–311 (2022)

[Google Scholar](#)

37. Gupta, S., Kumar, D., Singh, J.: Analytical study for MHD flow of Williamson nanofluid with the effects of variable thickness, nonlinear thermal radiation and improved Fourier's and Fick's Laws. *SN Appl. Sci.* **2**, 438 (2020)

[Article](#) [Google Scholar](#)

38. Tassaddiq, A., Khan, I., Nisar, K.S., Singh, J.: MHD flow of a generalized Casson fluid with Newtonian heating: a fractional model with Mittag-Leffler memory. *Alex. Eng. J.* **59**(5), 3049–3059 (2020)

[Article](#) [Google Scholar](#)

39. Sushila, S.J., Kumar, D., Baleanu, D.: A hybrid analytical algorithm for thin film flow problem occurring in non-Newtonian fluid mechanics. *Ain Shams Eng. J.* **12**(2), 2297–2302 (2021)

[Article](#) [Google Scholar](#)

40. Ferraro, V.C.A., Plumton, C.: *An Introduction to Magneto Fluid Mechanics*, 2nd edn., p. 58. Oxford University Press (1966)

[Google Scholar](#)

## Author information

---

### Authors and Affiliations

Department of Mathematics, JECRC University, Jaipur, 303905, India  
Abhishek Neemawat

Department of Mathematics, Sanskriti College, Jaipur, 302020, India  
Nimit Jain

Department of Physics, Vivekanand Global University, Jaipur, 303012, India  
Sushila

### Corresponding author

Correspondence to [Sushila](#).

## Editor information

---

### Editors and Affiliations

Department of Mathematics, JECRC University, Jaipur, Rajasthan, India

Jagdev Singh

Department of Mathematics, University of Memphis, Memphis, TN, USA

George A. Anastassiou

Department of Computer Science and Mathematics, Lebanese American University, Beirut, Lebanon

Dumitru Baleanu

Department of Mathematics, University of Rajasthan, Jaipur, Rajasthan, India

Devendra Kumar

## Rights and permissions

---

[Reprints and permissions](#)

## Copyright information

---

© 2024 The Author(s), under exclusive license to Springer Nature Switzerland AG

## About this paper

---

### Cite this paper

Neemawat, A., Jain, N., Sushila (2024). Numerical Investigation of Radiation and Magnetic Effects on Casson Fluid Flow Over a Porous Sheet in Presence of Constant Mass Flux. In: Singh, J., Anastassiou, G.A., Baleanu, D., Kumar, D. (eds) *Advances in Mathematical Modelling, Applied Analysis and Computation . ICMMAAC 2023. Lecture Notes in Networks and Systems*, vol 953. Springer, Cham. [https://doi.org/10.1007/978-3-031-56304-1\\_17](https://doi.org/10.1007/978-3-031-56304-1_17)

[.RIS](#) [.ENW](#) [.BIB](#)

DOI	Published	Publisher Name
<a href="https://doi.org/10.1007/978-3-031-56304-1_17">https://doi.org/10.1007/978-3-031-56304-1_17</a>	29 March 2024	Springer, Cham

Print ISBN	Online ISBN	eBook Packages
978-3-031-56303-4	978-3-031-56304-1	<a href="#">Engineering</a>
		<a href="#">Engineering (R0)</a>

## Publish with us

---

[Policies and ethics](#) 



# A comprehensive study of decay modes associated with Pb isotopes

R. Sharma<sup>1,2</sup>, A. Jain<sup>1,3</sup>, P. K. Sharma<sup>4</sup>, S. K. Jain<sup>1</sup>, and G. Saxena<sup>3</sup>

<sup>1</sup> Department of Physics, School of Basic Sciences, Manipal University Jaipur-303007, India

<sup>2</sup> Department of Physics, S. S. Jain Subodh P.G.(Autonomous) College, Jaipur-302004, India

<sup>3</sup> Department of Physics (H&S), Govt. Women Engineering College, Ajmer - 305002, India

<sup>4</sup> Govt. Polytechnic College, Rajsamand-313324, India

E-mail: gauravphy@gmail.com

December 2021

**Abstract.** Decay modes in Pb isotopes within the range  $176 \leq A \leq 266$  are investigated by the calculation of half-lives using several empirical formulas. These formulas along with various theoretical treatments are first tested to reproduce experimental half-lives and known decay modes of Pb isotopes, which are in consequence applied to estimate half-lives and decay modes of unknown Pb isotopes. A comparison between  $\alpha$ -decay and weak-decay from the stable to drip-line isotopes is canvassed which leads to the excellent match with experimental data and applicability of applied empirical formulas. In addition, the full chain of Pb isotopes is probed as potential daughter candidates of cluster emission from superheavy nuclei which ensued the predominant role of  $^{208}\text{Pb}$  and nearby isotopes in probable cluster emission.

*keywords:* Alpha Decay; Weak-decay; Cluster Decay; Half-lives.

## 1. Introduction

Nuclei with the heaviest well-established proton shell closure ( $Z=82$ ) i.e. Pb isotopes, out of which 43 are experimentally accessible, offer an excellent ground for testing the theories and their continuous growths. The most neutron-rich lead isotope identified experimentally is  $^{220}\text{Pb}$  [1] whereas  $^{178}\text{Pb}$  is the most neutron-deficient lead isotope known recently [2]. On the other hand,  $^{204,206,207,208}\text{Pb}$  are stable and rest of the isotopes decay via  $\alpha$ ,  $\beta^+/\text{EC}$  or  $\beta^-$  emissions. In addition, doubly magicity and core shape of  $^{208}\text{Pb}$  make it a predominant daughter nucleus of various cluster emissions as well as the terminating nucleus of several  $\alpha$ -decay chains of superheavy nuclei. Hence, interconnection among various decays in Pb isotopes classifies it uniquely for probing a variety of decay modes at the same time.



Recently,  $\alpha$ -decay has been contemplated in Pb isotopes using Coulomb and proximity potential model (CPPM) [3], the quantum-mechanical tunneling mechanism of penetration through a potential barrier [4], generalized liquid drop model [5] and modified generalized liquid drop model (MGLDM) [6]. Additionally,  $\beta$ -decay half-lives are reported for  $^{215-218}\text{Pb}$  beyond  $N=126$  by R. Caballero-Folch *et al.* [7]. Another decay mode which was first proposed theoretically in 1980 by Sandulescu *et al.* [8] before its experimental realization in 1984 by Rose and Jones [9], and intimately connected to closed-shell daughters as  $^{208}\text{Pb}$  or its neighbors, is the emission of heavy nuclei (clusters), such as carbon, oxygen, fluorine, neon, magnesium, silicon, etc. Therefore, the study of Pb isotopes which are either stable or decay via  $\alpha$ ,  $\beta^+ / EC$ ,  $\beta^-$ , along with their potential as daughter nuclei of cluster emission in superheavy nuclei, provide plenteousness base for testing and improvements of theoretical approaches or empirical formulas, which has invoked us for the present study.

In this study, various theoretical models and empirical formulas are examined to produce known half-lives of Pb isotopes ( $176 \leq A \leq 266$ ) considering  $\alpha$ -decay as good as the weak-decay. Consequently, these formulas are used to estimate half-lives of unknown Pb isotopes. In addition, half-lives for various cluster emissions considering Pb isotopes as daughter nuclei are examined to speculate various cluster emissions in the superheavy regions.

## 2. Theoretical Frameworks

As mentioned above, decay modes of Pb isotopes within the range  $176 \leq A \leq 266$  are investigated by evaluating the decay half-lives using empirical formulas that are predominantly dependent on the energy released in the specific transition. The energy released in  $\alpha$ -decay,  $\beta^-$ -decay, and electron capture (EC) are denoted by  $Q_\alpha$ ,  $Q_{\beta^-}$ , and  $Q_{EC}$ , respectively, and are estimated using a few widely used theories wherever the experimental values of these energies are not available. To evaluate the Q-values in the unknown regions, we have used various parameterizations/variants of the RMF models that have been practiced to a great extent. The commonly used variants are NL3\* [10], TMA [11], FSU-Gold [12], FSU-Garnet [13]. The relativistic mean-field approach and its variants are adequately described in various Refs. [12, 14–20] and our work [21] which can be referred for further details of the formalism. For comparison, the results of other theoretical models viz. RCHB [22], FRDM [23] and WS4 [24] are also taken into account. Aforesaid models are tested to reproduce the experimental Q-values [25] of Pb isotopes. Hence, we have calculated  $Q_\alpha$ ,  $Q_{\beta^-}$ , and  $Q_{EC}$  (respective equations are provided in the upcoming sections) values for approx 43 Pb isotopes in the range  $96 \leq N \leq 138$ . The root-mean-square error RMSE (which provides error in the estimated data) along with standard deviation  $\sigma$  (which gives deviation from experimental data) are given by the following equations, respectively, and are listed in Table 1.

$$RMSE = \sqrt{\frac{1}{N_{nucl}} \sum_{i=1}^{N_{nucl}} (x)^2} \quad (1)$$

$$\sigma = \sqrt{\frac{1}{N_{nucl} - 1} \sum_{i=1}^{N_{nucl}} (x - \bar{x})^2} \quad (2)$$

In these equations,  $x = Q_{Th} - Q_{Exp}$ ,  $\bar{x}$  is the mean of  $x$ , and  $N_{nucl}$  is the total number of data used for the calculations. The table ensuing exactitude of WS4 mass model in producing Q-values for all the considered decay modes. Hence, from here onwards, Q-values are taken from the WS4 mass model if the experimental Q-values are not available.

**Table 1.** RMSE and standard deviation ( $\sigma$ ) of  $Q_\alpha$ ,  $Q_{\beta^-}$ , and  $Q_{EC}$  for Pb isotopic chain.

Theory	RMSE			$\sigma$		
	$Q_\alpha$	$Q_{\beta^-}$	$Q_{EC}$	$Q_\alpha$	$Q_{\beta^-}$	$Q_{EC}$
WS4	0.36	0.29	0.53	0.06	0.13	0.56
FRDM	0.37	0.32	0.29	0.09	0.18	0.30
TMA	0.61	1.48	0.63	0.27	0.50	0.85
NL3*	1.06	1.89	1.70	0.37	0.23	0.08
FSU-Garnet	1.13	2.10	1.27	0.28	0.47	0.58
FSU-Gold	1.17	3.37	1.91	1.10	0.73	0.36
RCHB	2.06	0.62	0.79	1.35	0.23	0.31

It is crucial to point out here that we have performed quadrupole constrained calculations using RMF approach for obtaining corresponding potential energy surfaces (PESs) in addition to the determination of the corresponding ground-state deformations for all the Pb isotopes. Most of the isotopes are found spherical or near spherical shapes, however, some neutron deficient nuclei  $^{186,188}\text{Pb}$  are found in coexisting oblate and prolate shapes. These Pb nuclei are already speculated to show shape coexistence [26–28]. The pronounced shape coexistence with prolate and oblate shapes appears to be a remarkable feature and characteristic of the nuclei away from shell closure that may have a significant role in the above mentioned Q-values and consequently in determination of lifetime [29]. The enhanced lifetime obtained with the second minima, which is lying at a very small energy difference may get favored in certain situations and affect the half-lives. Dependence of half-lives on deformed nuclei as well as nuclei having co-existence will be investigated in more detail in our future work.

### 3. $\alpha$ -decay

One of the dominant decay modes in heavy and superheavy nuclei is the  $\alpha$ -decay for which energy release  $Q_\alpha$  in ground-state to ground-state decay is obtained from mass excesses or total binding energies through

$$\begin{aligned} Q_\alpha(\text{MeV}) &= M(Z, N) - M(Z - 2, N - 2) - M(2, 2) \\ &= B.E.(Z - 2, N - 2) + B.E.(2, 2) - B.E.(Z, N) \end{aligned} \quad (3)$$

**Table 2.** Coefficients of NMSF, NMHF, MTNF and QF formulas.

Formulas	a	b	c	d	e	f	g	$\overline{E}_i$
NMSF	0.6975	-0.1113	-27.1154	13.5610	-24.7796	0.0174	-	$\overline{E}_{i,ee} = 0.0000$ $\overline{E}_{i,eo} = -0.0396$ $\overline{E}_{i,oe} = -0.0350$ $\overline{E}_{i,oo} = 0.0438$
NMHF	107.0131	-206.5398	-160.6152	309.6165	19.7237	-31.1655	0.0238	-
MTNF	0.7208	-17.7056	0.0281	-	-	-	-	-
QF	-0.3980	9.2318	-75.3725	0.0354	-	-	-	-

where the  ${}^4\text{He}$  mass excess  $M(2, 2)$  is 2.42 MeV and the binding energy  $B.E.(2, 2)$  is 28.30 MeV. To calculate the  $\alpha$ -decay half-lives ( $\log_{10}T_{1/2}$ ), we have used four recently developed formulas. These formulas are fitted on latest experimental  $\alpha$ -decay half-lives, spin, and parity of 398 nuclei from NUBASE2020 [30] in the range  $50 \leq Z \leq 118$  which include an essential contribution of orbital angular momentum ( $l$ ) of the emitted  $\alpha$ -particle and hence evidently described favoured and unfavoured  $\alpha$ -transitions [31, 32]. These formulas with brief details are mentioned below:

### 3.1. New Modified Sobiczewski Formula (NMSF)

Parkhomenkho and Sobiczewski have proposed the phenomenological formula to calculate the  $\alpha$ -decay half-lives [33] in 2005 which has been modified in our recent work [34]. In the present work, we use another modified version referred to as the new modified Sobiczewski formula (NMSF) [31] which includes isospin dependency as well as the centrifugal term and given by:

$$\log_{10}T_{1/2}^{NMSF}(s) = aZ\sqrt{\mu}(Q_\alpha - \overline{E}_i)^{-1/2} + bZ\sqrt{\mu} + c + dI + eI^2 + fl(l+1) \quad (4)$$

where  $Z$ ,  $Q_\alpha$ ,  $l$ , and  $\overline{E}_i$  represent the proton number,  $\alpha$ -decay energy of parent nucleus, minimum angular momentum and average excitation energy (in MeV), respectively.  $\mu = \frac{A_d A_\alpha}{A_d + A_\alpha}$  represents reduced mass (where  $A_d$  and  $A_\alpha$  are mass number of the daughter nuclei and  $\alpha$ -particle, respectively), and  $I = \frac{N-Z}{A}$  exhibits nuclear isospin asymmetry. The values of fitted coefficients  $a$ ,  $b$ ,  $c$ ,  $d$ ,  $e$ , and  $f$  are given in Table 2.

### 3.2. New Modified Horoi Formula (NMHF)

Another formula for calculating  $\alpha$ -decay half-lives along with cluster decay was offered by Horoi *et al.* [35]. This formula has been modified in our recent work [31] which depends upon the proton number of an alpha particle ( $Z_\alpha$ ), proton number of daughter nucleus  $Z_d$ ,  $\alpha$ -decay energy of parent nucleus ( $Q_\alpha$ ), minimum angular momentum ( $l$ ), reduced mass ( $\mu$ ) and nuclear isospin asymmetry ( $I = \frac{N-Z}{A}$ ) given as:

$$\log_{10}T_{1/2}^{NMHF}(s) = (a\sqrt{\mu} + b)[(Z_\alpha Z_d)^{0.6} Q_\alpha^{-1/2} - 7] + (c\sqrt{\mu} + d) + eI$$

$$+ fI^2 + gl(l + 1) \quad (5)$$

where the coefficients (a, b, c, d, e, f, and g) are given in Table 2.

### 3.3. Modified TNF Formula (MTNF)

One of the very old formulas i.e Tagerpera-Nurmi formula [36] has also been modified in one of our recent work [32] and shapes as:

$$\log_{10}T_{1/2}^{MTNF}(s) = a\sqrt{\mu}(Z_dQ_\alpha^{-1/2} - Z_d^{2/3}) + b + cl(l + 1) \quad (6)$$

Here  $Z_d$ ,  $Q_\alpha$ ,  $\mu$ ,  $l$  are same as defined above, and the fitted coefficients (a, b, and c) are given in Table 2.

### 3.4. Quadratic Fitting Formula (QF)

An entirely new formula was also proposed [32] with only 4 fitted coefficients incorporating a quadratic fitting term. The formula is named as QF formula and given by:

$$\log_{10}T_{1/2}^{QF}(s) = a\sqrt{\mu}\left(\frac{Z_d^{0.6}}{\sqrt{Q_\alpha}}\right)^2 + b\sqrt{\mu}\left(\frac{Z_d^{0.6}}{\sqrt{Q_\alpha}}\right) + c + dl(l + 1) \quad (7)$$

where the symbols are defined above and the coefficients (a, b, c, and d) are given in Table 2.

Using these 4 formulas, the half-lives for the ground to ground state decay have been calculated for  $^{176-194}\text{Pb}$  and  $^{204}\text{Pb}$  isotopes that are given in Table 3. For these half-lives, the minimum angular momentum  $l_{min}$  (written as  $l$  in the formulas) taken away by  $\alpha$ -particle is obtained by using standard selection rules [37] based on spin and parity of parent and daughter nuclei. For comparison, experimental half-lives along with probable decay modes are also mentioned [30]. From Table 3, it is indulging to note that our formulas are adequate to estimate  $\alpha$ -decay half-lives and are in a close match with the experimental half-lives where the probability of  $\alpha$ -decay is found dominant. Towards the neutron deficient side, we have estimated half-lives of  $^{176-177}\text{Pb}$  for which Q-values are taken from the WS4 mass model (shown by an asterisk (\*)) as concluded in the previous section. It is important to note that the NMHF formula is found to be more accurate with minimum RMSE value among the considered formulas for Pb isotopes, specifically.

The study of Pb isotopes provides an excellent ground where the  $\alpha$ -decay competes with  $\beta^+/EC$ -decay towards neutron deficient side as can also be seen from Table 3 for the  $^{185-192}\text{Pb}$ . With this in view, we have estimated half-lives of weak-decay for isotopes of Pb having  $A > 184$ . The process to calculate half-life for weak-decay ( $\beta^-$  &  $\beta^+/EC$ ) is elaborated in the next section.

**Table 3.**  $\alpha$ -decay half-lives for Pb isotopes. Experimental data are taken from Refs. [25, 30].

A	Exp.				$\log_{10}T_{1/2}^{cal}$ (s)			
	$Q_\alpha$ (MeV)	$l_{min}$	$\log_{10}T_{1/2}$ (s)	Decay modes	NMSF	NMHF	MTNF	QF
176	7.88*	0	-	-	-4.06	-4.29	-3.54	-4.42
177	7.69*	3	-	-	-3.42	-3.49	-2.72	-3.37
178	7.79	0	-3.92	$\alpha$	-3.73	-3.95	-3.31	-4.12
179	7.60	2	-2.46	$\alpha$	-3.17	-3.26	-2.63	-3.25
180	7.42	0	-2.39	$\alpha$	-2.63	-2.88	-2.30	-2.84
181	7.24	2	-1.44	$\alpha$	-2.08	-2.19	-1.62	-1.99
182	7.07	0	-1.26	$\alpha$	-1.51	-1.79	-1.27	-1.56
183	6.93	2	-0.27	$\alpha$	-1.06	-1.18	-0.67	-0.82
184	6.77	0	-0.31	$\alpha$	-0.52	-0.80	-0.35	-0.44
185	6.70	2	0.80	$\alpha/\beta^+/EC$	-0.25	-0.36	0.08	0.09
186	6.47	0	0.68	$\beta^+/EC/\alpha$	0.57	0.28	0.67	0.78
187	6.39	2	1.18	$\beta^+/EC/\alpha$	0.84	0.73	1.11	1.31
188	6.11	0	1.40	$\beta^+/EC/\alpha$	1.94	1.63	1.98	2.31
189	5.92	2	1.59	$\beta^+/EC/\alpha$	2.67	2.55	2.90	3.38
190	5.70	0	1.85	$\beta^+/EC/\alpha$	3.63	3.31	3.62	4.16
191	5.46	0	1.90	$\beta^+/EC/\alpha$	4.51	4.36	4.65	5.29
192	5.22	0	2.32	$\beta^+/EC/\alpha$	5.81	5.48	5.75	6.48
193	5.01	0	2.54	$\beta^+/EC$	6.67	6.54	6.80	7.57
194	4.74	0	2.81	$\beta^+/EC$	8.33	8.00	8.24	9.05
204	1.97	0	$\geq 24.64$	$\alpha$	37.26	37.12	37.19	28.32

#### 4. $\beta$ -decay & Electron Capture (Weak-decay)

The energy released in ground-state to ground-state electron-decay ( $\beta^-$ -decay) and electron capture (EC) are given in terms of the atomic mass excess  $M(Z, N)$  or the total binding energy  $B.E.(Z, N)$  by:

$$\begin{aligned} Q_{\beta^-}(MeV) &= M(Z, N) - M(Z + 1, N - 1) \\ &= B.E.(Z + 1, N - 1) - B.E.(Z, N) + M_n - M_H \end{aligned} \quad (8)$$

$$\begin{aligned} Q_{EC}(MeV) &= M(Z, N) - M(Z - 1, N + 1) - B.E^{e^-} \\ &= B.E.(Z - 1, N + 1) - B.E.(Z, N) + M_H - M_n - B.E^{e^-} \end{aligned} \quad (9)$$

To look into the possibility of weak-decay, we adopt the empirical formula of Fiset and Nix [38] for estimating the corresponding half-lives. It is worthy to note that this formula of  $\beta$ -decay has recently been used successfully in a few of our works [39, 40] and the work by Ikram *et al.* [41].

$$T_\beta(s) = \frac{540m_e^5}{\rho(W_\beta^6 - m_e^6)} \times 10^{5.0} \quad (10)$$

This equation (10) is only logical for  $W_\beta \gg m_e$ . For the average density of states  $\rho$  in the daughter nucleus, we use the empirical results given by Seeger *et al.* [42], from

which  $\rho$  has values 0.97 and 1.67 for even and odd A isotopes of Pb, respectively. The formula for electron capture (EC) is given by

$$T_{EC}(s) = \frac{9m_e^2}{2\pi(\alpha Z_K)^{2s+1}\rho [Q_{EC} - (1-s)m_e]^3} \left(\frac{2R_0}{\hbar c/m_e}\right)^{2-2s} \times \frac{\Gamma(2s+1)}{1+s} \times 10^{6.5} \quad (11)$$

Here,  $Z_K$  is the effective charge of the parent nucleus for an electron in the K-shell; it is given approximately by  $Z_K = Z_P - 0.35$ , The energy  $W_\beta$  is sum of energy of the emitted  $\beta$  - particle and its rest mass  $m_e$ . i.e.  $W_\beta = Q_\beta + m_e$ . Also, the quantity s is given by  $s = [1 - (\alpha Z_K)^2]^{\frac{1}{2}}$  and represents the rest mass of an electron minus its binding energy in the K-shell, in units of  $m_e$ . The quantity  $\alpha$  is the fine-structure constant, and  $R_0$  is the nuclear radius, which is taken to be  $R_0 = 1.2249A^{\frac{1}{3}} fm$ .

In this paper, we follow Eqn.(10) to calculate half-lives for  $\beta^-$ -decay whereas the Eqn.(11) is used to calculate half-lives for electron capture (EC). The Table 4 consists of half-lives of  $^{185-203} Pb$  calculated for  $\beta^+/EC$ -decay. In a similar manner,  $\beta^-$ -decay half-lives are estimated for a wide range which are mentioned in Table 5 for  $^{209-266} Pb$ . The experimental half-lives using the empirical formulas are in reasonable match with experimental data, which automatically validates the use of the formula in the unknown region. As mentioned above, the majority of the Q-values are taken from the WS4 mass model for  $\beta^-$ -decay.

**Table 4.**  $\beta^+/EC$ -decay half-lives for Pb isotopes. Experimental data are taken from Refs. [25, 30].

A	Exp.			$\log_{10} T_{1/2}^{cal} (s)$ $\beta^+/EC$	A	Exp.			$\log_{10} T_{1/2}^{cal} (s)$ $\beta^+/EC$
	$Q_{EC}$ (MeV)	$\log_{10} T_{1/2}$ (s)	Decay modes			$Q_{EC}$ (MeV)	$\log_{10} T_{1/2}$ (s)	Decay modes	
185	8.22	0.80	$\alpha/\beta^+/EC$	3.04	194	2.73	2.81	$\beta^+/EC$	4.75
186	5.20	0.68	$\beta^+/EC/\alpha$	3.88	195	4.45	2.95	$\beta^+/EC$	3.86
187	7.46	1.18	$\beta^+/EC/\alpha$	3.17	196	2.15	3.35	$\beta^+/EC$	5.07
188	4.52	1.40	$\beta^+/EC/\alpha$	4.07	197	3.60	2.69	$\beta^+/EC$	4.14
189	6.77	1.59	$\beta^+/EC/\alpha$	3.30	198	1.46	3.94	$\beta^+/EC$	5.61
190	3.96	1.85	$\beta^+/EC/\alpha$	4.25	199	2.83	3.73	$\beta^+/EC$	4.46
191	6.05	1.90	$\beta^+/EC/\alpha$	3.45	200	0.80	4.89	$\beta^+/EC$	6.48
192	3.32	2.32	$\beta^+/EC/\alpha$	4.48	201	1.91	4.53	$\beta^+/EC$	5.00
193	5.28	2.54	$\beta^+/EC$	3.63	203	0.98	5.27	$\beta^+/EC$	5.95

To visualize the competition among all these concerned decay modes and their agreement with available experimental half-lives, we have plotted our calculated half-lives for  $\alpha$ ,  $\beta^-$ -decays as well as electron capture (EC) in Fig. 1 along with experimental half-lives [30]. An excellent match with experimental data renders our estimation of half-lives with a good accuracy which is adequate to use in all regions of the periodic chart. A close look of Fig. 1 suggests shell effect near N=126 as the  $\alpha$ -decay half-lives approach to very high values. This region is also marked as 'stable' in the figure. The competition among considered decays demonstrates a clear possibility of  $\alpha$ -decay in the neutron deficient region which is subsequently overtaken by  $\beta^+/EC$ -decay upto

**Table 5.**  $\beta^-$ -decay half-lives for Pb isotopes. Experimental data are taken from Refs. [25,30]. Other Q-values are taken from WS4 mass model (kindly refer to section 2).

Exp.					WS4			WS4			WS4		
A	$Q_{\beta^-}$ (MeV)	$\log_{10}T_{1/2}$ (s)	Decay modes	$\log_{10}T_{1/2}^{cal}$ ( $\beta^-$ ) (s)	A	$Q_{\beta^-}$ (MeV)	$\log_{10}T_{1/2}^{cal}$ ( $\beta^-$ ) (s)	A	$Q_{\beta^-}$ (MeV)	$\log_{10}T_{1/2}^{cal}$ ( $\beta^-$ ) (s)	A	$Q_{\beta^-}$ (MeV)	$\log_{10}T_{1/2}^{cal}$ ( $\beta^-$ ) (s)
209	0.64	4.07	$\beta^-$	5.68	221	5.21	1.51	237	10.49	-0.20	253	14.48	-1.00
210	0.06	8.80	$\beta^-$	8.03	222	4.43	2.13	238	9.62	0.25	254	13.82	-0.65
211	1.37	3.34	$\beta^-$	4.41	223	6.36	1.03	239	11.02	-0.32	255	15.20	-1.12
212	0.57	4.58	$\beta^-$	6.09	224	5.45	1.64	240	10.12	0.13	256	14.49	-0.77
213	2.03	2.79	$\beta^-$	3.62	225	7.03	0.79	241	11.50	-0.43	257	15.68	-1.20
214	1.02	3.21	$\beta^-$	5.18	226	6.04	1.39	242	10.65	0.00	258	14.95	-0.85
215	2.71	2.17	$\beta^-$	3.00	227	7.56	0.61	243	12.09	-0.55	259	16.10	-1.27
216	1.61	> -6.52	$\beta^-$	4.33	228	6.53	1.20	244	11.11	-0.10	260	15.44	-0.93
217	3.50	> -6.52	$\beta^-$	2.43	229	8.08	0.45	245	12.00	-0.53	261	16.68	-1.36
218	2.20	> -6.52	$\beta^-$	3.69	230	7.08	1.00	246	10.79	-0.03	262	15.92	-1.01
219	4.00	> -6.52	$\beta^-$	2.13	231	8.57	0.30	247	12.47	-0.63	263	17.04	-1.41
220	2.90	> -6.52	$\beta^-$	3.09	232	7.73	0.79	248	11.82	-0.26	264	16.37	-1.08
					233	9.25	0.11	249	13.29	-0.79	265	17.44	-1.47
					234	8.37	0.60	250	12.49	-0.40	266	16.88	-1.15
					235	9.84	-0.04	251	13.83	-0.89			
					236	9.01	0.41	252	13.15	-0.53			

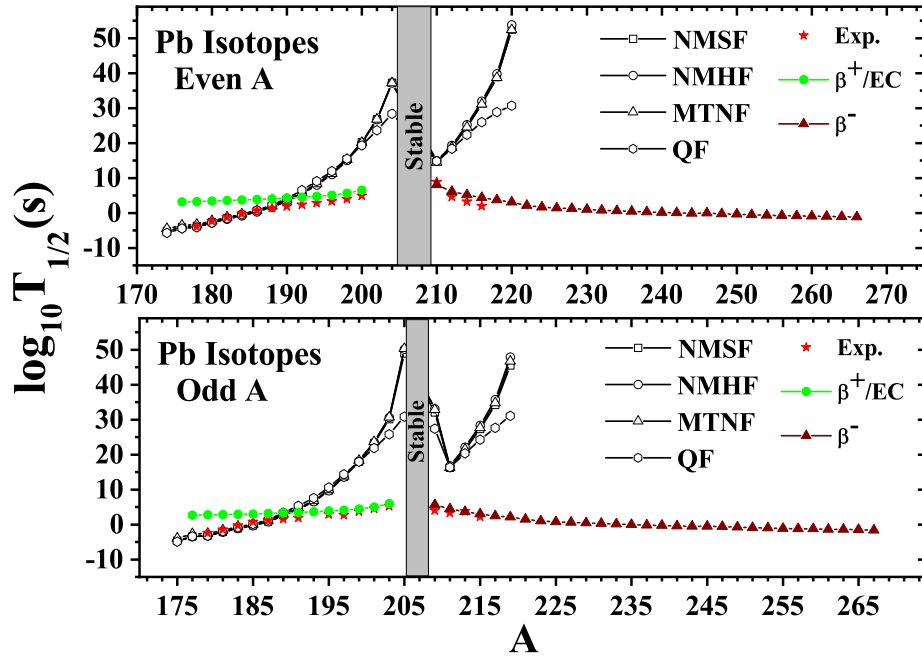


**Figure 1.** (Colour online) The comparison of half-lives of  $\alpha$ ,  $\beta^-$ ,  $\beta^+/\text{EC}$ -decays.

the stable region. After stable region,  $\beta^+/\text{EC}$ -decay is energetically forbidden, however,  $\beta^-$ -decay becomes more probable and holds up to the neutron drip-line.

To examine the competition among various decay modes, we have calculated the total half-lives of Pb isotopes in the range  $103 \leq N \leq 117$  (using Eqn. 12), and compared them with the available experimental data.

$$\frac{1}{T_{1/2}^{Th.}} = \frac{1}{T_{1/2}^{\alpha}} + \frac{1}{T_{1/2}^{\beta^+/\text{EC}}} \quad (12)$$

where  $\alpha$ -decay half-lives ( $T_{1/2}^\alpha$ ) have calculated by using NMHF (as mentioned in subsection 3.2),  $\beta^+$ /EC-decay half-lives calculated with the help of Eqn. (11). Thereafter, to quantize the competition among various decay-modes, we have calculated the branching ratios for respective decay modes as:

$$b = \begin{cases} \frac{T_{1/2}^{Th.}}{T_{1/2}^\alpha} & \text{for } \alpha\text{-decay} \\ \frac{T_{1/2}^{Th.}}{T_{1/2}^{\beta^+/EC}} & \text{for } \beta^+/\text{EC-decay} \end{cases} \quad (13)$$

The values of total half-lives and branching ratios are listed in Table 6. It is to be noted that the nuclei with  $A \leq 184$  own  $\alpha$ -decay as the only dominant mode. Similarly, nuclei with  $A \geq 209$  have only  $\beta^-$ -decay mode predominantly. For the rest of the nuclei, the competition is clearly evident from the Table 6 where the probability of  $\alpha$ -decay decreases gradually towards neutron-rich side and chances of  $\beta^+$ /EC-decay turn more probable. It is also satisfactory to note that total half-lives calculated by using Eqn. (12) is in a reasonable match with the experimental data.

**Table 6.**  $\alpha$ -decay total half-lives and branching ratio for Pb isotopes. Experimental data are taken from Ref. [30].

A	Total $\log_{10}T_{1/2}$ (s)		Branching ratio		A	Total $\log_{10}T_{1/2}$ (s)		Branching ratio	
	Exp.	Theoretical	$\alpha$	$\beta^+/EC$		Exp.	Theoretical	$\alpha$	$\beta^+/EC$
185	0.80	-0.36	99.96	0.04	194	2.81	4.51	0.03	99.97
186	0.68	0.28	99.98	0.02	195	2.95	4.09	0.00	100.00
187	1.18	0.73	99.64	0.36	196	3.35	4.84	0.00	100.00
188	1.40	1.63	99.37	0.63	197	2.69	4.38	0.00	100.00
189	1.59	2.51	90.53	9.47	198	3.94	5.37	0.00	100.00
190	1.85	3.23	83.30	16.70	199	3.73	4.70	0.00	100.00
191	1.90	3.60	17.34	82.66	200	4.89	6.25	0.00	100.00
192	2.32	4.22	5.50	94.50	201	4.53	5.24	0.00	100.00
193	2.54	3.86	0.21	99.79	203	5.27	6.18	0.00	100.00

## 5. Cluster Decay

Another exotic decay, in which a heavy nucleus decays into a light daughter nucleus and emits a fragment, is named cluster-decay. This kind of decay was first studied by Sandulescu *et al.* in 1980 [8] which is subsequently observed experimentally [9] in  $^{223}\text{Ra}$  which decays into a large fragment near doubly-magic  $^{208}\text{Pb}$  and a lighter cluster  $^{14}\text{C}$ . Many of the experiments have been done in this region [43–45] and several other clusters like  $^{20}\text{O}$ ,  $^{22,24-26}\text{Ne}$ ,  $^{28-30}\text{Mg}$  and  $^{32,34}\text{Si}$  have been experimentally observed so far [46–48] which predominantly diverge towards Pb isotopes. Hence the emission of the cluster is closely related to the Pb isotopes in the heavy and superheavy regions which incited our investigation towards cluster emission. At this point, it is clearly mentioned that unlikely to above-considered decay modes, the probability of cluster emission from Pb isotopes is insignificant or negligible, however, Pb isotopes own their candidature to become daughter nuclei in cluster emission of heavier and superheavy nuclei. With this



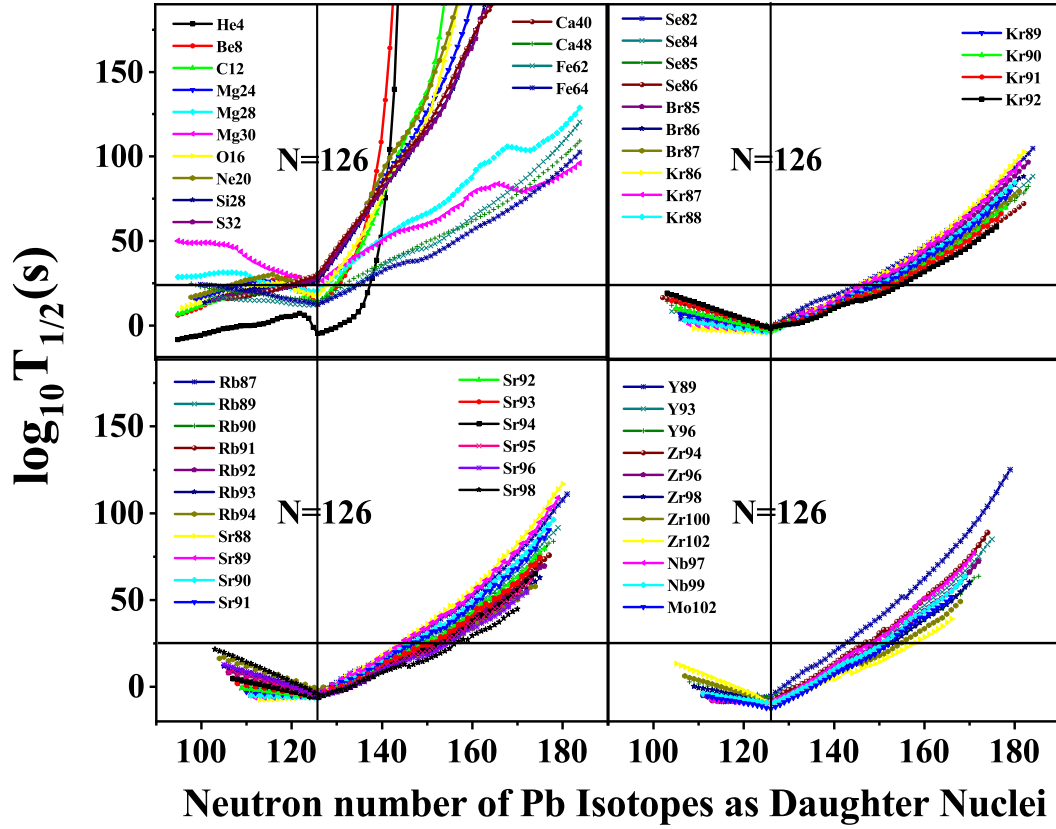


**Figure 2.** (Colour online) Half-lives for various cluster emission considering Pb isotopes as daughter nuclei.

in view, considering daughter nuclei as Pb nuclei the cluster emission is looked in for heavy and superheavy nuclei. To calculate the energy released in cluster decay, we have used the following formula:

$$Q(\text{MeV}) = B.E.(d) + B.E.(c) - B.E.(p) \quad (14)$$

where  $B.E.(d)$ ,  $B.E.(c)$ , and  $B.E.(p)$  are the binding energies of the daughter, cluster, and parent nucleus, respectively and taken from WS4 mass table [24]. To estimate half-life of cluster decay, a very widely known formula proposed by Qi *et al.* [49] is used which is also called universal decay law (UDL) and given as:

$$\log_{10} T_{1/2}^{UDL}(s) = a Z_c Z_d \sqrt{\frac{\mu}{Q}} + b [\mu Z_c Z_d (A_c^{1/3} + A_d^{1/3})]^{1/2} + c \quad (15)$$

where  $\mu$  is the reduced mass as mentioned above, and  $Z_c$ ,  $Z_d$ ,  $Q$  are proton number of cluster nucleus, proton number of daughter nucleus, the energy released during decay, respectively. Also,  $a=0.3949$ ,  $b=-0.3693$ , and  $c=-23.7615$  are fitting coefficients. The formula is applied for a wide range of Pb nuclei considered as daughter nuclei and covering clusters from  ${}^4\text{He}$  to  ${}^{102}\text{Mo}$  to calculate half-lives, which is plotted in Fig. 2. The strong stability of  ${}^{208}\text{Pb}$  clearly visible in all the panels of Fig. 2 as all the half-lives are found minimum for all the considered clusters. This investigation evidently

establishes cluster decay as one of the important decay modes in heavy and superheavy nuclei which needs separate investigation.

## 6. Conclusions

Various decay modes are probed on equal footing which are mainly concerned with Pb isotopes. Towards the neutron deficient side, half-lives are estimated using four newly proposed empirical formulas of  $\alpha$ -decay (NMSF, NMHF, MTNF, and QF). Similarly, half-lives towards both sides of the valley of  $\beta$ -stability are calculated using the empirical formula of weak-decay. Calculated half-lives along with the competition of these decay modes are found consistent with experimental values as a result these formulas are utilized to estimate half-lives for other unknown isotopes of Pb. It is concluded that for the Pb isotopes the WS4 mass table results more accurately for calculating Q-values of decay modes. In particular, for  $\alpha$ -decay, the NMHF formula is found to be more precise for Pb isotopes and hence can be used to estimate  $\alpha$ -decay half-lives of unknown nuclei in this region of the periodic chart. Another important outcome of our study is to bring in the possibility of cluster emission from superheavy nuclei which produces Pb isotopes as one of the daughter nuclei by emitting clusters ranging from He to Mo isotopes. This comprehensive study of decay modes linked with Pb isotopes is expected to provide a reasonable drive to the experiments eyeing on Pb or heavier nuclei.

## 7. Acknowledgement

The support provided by SERB (DST), Govt. of India under CRG/2019/001851 is acknowledged.

## 8. References

- [1] H. Alvarez-Pol *et al.* 2010 *Phys. Rev. C* **82** 041602.
- [2] H. Badran *et al.* 2016 *Phys. Rev. C* **94** 054301.
- [3] K. P. Santhosh, I. Sukumaran and B. Priyanka 2015 *Nuclear Physics A* **935** 28.
- [4] S. S. Hosseini, H. Hassanabadi and D. T. Akrawy 2019 *Int. J. Mod. Phys. E* **28** 1950017.
- [5] H. -M. Liu *et al.* 2020 *Chinese Phys. C* **44** 094106.
- [6] K. P. Santhosh *et al.* 2020 *Phys. Rev. C* **101** 064610.
- [7] R. Caballero-Folch *et al.* 2017 *Phys. Rev. C* **95** 064322.
- [8] A. Sandulescu, D. N. Poenaru and W. Greiner 1980 *Sov. J. Part. Nucl.* **11** 528.
- [9] H. J. Rose and G. A. Jones 1984 *Nature* **307** 245.
- [10] G. Lalazissis *et al.* 2009 *Phys. Lett. B* **671** 36.
- [11] Y. Sugahara and H. Toki 1994 *Nucl. Phys. A* **579** 557.
- [12] B. G. Todd-Rutel and J. Piekarewicz 2005 *Phys. Rev. Lett.* **95** 122501.
- [13] W. C. Chen and J. Piekarewicz 2015 *Phys. Lett. B* **748** 284.
- [14] B. D. Serot and J. D. Walecka 1986 *Adv. Nucl. Phys.* **16** 1.
- [15] P. Ring 1996 *Prog. Part. Nucl. Phys.* **37** 193.
- [16] G. A. Lalazissis, J. Konig and P. Ring 1997 *Phys. Rev. C* **55**, 540.
- [17] G. A. Lalazissis, T. Niksic, D. Vretenar and P. Ring 2005 *Phys. Rev. C* **71** 024312.
- [18] T. Niksic, D. Vretenar and P. Ring 2008 *Phys. Rev. C* **78** 034318.

- [19] G. Saxena, M. Kumawat, B. K. Agrawal and M. Aggarwal 2019 *J. Phys. G: Nucl. Part. Phys.* **46** 065105.
- [20] G. Saxena, M. Kumawat, R. Sharma and Mamta. Aggarwal 2021 *J. Phys. G: Nucl. Part. Phys.* **48** 125102.
- [21] R. Sharma, A. Jain, M. Kaushik, S. K. Jain and G. Saxena 2021 *Int. J. Mod. Phys. E* **38** 2150070.
- [22] X. W. Xia *et al.* 2018 *Atomic Data and Nuclear Data Tables* **121** 1.
- [23] P. Moller, A. J. Sierk, T. Ichikawa and H. Sagawa 2016 *Atomic Data and Nuclear Data Tables* **109** 1.
- [24] N. Wang, M. Liu, X. Wu and J. Meng 2014 *Phys. Lett. B* **734** 215.
- [25] M. Wang, W. Huang, F. Kondev, G. Audi, and S. Naimi 2020 *Chinese Physics C* **45** 030003.
- [26] A. N. Andreyev *et al.* 2000 *Nature* **405** 430.
- [27] T. Duguet, M. Bender, P. Bonche, P. -H. Heenen 2003 *Phys. Lett. B* **559** 201.
- [28] V. Hellemans, R. Fossion, S. D. Baerdemacker, and K. Heyde 2005 *Phys. Rev. C* **71** 034308.
- [29] B. P. Crider *et al.* 2016 *Phys. Lett. B* **763** 108.
- [30] F. G. Kondev, Meng Wang, W. J. Huang, S. Naimi and G. Audi 2020 *Chinese Physics C* **45** 030001.
- [31] P. K. Sharma, A. Jain and G. Saxena 2021 *Nucl. Phys. A* **1016** 122318.
- [32] G. Saxena, P. K. Sharma and A. Jain 2021 *Phys. Scr.* **96** 125304.
- [33] A. Parkhomenko and A. Sobiczewski 2005 *Acta Phys. Pol. B* **36** 3095.
- [34] G. Saxena, P. K. Sharma and Prafulla Saxena 2021 *J. Phys. G: Nucl. Part. Phys.* **48**, 055103.
- [35] M. Horoi, B. A. Brown and A. Sandulescu 2004 *J. Phys. G* **30** 945.
- [36] R. Taguepera, M. Nurmia 1961 *Ann. Acad. Sci. Fenn. Ser. A* **6** 78.
- [37] V. Yu. Denisov and A. A. Khudenko 2009 *At. Data Nucl. Data Tables* **95** 815.
- [38] E. Fiset and J. Nix 1972 *Nucl. Phys. A* **193**, 647.
- [39] G. Saxena, M. Kumawat, S. S. Singh and M. Aggarwal 2019 *Int. J. Mod. Phys. E* **28** 1950008.
- [40] U. K. Singh, P. K. Sharma, M. Kaushik, S. K. Jain, D. T. Akrawy and G. Saxena 2020 *Nucl. Phys. A* **1004** 122035.
- [41] M. Ikram, A. A. Rather, A. A. Usmani, B. Kumar and S. K. Patra 2017 *arXiv:1709.07311 [nucl-th]*.
- [42] A. S. Philip, A. F. William and D. C. Donald 1965 *Astrophysical Journal Supplement* **11** 121.
- [43] D. V. Aleksandrov, A. F. Belyatskii, Yu. A. Glukhov, E. Yu. Nikol'Skii, B. G. Novataskii, A. A. Ogloblin and D. N. Stepanov 1984 *JETP Lett.* **40** 4.
- [44] S. Gales, E. Hourany, M. Houssonnois, J. P. Shapira, L. Stab and M. Vergnes 1984 *Phys. Rev. Lett.* **53** 759.
- [45] W. Kutschera, I. Ahmad, S. G. Armato, A. M. Friedman, J. E. Gindler, W. Henning, T. Ishii, M. Paul and K. E. Rehm 1985 *Phys. Rev. C* **32** 2036.
- [46] S. W. Barwick, P. B. Price, H. L. Ravn, E. Hourani and Houssonnois, 1986 *Phys. Rev. C* **34** 362.
- [47] R. Bonetti, C. Chiesa, A. Guglielmetti, C. Migliorino, R. Matheoud, A. L. Pasinetti and H. L. Ravn 1993 *Nucl. Phys. A* **562** 32.
- [48] R. Bonetti, C. Chiesa, A. Guglielmetti, C. Migliorino, P. Monti, A. L. Pasinetti and H. L. Ravn 1994 *Nucl. Phys. A* **576** 21.
- [49] C. Qi, F. R. Xu, R. J. Liotta and R. Wyss 2009 *Phys. Rev. Lett.* **103** 072501.

# Cluster radioactivity from trans-tin to superheavy region using an improved empirical formula

Regular Article – Theoretical Physics Published: 23 August 2023

Volume 59, article number 189, (2023) Cite this article



The European Physical Journal

A

Aims and scope

Submit manuscript

G. Saxena  & A. Jain 178 Accesses  4 Citations [Explore all metrics](#) →

## Abstract

A simple relation  $(aZ_c + b)(Z_d/Q)^{1/2} + (cZ_c + d)$  of estimation of the half-life of cluster emission is further improved for cluster and  $\alpha$ -decays, separately, by incorporating isospin of parent nucleus as well as angular momentum taken away by the emitted particle. This improved version is not only found robust in producing experimental half-lives belonging to the trans-tin and trans-lead regions but also elucidates cluster emission in superheavy nuclei over the usual  $\alpha$ -decay. Considering daughter nuclei around the doubly magic  $^{100}\text{Sn}$  and  $^{208}\text{Pb}$  nuclei for trans-tin and trans-lead (including superheavy) parents, respectively, a systematic and extensive study of  $56 \leq Z \leq 120$  isotopes is performed for the light and heavy cluster emissions. A fair competition among cluster emission,  $\alpha$ -decay, spontaneous fission, and  $\beta$ -decay is observed in this broad range resulting in a substantial probability of C to Sr clusters from several nuclei, which demonstrates the adequacy of shell effects. The present article proposes a single, improved, latest-fitted, and effective formula of cluster radioactivity that can be used to estimate precise half-lives for a wide range of the periodic chart from trans-tin to superheavy nuclei.

 This is a preview of subscription content, [log in via an institution](#)  to check access.

Access this article

Log in via an institution

## Subscribe and save

 Springer+ Basic

€32.70 /Month

Get 10 units per month

Download Article/Chapter or eBook

1 Unit = 1 Article or 1 Chapter

Cancel anytime

[Subscribe now →](#)

## Buy Now

[Buy article PDF 39,95 €](#)

Price includes VAT (India)

Instant access to the full article PDF.

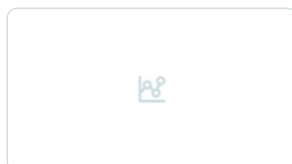
[Rent this article via DeepDyve ↗](#)
[Institutional subscriptions →](#)

## Similar content being viewed by others



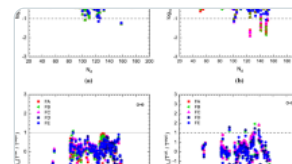
### Exploring $\alpha$ -decay chains and cluster radioactivities of superheavy $^{293-295}_{119}$ isotopes

Article | 26 March 2024



### Cluster radioactivity in $^{294,296}\text{Og}$

Article | 18 December 2021



### An improved unified formula for $\alpha$ -decay and cluster radioactivity of heavy and superheavy nuclei

Article | Open access  
17 November 2022

## Data Availability Statement

This manuscript has no associated data or the data will not be deposited. [Authors' comment: The data in manuscript is already in the various tables. Rest other data can be made available on request.]

## References

1. A. Sandulescu, D. N. Poenaru, W. Greiner, Sov. J. Part. Nucl. II. **11**, 528 (1980)
2. H.J. Rose, G.A. Jones, Nature **307**, 245 (1984)

[ADS](#) [Google Scholar](#)

3. R. Bonetti, A. Guglielmetti, Rom. Rep. Phys. **59**, 301 (2007)

[Google Scholar](#)

4. S. Kumar et al., J. Phys. G Nucl. Part. Phys. **29**, 625 (2003)

[ADS](#) [Google Scholar](#)

5. S. Kumar, R. Rani, R. Kumar, J. Phys. G Nucl. Part. Phys. **36**, 015110 (2009)

[ADS](#) [Google Scholar](#)

6. R.K. Gupta et al., Phys. Rev. C **68**, 034321 (2003)

[ADS](#) [Google Scholar](#)

7. R.K. Gupta, W. Greiner, Int. J. Mod. Phys. E **03**, 335 (1994)

[ADS](#) [Google Scholar](#)

8. P.B. Price, Annu. Rev. Nucl. Part. Sci. **39**, 19 (1989)

[ADS](#) [Google Scholar](#)

9. K.P. Santhosh, B. Priyanka, M.S. Unnikrishnan, Nucl. Phys. A **889**, 29 (2012)

[ADS](#) [Google Scholar](#)

10. E. Hourani, M. Hussonnois, D.N. Poenaru, Ann. Phys. (Paris) **14**, 311 (1989)

[ADS](#) [Google Scholar](#)

11. G. Royer, R. Moustabchir, Nucl. Phys. A **683**, 182 (2001)

[ADS](#) [Google Scholar](#)

12. A. Singh et al., J. Phys. G Nucl. Part. Phys. **49**, 025101 (2022)

[ADS](#) [Google Scholar](#)

13. S.N. Kuklin, G.G. Adamian, N.V. Antonenko, Phys. Rev. C **71**, 014301 (2005)

[ADS](#) [Google Scholar](#)

14. Y.T. Oganessian et al., *Z. Fur Phys. A Hadron. Nucl.* **349**, 341 (1994)

[ADS](#) [Google Scholar](#)

15. A. Guglielmetti et al., *Phys. Rev. C* **52**, 740 (1995)

[ADS](#) [Google Scholar](#)

16. A. Guglielmetti et al., *Nucl. Phys. A* **583**, 867 (1995)

[ADS](#) [Google Scholar](#)

17. K. Prathapan, R.K. Biju, *Int. J. Mod. Phys. E* **30**, 2150106 (2021)

[ADS](#) [Google Scholar](#)

18. K.P. Santhosh, T.A. Jose, N.K. Deepak, *Phys. Rev. C* **105**, 054605 (2022)

[ADS](#) [Google Scholar](#)

19. G. Royer, Q. Ferrier, M. Pineau, *Nucl. Phys. A* **1021**, 122427 (2022)

[Google Scholar](#)

20. C. Nithya, K.P. Santhosh, *Nucl. Phys. A* **1020**, 122400 (2022)

[Google Scholar](#)

21. D.N. Poenaru, R.A. Gherghescu, *Phys. Rev. C* **97**, 044621 (2018)

[ADS](#) [Google Scholar](#)

22. D.N. Poenaru, H. Stöcker, R.A. Gherghescu, *Eur. Phys. J. A* **54**, 14 (2018)

[ADS](#) [Google Scholar](#)

23. Z. Matheson, S.A. Giuliani, W. Nazarewicz, J. Sadhukhan, N. Schunck, *Phys. Rev. C* **99**, 041304 (2019)

[ADS](#) [Google Scholar](#)

24. M. Warda, A. Zdeb, L.M. Robledo, *Phys. Rev. C* **98**, 041602(R) (2018)

[ADS](#) [Google Scholar](#)

25. D.N. Poenaru, R.A. Gherghescu, W. Greiner, *Phys. Rev. C* **85**, 034615 (2012)

[ADS](#) [Google Scholar](#)

26. Y.L. Zhang, Y.Z. Wang, Phys. Rev. C **97**, 014318 (2018)

[ADS](#) [Google Scholar](#)

27. K.P. Santhosh, R.K. Biju, J. Phys. G Nucl. Part. Phys. **36**, 015107 (2009)

[ADS](#) [Google Scholar](#)

28. K.P. Santhosh, C. Nithya, Phys. Rev. C **97**, 064616 (2018)

[ADS](#) [Google Scholar](#)

29. A. Soylu, F. Koyuncu, Eur. Phys. J. A **55**, 118 (2019)

30. A. Jain, P.K. Sharma, S.K. Jain, D.T. Akrawy, G. Saxena, Phys. Scr. **98**, 085304 (2023)

[ADS](#) [Google Scholar](#)

31. D.N. Poenaru, M. Ivascu, D. Mazilu, Comput. Phys. Commun. **25**, 297 (1982)

[ADS](#) [Google Scholar](#)

32. D.S. Delion, J. Suhonen, Phys. Rev. C. **64**, 064302 (2001)

[ADS](#) [Google Scholar](#)

33. D.N. Poenaru, W. Greiner, Handbook of Nuclear Properties. Clarendon Press, Oxford, (1996)

34. D.N. Poenaru, Nuclear Decay Modes. Institute of Physics Publishing, Bristol, (1996)

35. S.K. Arun et al., Phys. Rev. C **79**, 064616 (2009)

[ADS](#) [Google Scholar](#)

36. M. Brack et al., Rev. Mod. Phys. **44**, 320 (1972)

[ADS](#) [Google Scholar](#)

37. A.C. Wahl, At. Data Nucl. Data Tables **39**, 1 (1988)

[ADS](#) [Google Scholar](#)



38. D.N. Poenaru et al., Phys. Rev. C **32**, 572 (1985)

[ADS](#) [MathSciNet](#) [Google Scholar](#)

39. D.N. Poenaru et al., At. Data Nucl. Data Tables **34**, 423 (1986)

[ADS](#) [Google Scholar](#)

40. Joshua T. Majekodunmi et al., Phys. Rev. C **105**, 044617 (2022)

[ADS](#) [Google Scholar](#)

41. W.A. Yahya, T.T. Ibrahim, Eur. Phys. J. A **58**, 48 (2022)

[ADS](#) [Google Scholar](#)

42. S.S. Hosseini, S.M. Motevalli, Phys. Rev. C **107**, 034611 (2023)

[ADS](#) [Google Scholar](#)

43. R. Dagtas, O. Bayrak, Phys. Scr. **97**, 105301 (2022)

44. H-M. Liu et al., Phys. Scr. **96**, 125322 (2021)

45. Mihai Horoi, J. Phys. G Nucl. Part. Phys. **30**, 945 (2004)

[ADS](#) [Google Scholar](#)

46. M. Balasubramaniam et al., Phys. Rev. C **70**, 017301 (2004)

47. Z. Ren, C. Xu, Z. Wang, Phys. Rev. C **70**, 034304 (2004)

[ADS](#) [Google Scholar](#)

48. D. Ni, Z. Ren, T. Dong, C. Xu, Phys. Rev. C **78**, 044310 (2008)

[ADS](#) [Google Scholar](#)

49. C. Qi, F.R. Xu, R.J. Liotta, R. Wyss, Phys. Rev. Lett. **103**, 072501 (2009)

[ADS](#) [Google Scholar](#)

50. D.N. Poenaru, R.A. Gherghescu, W. Greiner, Phys. Rev. C **83**, 014601 (2011)

[ADS](#) [Google Scholar](#)

51. O.A.P. Tavares, E.L. Medeiros, Eur. Phys. J. A **49**, 6 (2013)

[ADS](#) [Google Scholar](#)

52. A. Jain, P.K. Sharma, S.K. Jain, J.K. Deegwal, G. Saxena, Nucl. Phys. A **1031**, 122597 (2023)

[Google Scholar](#)

53. A. Soylu, C. Qi, Nucl. Phys. A **1013**, 122221 (2021)

[Google Scholar](#)

54. M. Ismail, A.Y. Ellithi, A. Adela, M.A. Abbas, Eur. Phys. J. A **58**, 225 (2022)

[ADS](#) [Google Scholar](#)

55. Y. Wang et al., Chin. Phys. C **45**, 044111 (2021)

[ADS](#) [Google Scholar](#)

56. S. Cheng et al., Eur. Phys. J. A **58**, 168 (2022)

[ADS](#) [Google Scholar](#)

57. Lin-Jing. Qi et al., Chin. Phys. C **47**, 064107 (2023)

[ADS](#) [Google Scholar](#)

58. Y. Gao, J. Cui, Y. Wang, J. Gu, Sci. Rep. **10**, 9119 (2020)

[ADS](#) [Google Scholar](#)

59. A. Guglielmetti et al., Phys. Rev. C. **56**, R2912 (1997)

[ADS](#) [Google Scholar](#)

60. F.G. Kondev et al., Chin. Phys. C **45**, 030001 (2021)

[ADS](#) [Google Scholar](#)

61. P.K. Sharma, A. Jain, G. Saxena, Nucl. Phys. A **1016**, 122318 (2021)

[Google Scholar](#)

62. G. Saxena et al., J. Phys. G Nucl. Part. Phys. **50**, 015102 (2023)

[ADS](#) [Google Scholar](#)

63. A. Soylu et al., Eur. Phys. J. A **48**, 128 (2012)

[ADS](#) [Google Scholar](#)

64. K. Wei, H.F. Zhang, Phys. Rev. C **96**, 021601(R) (2017)

[ADS](#) [Google Scholar](#)

65. G. Saxena, A. Jain, P.K. Sharma, P. Saxena, Communicated to Scientific Reports (2023) (under communication)

66. J-G. Deng, H-F. Zhang, Phys. Lett. B **816**, 136247 (2021)

67. VYu. Denisov, A.A. Khudenko, Phys. Rev. C **79**, 054614 (2009)

[ADS](#) [Google Scholar](#)

68. K.N. Huang et al., At. Data Nucl. Data Tables **18**, 243 (1976)

[ADS](#) [Google Scholar](#)

69. N. Wang, M. Liu, X. Wu, J. Meng, Phys. Lett. B **734**, 215 (2014)

[ADS](#) [Google Scholar](#)

70. P. Möller, M.R. Mumpower, T. Kawano, W.D. Myers, At. Data Nucl. Data Tables **125**, 1 (2019)

[ADS](#) [Google Scholar](#)

71. J. Dobaczewski, M.V. Stoitsov, W. Nazarewicz, AIP Conference Proceedings **726**, 51 (2004)

[ADS](#) [Google Scholar](#)

72. G. Saxena, M. Kumawat, M. Kaushik, S.K. Jain, M. Aggarwal, Phys. Lett. B **788**, 1 (2019)

[ADS](#) [Google Scholar](#)

73. G. Saxena, M. Kumawat, M. Kaushik, U.K. Singh, S.K. Jain, S. Somorendro Singh, M. Aggarwal, Int. J. Mod. Phys. E **26**, 1750072 (2017)

[ADS](#) [Google Scholar](#)

74. G. Saxena, M. Kumawat, M. Kaushik, S.K. Jain, M. Aggarwal, Phys. Lett. B **775**, 126 (2017)

[ADS](#) [Google Scholar](#)

75. U.K. Singh, P.K. Sharma, M. Kaushik, S.K. Jain, D.T. Akrawy, G. Saxena, Nucl. Phys. A **1004**, 122035 (2020)

[Google Scholar](#)

76. E.O. Fiset, J.R. Nix, Nucl. Phys. A **193**, 647 (1972)

[ADS](#) [Google Scholar](#)

77. G. Saxena, P.K. Sharma, P. Saxena, J. Phys. G Nucl. Part. Phys. **48**, 055103 (2021)

78. R. Sharma, A. Jain, P.K. Sharma, S.K. Jain, G. Saxena, Phys. Scr. **97**, 045307 (2022)

[ADS](#) [Google Scholar](#)

79. G. Saxena, A. Jain, P.K. Sharma, Phys. Scr. **96**, 125304 (2021)

[ADS](#) [Google Scholar](#)

## Acknowledgements

---

GS acknowledges the support provided by SERB (DST), Govt. of India under SIR/2022/000566, and would like to thank Prof. Nils Paar for his kind hospitality at the University of Zagreb, Croatia. AJ is indebted to Prof. S. K. Jain, Manipal University, Jaipur, India for his guidance.

## Author information

---

### Authors and Affiliations

Department of Physics (H & S), Govt. Women Engineering College, Ajmer, 305002, India

G. Saxena

Department of Physics, Faculty of Science, University of Zagreb, Bijenička c. 32, 10000, Zagreb, Croatia

G. Saxena

Department of Physics, School of Basic Sciences, Manipal University Jaipur, Jaipur, 303007, India

A. Jain

Department of Physics, S. S. Jain Subodh P. G. (Autonomous) College, Jaipur, 302004, India

A. Jain

### Corresponding author

Correspondence to [G. Saxena](#).

## Additional information

---

Communicated by Chong Qi.

## Rights and permissions

---

Springer Nature or its licensor (e.g. a society or other partner) holds exclusive rights to this article under a publishing agreement with the author(s) or other rightsholder(s); author self-archiving of the accepted manuscript version of this article is solely governed by the terms of such publishing agreement and applicable law.

[Reprints and permissions](#)

## About this article

---

### Cite this article

Saxena, G., Jain, A. Cluster radioactivity from trans-tin to superheavy region using an improved empirical formula. *Eur. Phys. J. A* **59**, 189 (2023). <https://doi.org/10.1140/epja/s10050-023-01102-8>

Received  
19 May 2023

Accepted  
02 August 2023

Published  
23 August 2023

DOI  
<https://doi.org/10.1140/epja/s10050-023-01102-8>

# Cluster radioactivity in $^{294,296}\text{Og}$

Published: 18 December 2021




Volume 242, article number 60, (2021) Cite this article



## Hyperfine Interactions


Aims and scope

Submit manuscript

A. Jain , R. Sharma, S. K. Jain, P. K. Sharma & G. Saxena 91 Accesses  2 Citations [Explore all metrics](#) →

## Abstract

Cluster radioactivity is one of the exotic phenomena which offers an alternate emission in heavy and superheavy nuclei in addition to the  $\alpha$ -decay and spontaneous fission. In the present work, we predict half-lives of cluster decay in superheavy nuclei  $^{294,296}\text{Og}$  by picking up the emission of all possible even-even isotopes from He to Mo ( $Z = 2-42$ ). These half-lives are compared with the half-lives of  $\alpha$ -decay, and accordingly the possibility of most probable cluster emission is ascertained. For these decay processes, the disintegration energies ( $Q$ -values) are taken from WS4 mass model. To estimate cluster emission half-lives, we use few widely known empirical formulas i.e. Horoi [J. Phys. G: Nucl. Part. Phys. 30, 945 (2004)], RenA [Phys. Rev. C 70, 034304 (2004)], NRDX [Phys. Rev. C 78, 044310 (2008)], UDL [Phys. Rev. 103, 072501 (2009)], and UNIV [Phys. Rev. C 83, 014601 (2011)]. The emission of  $^{86,92}\text{Kr}$  from  $^{294}\text{Og}$  and  $^{88,92}\text{Kr}$  clusters from  $^{296}\text{Og}$  are found to be the dominant clusters. Details of this study will be certainly useful for future experiments eyeing on synthesis of new elements.

 This is a preview of subscription content, [log in via an institution](#)  to check access.

### Access this article

[Log in via an institution](#)

### Subscribe and save

 Springer+ Basic

€32.70 /Month

Get 10 units per month

Download Article/Chapter or eBook

1 Unit = 1 Article or 1 Chapter

Cancel anytime

[Subscribe now →](#)
**Buy Now**
**Buy article PDF 39,95 €**

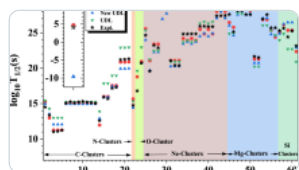
Price includes VAT (India)

Instant access to the full article PDF.

 Rent this article via [DeepDyve](#) ↗

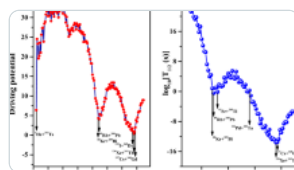
[Institutional subscriptions](#) →

### Similar content being viewed by others



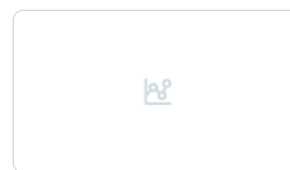
**Cluster radioactivity from trans-tin to superheavy region using an improved empirical formula**

Article | 23 August 2023



**Systematic study on heavy-particle radioactivity of superheavy nuclei <sup>297-300</sup>119**

Article | 12 October 2024



**Cluster and alpha decay of superheavy nuclei**

Article | 19 February 2018

## References

1. Sandulescu, A., Poenaru, D.N., Greiner, W.: New type of decay of heavy nuclei intermediate between fission and  $\alpha$  decay. Sov. J. Part. Nucl. II(11), 528 (1980). <https://www.osti.gov/biblio/6189038-new-type-decay-heavy-nuclei-intermediate-between-fission-cap-alpha-decay>
2. Rose, H.J., Jones, G.A.: A new kind of natural radioactivity. Nature 307, 245 (1984). <https://doi.org/10.1038/307245a0>
3. Gales, S., Hourany, E., Houssonnois, M., Shapira, J.P., Stab, L., Vergnes, M.: Exotic Nuclear Decay of <sup>223</sup>Ra by Emission of <sup>14</sup>C. Nuclei Phys. Rev. Lett. 53, 759 (1984). <https://doi.org/10.1103/PhysRevLett.53.759>

[Google Scholar](#)
[Article](#) [ADS](#) [Google Scholar](#)
[Article](#) [ADS](#) [Google Scholar](#)

4. Kutschera, W., Ahmad, I., Armato, S.G., Friedman, A.M., Gindler, J.E., Henning, W., Ishii, T., Paul, M., Rehm, K.E.: Spontaneous  $^{14}\text{C}$  emission from  $^{223}\text{Ra}$ . Phys. Rev. C. **32**, 2036 (1985). <https://doi.org/10.1103/PhysRevC.32.2036>  
[Article](#) [ADS](#) [Google Scholar](#)
  
5. Barwick, S.W., Price, P.B., Ravn, H.L., Hourani, E.: Hussonnois,:systematics of spontaneous emission of intermediate mass fragments from heavy nuclei. Phys. Rev. C. **34**, 362 (1986). <https://doi.org/10.1103/PhysRevC.34.362>  
[Article](#) [ADS](#) [Google Scholar](#)
  
6. Bonetti, R., Chiesa, C., Guglielmetti, A., Migliorino, C., Matheoud, R., Pasinetti, A.L., Ravn, H.L.: Nuclear structure effects in the exotic decay of  $^{225}\text{Ac}$  via  $^{14}\text{C}$  emission. Nucl. Phys. A. **562**, 32 (1993). [https://doi.org/10.1016/0375-9474\(93\)90030-2](https://doi.org/10.1016/0375-9474(93)90030-2)  
[Article](#) [ADS](#) [Google Scholar](#)
  
7. Bonetti, R., Chiesa, C., Guglielmetti, A., Migliorino, C., Monti, P., Pasinetti, A.L., Ravn, H.L.: Carbon radioactivity of  $^{221}\text{Fr}$  and  $^{221}\text{Ra}$  and the hindered decay of exotic odd-A emitters. Nucl. Phys. A. **576**, 21 (1994). [https://doi.org/10.1016/0375-9474\(94\)90736-6](https://doi.org/10.1016/0375-9474(94)90736-6)  
[Article](#) [ADS](#) [Google Scholar](#)
  
8. Sobiczewski, A., Patyk, Z., Cwiok, S.: Deformed superheavy nuclei. Phys. Lett. B. **224**, 1 (1989). [https://doi.org/10.1016/0370-2693\(89\)91038-1](https://doi.org/10.1016/0370-2693(89)91038-1)  
[Article](#) [ADS](#) [Google Scholar](#)
  
9. Parkhomenko, A., Sobiczewsk, A.: Phenomenological formula for  $\alpha$ ,-decay half-lives of heaviest nuclei. Acta Phys. Pol. B. **36**, 3095 (2005). <https://www.actaphys.uj.edu.pl/R/36/10/3095/pdf>  
[ADS](#) [Google Scholar](#)
  
10. Budaca, A.I., Budaca, R., Silisteanu, I.: Extended systematics of alpha decay half lives for exotic superheavy nuclei. Nucl. Phys. A. **951**, 60 (2016). <https://doi.org/10.1016/j.nuclphysa.2016.03.048>  
[Article](#) [ADS](#) [Google Scholar](#)
  
11. Poenaru, D.N., Gherghescu, R.A., Carjan, N.: Alpha-decay lifetimes semiempirical relationship including shell effects. Euro Physics Letters. **77**, 62001 (2007). <https://iopscience.iop.org/article/10.1209/0295-5075/77/62001/pdf>  
[Article](#) [ADS](#) [Google Scholar](#)
  
12. Royer, G.: Analytic expressions for alpha-decay half-lives and potential barriers. Nucl. Phys. A. **848**, 279 (2010). <https://doi.org/10.1016/j.nuclphysa.2010.09.009>



13. Jun-Gang, D., Hong-Fei, Z., Royer, G.: Improved empirical formula for  $\alpha$ -decay half-lives. Phys. Rev. C. **034307**, 101 (2020). <https://doi.org/10.1103/PhysRevC.101.034307>  
[Google Scholar](#)
14. Dashty, T., Akrawy, Hassanabadi, H., Hosseini, S.S., Santhosh, K.P.: Nuclear isospin effect on  $\alpha$ -decay half-lives. Nucl. Phys. A. **975**, 19228 (2018). <https://doi.org/10.1016/j.nuclphysa.2018.04.001>  
[Google Scholar](#)
15. Dashty, T., Akrawy, A., Ahmed, H.: New empirical formula for  $\alpha$ -decay calculations. Int. J. Mod. Phys. E **27**, 1850068 (2018). <https://doi.org/10.1142/S0218301318500684>  
[Article](#) [Google Scholar](#)
16. Dashty, T., Akrawy, A., Ahmed, H.:  $\alpha$ -decay systematics for superheavy nuclei. Phys. Rev. C **100**, 044618 (2019). <https://doi.org/10.1103/PhysRevC.100.044618>  
[Article](#) [ADS](#) [Google Scholar](#)
17. Dashty, T., Akrawy, Hassanabadi, H., Qian, Y., Santhosh, K.P.: Influence of nuclear isospin and angular momentum on. Nucl. Phys. A **983**, 310 (2019). <https://doi.org/10.1016/j.nuclphysa.2018.10.091>  
[Article](#) [ADS](#) [Google Scholar](#)
18. Hamilton, J.M., Hofmann, D., Oganessian, Y.T.: Search for Superheavy Nuclei. Annu. Rev. Nucl. Part. Sci. **63**, 383 (2013). <https://doi.org/10.1146/annurev-nucl-102912-144535>  
[Article](#) [ADS](#) [Google Scholar](#)
19. Oganessian, Y.T., et al.: Synthesis of the isotopes of elements 118 and 116 in the  $^{249}\text{Cf}$  and  $^{245}\text{Cm} + ^{48}\text{Ca}$  fusion reactions. Phys. Rev. C. **74**, 044602 (2006). <https://doi.org/10.1103/PhysRevC.74.044602>  
[Article](#) [ADS](#) [Google Scholar](#)
20. Oganessian, Y.T., et al.: Production and Decay of the Heaviest Nuclei  $^{293,294}\text{117}$  and  $^{294}\text{118}$ . Phys. Rev. Lett. **109**, 162501 (2012). <https://doi.org/10.1103/PhysRevLett.109.162501>  
[Article](#) [ADS](#) [Google Scholar](#)
21. Brewer, N., et al.: Search for the heaviest atomic nuclei among the products from reactions of mixed-Cf with a  $^{48}\text{Ca}$  beam. Phys. Rev. C. **98**, 024317 (2018). <https://doi.org/10.1103/PhysRevC.98.024317>

[Article](#) [ADS](#) [Google Scholar](#)

22. Zhang, Y.L., Wnag, Y.Z.: Systematic study of cluster radioactivity of superheavy nuclei. *Phys. Rev. C.* **97**, 014318 (2018). <https://doi.org/10.1103/PhysRevC.97.014318>

[Article](#) [ADS](#) [Google Scholar](#)

23. Carmel Vigila Bai, G.M., Revathi, R.: Alpha and heavy cluster radioactivity of superheavy nuclei  $100 \leq Z \leq 120$ . *J. Phys. Conf. Ser.* **1706**, 012021 (2020). <https://doi.org/10.1088/1742-6596/1706/1/012021>

[Article](#) [Google Scholar](#)

24. Santhosh, K.P., Nithya, C.: Systematic studies of  $\alpha$ , and heavy-cluster emissions from superheavy nuclei. *Phys. Rev. C.* **97**, 064616 (2018). <https://doi.org/10.1103/PhysRevC.97.064616>

[Article](#) [ADS](#) [Google Scholar](#)

25. Anjali, K.P., et al.: Studies on the emission of various exotic fragments from superheavy nuclei via cluster decay process. *Nucl. Phys. A.* **993**, 121644 (2020). <https://doi.org/10.1016/j.nuclphysa.2019.121644>

[Article](#) [Google Scholar](#)

26. Pradeep Kumar, K., Santhosh, K.P.: Proton shell closure in the superheavy region: Cluster radioactivity study in the isotopic set  $^{270-318}118$ . *Pramana – J. Phys.* **94**, 114 (2021). <https://doi.org/10.1007/s12043-021-02138-5>

[Article](#) [Google Scholar](#)

27. Matheson, Z., et al.: Cluster radioactivity of  $^{294}\text{Og}$ . *Phys. Rev. C.* **99**, 041304 (2019). <https://doi.org/10.1103/PhysRevC.99.041304>

[Article](#) [ADS](#) [Google Scholar](#)

28. Poenaru, D.N., et al.: Cluster and alpha decay of superheavy nuclei. *Eur. Phys. J. A* **54**, 14 (2018). <https://doi.org/10.1140/epja/i2018-12469-6>

[Article](#) [ADS](#) [Google Scholar](#)

29. Soylu, A., et al.: The predictions on the heavier cluster decays of superheavy nuclei. *Eur. Phys. J. A* **55**, 118 (2019). <https://doi.org/10.1140/epja/i2019-12790-6>

[Article](#) [ADS](#) [Google Scholar](#)

30. Dmitriev, S., Itkis, M., Oganessian, Y.T.: Status and perspectives of the Dubna superheavy element factory. *Eur. Phys. J. WOC* **131**, 08001 (2016). <https://doi.org/10.1051/epjconf/201613108001>

31. Oganessian, Y.T., Dmitriev, S.N.: Synthesis and study of properties of superheavy atoms. *Factory of Superheavy Elements. Russ. Chem. Rev.* **85**, 901 (2016). <https://iopscience.iop.org/article/10.1070/RCR4607/meta>  
[Article](#) [ADS](#) [Google Scholar](#)
32. Hofmann, S., et al.: Review of even element super-heavy nuclei and search for element 120. *Eur. Phys. J. A.* **52**, 180 (2016). <https://doi.org/10.1140/epja/i2016-16180-4>  
[Article](#) [ADS](#) [Google Scholar](#)
33. Roberto, J.B., Rykaczewski, K.P.: Discovery of element 117: Super-heavy elements and the “island of stability”. *Sep. Sci. Technol* **53**, 1813 (2018). <https://doi.org/10.1080/01496395.2017.1290658>  
[Article](#) [Google Scholar](#)
34. Düllmann, C. E., Block, M.: The quest for superheavy elements and the island of stability. *Sci. Am.* **318**, 48 (2018). <https://www.scientificamerican.com/article/the-quest-for-superheavy-elements-and-the-island-of-stability/>  
[Google Scholar](#)
35. Jerabek, P., Schuetrumpf, B., Schwerdtfeger, P., Nazarewicz, W.: Electron and Nucleon Localization Functions of Oganesson: Approaching the Thomas-Fermi Limit. *Phys. Rev. Lett.* **120**, 053001 (2018). <https://doi.org/10.1103/PhysRevLett.120.053001>  
[Article](#) [ADS](#) [Google Scholar](#)
36. Nazarewicz, W.: The limits of nuclear mass and charge. *Nature Phys.* **14**, 537 (2018). <https://doi.org/10.1038/s41567-018-0163-3>  
[Article](#) [ADS](#) [Google Scholar](#)
37. Giuliani, S.A., Matheson, Z., Nazarewicz, W., Olsen, E., Reinhard, P.G., Sadhukhan, J., Schuetrumpf, B., Schunck, N., Schwerdtfeger, P.: Oganesson and beyond, *Rev. Mod. Phys.*, in press. <https://www.osti.gov/servlets/purl/1513128> (2019)
38. Singh, U.K., Sharma, P.K., Kaushik, M., Jain, S.K., Dashty, T., Akrawy, Saxena, G.: Study of decay modes in transfermium isotopes. *Nucl. Phys. A.* **1004**, 122035 (2020). <https://doi.org/10.1016/j.nuclphysa.2020.122035>  
[Article](#) [Google Scholar](#)
39. Singh, U.K., Sharma, R., Sharma, P.K., Kaushik, M., Jain, S.K., Saxena, G.: Structural properties and  $\alpha$ -decay chains of transfermium nuclei ( $101 \leq Z \leq 110$ ). *Nucl. Phys. A.* **1006**, 122026 (2021). <https://doi.org/10.1016/j.nuclphysa.2020.122066>

40. Saxena, G., Sharma, P.K., Saxena, P.: Modified empirical formulas and machine learning for  $\alpha$ -decay systematics. *J. Phys. G: Nucl. Part. Phys.* **48**, 055103 (2021). <https://doi.org/10.1088/1361-6471/abcd1c>

[Article](#) [ADS](#) [Google Scholar](#)

41. Saxena, G., Kumawat, M., Somorendro, Singh, S., Aggarwal, M.: Structural properties and decay modes of  $Z = 122, 120$  and 118 superheavy nuclei. *Int. J. Mod. Phys. E.* **28**, 1950008 (2019). <https://doi.org/10.1142/S0218301319500083>

[Article](#) [ADS](#) [Google Scholar](#)

42. Geiger, H., Nuttall, J.M.: The ranges of the  $\alpha$  particles from various radioactive substances and a relation between range and period of transformation. *Philos. Mag.* **23**, 613 (1991). <https://doi.org/10.1080/14786441008637156>

[Google Scholar](#)

43. Ning, W., Min, L., Xizhen, W., Jie, M.: Surface diffuseness correction in global mass formula. *Phys. Lett. B.* **734**, 215 (2014). <https://doi.org/10.1016/j.physletb.2014.05.049>

[Article](#) [Google Scholar](#)

44. Saxena, G., Jain, A., Sharma, P.K.: A new empirical formula for  $\alpha$ -decay half-life and decay chains of  $Z = 120$  isotopes. *Phys. Scr.* **96**, 125304 (2021). <https://iopscience.iop.org/article/10.1088/1402-4896/ac1a4d/meta>

[Article](#) [ADS](#) [Google Scholar](#)

45. Mihai, H.: Scaling behaviour in cluster decay. *J. Phys. G: Nucl. Part. Phys.* **30**, 945–955 (2004). <https://iopscience.iop.org/article/10.1088/0954-3899/30/7/010/meta>

[Article](#) [Google Scholar](#)

46. Ren, Z., Xu, C., Wang, Z.: New perspective on complex cluster radioactivity of heavy nuclei. *Phys Rev C* **034304**, 70 (2004). <https://doi.org/10.1103/PhysRevC.70.034304>

[Google Scholar](#)

47. Ni, D., Ren, Z., Dong, T., Xu, C.: Unified formula of half-lives for  $\alpha$ ,-decay and cluster radioactivity. *Phys. Rev. C* **78**, 044310 (2008). <https://doi.org/10.1103/PhysRevC.78.044310>

[Article](#) [ADS](#) [Google Scholar](#)

48. Qi, C., Xu, F.R., Liotta, R.J., Wyss, R.: Universal Decay Law in Charged-Particle Emission and Exotic Cluster Radioactivity. *Phys. Rev. Lett* **103**, 072501 (2009). <https://doi.org/10.1103/PhysRevLett.103.072501>

49. Poenaru, D.N., Gherghescu, R.A., Greife, W.: Single universal curve for cluster radioactivities and  $\alpha$ -decay. Phys. Rev. C. **83**, 014601 (2011). <https://doi.org/10.1103/PhysRevC.83.014601>

[Article](#) [ADS](#) [Google Scholar](#)

50. Price, P.B., Bonetti, R., Guglielmetti, A., Chiesa, C., Matheoud, R., Migiliorino, C., Moody, K.J.: Emission of  $^{23}\text{F}$  and  $^{24}\text{Ne}$  in cluster radioactivity of  $^{231}\text{Pa}$ . Phys. Rev. C. **46**, 1939 (1992). <https://doi.org/10.1103/PhysRevC.46.1939>

[Article](#) [ADS](#) [Google Scholar](#)

51. Bonetti, R., Chiesa, C., Guglielmetti, A., Matheoud, R., Poli, G., Mikheev, V.L., Tretyakova, S.P.: First observation of spontaneous fission and search for cluster decay of  $^{232}\text{Th}$ . Phys. Rev. C. **51**, 2530 (1995).

<https://doi.org/10.1103/PhysRevC.51.2530>

[Article](#) [ADS](#) [Google Scholar](#)

## Acknowledgements

---

Authors gratefully acknowledge the support provided by Science and Engineering Research Board (DST), Govt. of India under CRG/2019/001851.

## Author information

---

### Authors and Affiliations

Department of Physics, School of Basic Sciences, Manipal University Jaipur, Jaipur, 303007, Rajasthan, India

A. Jain, R. Sharma & S. K. Jain

Department of Physics (H&S), Govt. Women Engineering College, Ajmer, 305002, Rajasthan, India

A. Jain & G. Saxena

Department of Physics, S. S. Jain Subodh P.G.(Autonomous) College, Jaipur, 302004, Rajasthan, India

R. Sharma

Department of Physics, Govt. Polytechnic College, Rajsamand, 313324, Rajasthan, India

P. K. Sharma

### Corresponding author

Correspondence to [A. Jain](#).

## Additional information

---

### Publisher's note

Springer Nature remains neutral with regard to jurisdictional claims in published maps and institutional affiliations.

These authors contributed equally to this work.

This article is part of the Topical Collection on *Proceedings of the International Conference on Hyperfine Interactions (HYPERFINE 2021), 5–10 September 2021, Brasov, Romania*

Edited by Ovidiu Crisan

## Rights and permissions

---

[Reprints and permissions](#)

## About this article

---

### Cite this article

Jain, A., Sharma, R., Jain, S.K. *et al.* Cluster radioactivity in  $^{294,296}\text{Og}$ . *Hyperfine Interact* **242**, 60 (2021). <https://doi.org/10.1007/s10751-021-01748-0>

Accepted  
18 October 2021

Published  
18 December 2021

DOI  
<https://doi.org/10.1007/s10751-021-01748-0>



### Keywords

[Cluster radioactivity](#)

[Superheavy nuclei](#)

[Empirical formulas](#)

# Cluster radioactivity in trans-lead region: A systematic study with modified empirical formulas

A. Jain <sup>a, b, c</sup>, P.K. Sharma <sup>d</sup>, S.K. Jain <sup>a</sup>, J.K. Deegwal <sup>e</sup>, G. Saxena <sup>c, f</sup>  

Show more 

 Share  Cite

<https://doi.org/10.1016/j.nuclphysa.2022.122597>

[Get rights and content](#)

## Abstract

The possibility of cluster emission from trans-lead ( $86 \leq Z \leq 96$ ) region of periodic chart has been explored comprehensively by employing few empirical formulas which are modified by adding angular momentum ( $l$ ) or isospin-dependent ( $I = (N - Z)/A$ ) or both terms for the calculation of cluster decay half-lives. These modified versions of the formulas are found with lesser  $\chi^2$  per degree of freedom and root mean-square error, in addition to the smaller values of some other statistical parameters, while compared to their corresponding old versions on available 61 experimental data of cluster radioactivity. By applying the modified version of the formula given by Balasubramaniam et al. (2004) [12], the most accurate formula among these, half-lives of several clusters i.e. isotopes of Be, B, C, N, O, F, Ne, Na, Mg, and Si are predicted systematically for the several isotopes in the trans-lead region. The contest of cluster emission with  $\alpha$ -decay has been investigated in form of branching ratio which brings several potential cluster emissions into the probable decay modes of these nuclei. The accurate prediction of half-lives of such clusters is expected to be crucial for the future experimental observations where  $\alpha$ -decay is observed dominantly.

## Introduction

In 1980, Sandulescu et al. [1] firstly predicted a new type of radioactivity: cluster radioactivity, which was based on fragmentation theory, where fusion and fission reaction valleys were generated by the shell closure effect [2]. Later in 1984, Rose and Jones experimentally proved the existence of this new type of exotic decay [3], in which  $^{14}\text{C}$  decays from actinide parent nucleus  $^{223}\text{Ra}$  and forms a stable doubly magic ( $Z=82$ ,  $N=126$ ) nucleus  $^{208}\text{Pb}$ . Till now, many clusters decays from light to heavy clusters ( $^{14}\text{C}$  to  $^{32}\text{Si}$ ) have been observed from various trans-lead nuclei (Fr, Ra, Ac, Pa, Th, U, Pu, etc.) resulting the corresponding daughter nuclei as magic nuclei ( $Z=82$ ) or neighboring ones ( $Z=80$ ,  $81$ , and  $83$ ), which indicate the importance of shell and pairing effects in cluster radioactivity [4], [5], [6]. These clusters are observed with long half-lives ( $T_{1/2}$ ) in the range  $10^{11}$ - $10^{30}$  sec. [7].

Theoretically, the half-lives of cluster emissions are predicted using various models such as unified fission model (UFM) [8], generalized liquid drop model (GLDM) [9], super-asymmetric fission model (SAFM) [10], preformation cluster model (PCM) [11], etc. Cluster decay half-lives are also calculated by using various semi-empirical formulas such as (i) the empirical relation suggested by Balasubramaniam et al. (BKAG formula) for cluster decay half-lives with only three parameters [12], (ii) the empirical relation suggested by Ren et al. (RenA formula) using a microscopic density-dependent cluster model with the re-normalized M3Y nucleon-nucleon interaction [13]. Concomitantly, based on experimental observations about the characteristics of exotic cluster decays, scaling law proposed by Horoi [14] in which logarithmic half-life is proportional to scaling variable  $(Z_c Z_d)^{0.6} / \sqrt{Q}$  and also proportional to  $\sqrt{\mu}$ , where  $\mu$  is the reduced mass of cluster and daughter nucleus which was followed by another semi-empirical formula (NRDX), proposed by Ni et al. [15] considering WKB barrier penetration probability with some approximations. In 2009, Qi et al. introduced universal decay law (UDL) [16] that originates from the mechanism of charge particle decay and R-matrix for all sort of decays of clusters, which includes monopole radioactive decays as well. Poenaru et al. [17] plotted a universal curve (UNIV) which is found to be a straight line for cluster decay and  $\alpha$ -decay.

Full Text

Help

All the above-mentioned formulas have been fitted to the available experimental data without considering the dependence of half-lives on angular momentum taken away by the cluster: expected to be crucial alike to the  $\alpha$ -decay [18] to delineate all sets of experimental data. The importance of angular momentum on the  $\alpha$ -decay half-lives has already been established in a few of our recent works [19], [20] which has invoked us to probe similar dependence on the cluster decay half-lives. In addition to this, isospin ( $I = (N - Z)/A$ ) of parent nucleus is found to be pivotal for the case of  $\alpha$ -decay in heavy and superheavy nuclei [20], [21], [22], [23], [24], [25] pointing towards its significance in terms of cluster decay as well. Considering these two effects together, modified UDL formula (new UDL) by Soyulu and Qi [26], and improved NRDX formula (named as improved unified formula (IUF)) by Ismail et al. [27] have explained recently that angular momentum and isospin are indeed crucial quantities in determining the cluster decay half-lives. Importance of isospin effect is also probed by improving semi-empirical formula (ISEM) for the cluster radioactivity in Ref. [28].

In this article, we have modified the BKAG [12], RenA [13], Horoi [14], NRDX [15], UDL [16], and UNIV [17] formulas by investigating the effect of centrifugal barrier and isospin terms. These six modified formulas are fitted by using 61 experimental cluster decay data [7], [9], [26], [29]. The comparison of RMSE (root mean square error) between the older and modified version manifestly shows the significance of inclusion of angular momentum and isospin-dependent terms in cluster emission. Furthermore, one of the modified formulas i.e. MBKAG formula (emerged with least RMSE) is employed to calculate the cluster decay half-lives for various cluster emissions like isotopes of Be, B, C, N, O, F, Ne, Na, Mg, and Si in trans-lead region ( $86 \leq Z \leq 96$ ). For these theoretical estimates, the requirement of disintegration energy ( $Q$ -value) is tested by 121 available experimental  $Q$ -values [7], [9], [26], [29] from various mass models [30], [31], [32], [33]. Consequently, various potential clusters are proposed from trans-lead region along with their accurate estimation of half-lives.

### Access through your organization

Check access to the full text by signing in through your organization.

Access through your organization

## Section snippets

### Formalism

In 2004, Balasubramaniam et al. fitted a formula (BKAG) [12] for cluster decay. In the course of that year, Ren et al. established a formula [13] that can be treated as a natural extension of the Geiger-Nuttall law [34] as well as the Viola-Seaborg formula [35] from simple  $\alpha$ -decay to complex cluster radioactivity. In the same year, Horoi also suggested an independent model for  $\alpha$ -decay which was generalized for cluster emission [14]. In 2008, Ni et al. established NRDX semi-empirical formula for

### Results and discussions

To ascertain the impact on accuracy for the estimation of half-lives of cluster decay by the addition of the above mentioned terms, we have plotted the ratio of decay widths  $W_{Exp.}/W_{Th.} = \log_{10} T_{1/2}^{Th.} / \log_{10} T_{1/2}^{Exp.}$  as a function of  $A$  for our six modified formulas (MBKAG, MRenA, MHoroi, MNRDX, MUDL, and MUNIV) along with their original versions in Fig. 1. Most of the points corresponding to our modified formulas (red diamonds) are between half order of magnitude while the points corresponding to

### Conclusions

Several empirical formulas are investigated by adding angular momentum and isospin dependence. Their modified versions are turned into MBKAG, MRenA, MHoroi, MNRDX, MUDL, and MUNIV formulas. Experimental data of a total of 61 nuclei have been utilized for fitting which offers improved results of all the modified formulas while compared to their earlier versions. Among these six modified formulas, after comparison of several statistical parameters the MBKAG formula is found most precise which is

### CRedit authorship contribution statement

**A. Jain:** Formal analysis, Validation, Visualization, Writing – original draft. **P.K. Sharma:** Conceptualization, Formal analysis, Writing – & editing. **S.K. Jain:** Formal analysis, Resources, Validation. **J.K. Deegwal:** Formal analysis, Resources, Validation. **G. Saxena:** Conceptualization, Formal analysis, Writing – original draft, Writing – review & editing.

### Declaration of Competing Interest

Full Text

Help



The authors declare the following financial interests/personal relationships which may be considered as potential competing interests: G. Saxena reports financial support was provided by Science and Engineering Research Board, grant nos CRG/2019/001851, SIR/2022/000566.

## Acknowledgement

AJ and GS acknowledge the support provided by SERB (DST), Govt. of India under CRG/2019/001851 and SIR/2022/000566, respectively.

[Recommended articles](#)

---

## References (49)

G. Royer *et al.*

Nucl. Phys. A (2001)

V.Yu. Denisov *et al.*

At. Data Nucl. Data Tables (2009)

P.K. Sharma *et al.*

Nucl. Phys. A (2021)

U.K. Singh

Nucl. Phys. A (2021)

A. Soylu *et al.*

Nucl. Phys. A (2021)

Ning Wang *et al.*

Phys. Lett. B (2014)

P. Möller *et al.*

At. Data Nucl. Data Tables (2019)

V.E. Viola *et al.*

J. Inorg. Nucl. Chem. (1966)

K-N. Huang

At. Data Nucl. Data Tables (1976)

G. Saxena *et al.*

Phys. Lett. B (2019)



View more references

---

## Cited by (9)

[Theoretical investigation of probable decay modes in potential nuclei  \$^{296,297}\text{Og}\$ ,  \$^{297}\text{119}\$ , and  \$^{298}\text{120}\$  for future experiments](#) ↗

2024, AIP Conference Proceedings

[Systematic study of cluster radioactivity in trans-lead nuclei with various versions of proximity potential formalisms](#) ↗

2024, Chinese Physics C

[Simple model for cluster radioactivity half-lives in trans-lead nuclei](#) ↗

2023, Chinese Physics C

[Cluster radioactivity from trans-tin to superheavy region using an improved empirical formula](#) ↗

2023, European Physical Journal A

[Decay properties of undetected superheavy nuclei with  \$Z > 110\$](#)

2023, Physica Scripta

[Alpha decay and cluster radioactivity investigation of actinide nuclei](#)

2023, International Journal of Modern Physics E



[View all citing articles on Scopus](#)

[View full text](#)

© 2023 Elsevier B.V. All rights reserved.



All content on this site: Copyright © 2024 Elsevier B.V., its licensors, and contributors. All rights are reserved, including those for text and data mining, AI training, and similar technologies. For all open access content, the Creative Commons licensing terms apply.



Full Text

Help

# Consumer Buying Behavior of Personal Care Product: A Comparative Study of Male and Female Users

**Dr. Neelu Lamba**  
**Researcher**

## **Abstract**

In today's world, the customer's demand and the power of the retailers is tremendously growing due to competitive environment and changing business. It is vital to have a sustainable relationship with customers for the survival and success of producers. Nowadays in the market a tremendous growth is experienced by the beauty products and has become one of the leading industries in the world. In Indian scenario too, the consumption and using of cosmetic products have increased rapidly. In our country, annually 15-20% of cosmetics market is reportedly growing. Comparing to other beauty products, demand for skin whitening is driving the trend. As consumer's awareness about their appearance and beauty results in the increasing demand of cosmetic and beauty products in the market.

Manufactures are likely to be aggressive to identify consumers' needs and requirements across all categories in cosmetics. Customers purchase products based on their preferences, needs and buying power.

Keywords: Beauty products, Cosmetics, Sustainable relationship

---

## Introduction

The word cosmetics is derived from the Greek word *kosmetikos* which means skilled at decorating. Cosmetics colloquially known as makeup or make-up are care substances used to enhance the appearance or odour of the human body. The U.S., the Food and Drug Administration (FDA), which regulates cosmetics, defines cosmetics as intended to be applied to the human body for cleansing, beautifying, promoting attractiveness, or altering the appearance without affecting the body's structure or functions.

According to Euromonitor, the cosmetics and toiletries is divided in 11 categories which are baby care, bath and shower products, deodorants, hair care, color cosmetic, men's grooming products, oral hygiene, fragrances, skin care, depilatories and sun care. The beauty and cosmetics sector is experiencing outstanding growth. It has been one of the world's leading industries. In India the cosmetic and toiletries market has developed rapidly. Our country cosmetics market is reportedly growing at 15-20% annually. Specifically, Demand for skin whitening products by men as well as women, is driving the trend, but other beauty products are not far behind (Alexander, 2011). The growth of cosmetics and beauty products markets have surged significantly as consumers are increasingly becoming aware about appearance, beauty grooming and choice of personal care products (Hamza salimkhraim). To meet consumers' needs, manufacturers are likely to be aggressive across all categories in cosmetics. However, the concentration of new product launches will be particularly visible in dynamic categories such as skin care and emerging categories such as mouthwashes/dental rinses.

Consumers buy products according to their needs, preferences and buying power. Consumer buying behaviour depends on his perception, self-concept, social and cultural background and their age and family cycle, their attitudes, beliefs values, motivation, personality, social class and many other factors that are both internal and external. Specifically, the attitudes of consumers can have a significant effect on buying behaviour. This paper examines the influence of attitude on cosmetics buying behaviour.

The higher paying jobs and an increase in the awareness of Indian women consumers towards the cosmeceutical products and to their benefits leads to the change in the mind setup of Indian women consumers and now they are ready to pay more for their cosmeceutical products. This impact of such changes is observed more in the middle class consumers. Numbers of women, especially from the middle-class population, have more disposable income leading to a change in cosmetic and skin care products consumption.

MAJOR INDIAN COSMETIC COMPANIES:-

In India, there is a complete range of cosmetic companies. It includes regional companies, national and MNCs. Hindustan Unilever leads the companies which is followed by Godrej consumer care, Procter & Gamble, Emami, Dabur and Calvin Care.

A broad list of these companies has been given below:-

1. Hul
2. Godrej Consumer Care.
3. Emami
4. ITC.
5. Dabur.
6. Procter & Gamble.
7. Calvin Care.
8. Hankel India Ltd.
9. Marico.
10. Reckitt Benckiser (India) Ltd.
11. Colgate Palmolive Pvt. Ltd.
12. Cholyil Pvt. Ltd.
13. J.K. Helen Couties Ltd.
14. J L Morison India Ltd.
15. Modi Ravlon Ltd.

### Literature Review

Dr. Anandrajan S., Sivagami T. (2016) studied consumer purchase decision behavior towards cosmetic marketing. The aim of the study was to study consumer behavior marketing of cosmetic products. They also want to know the influence of various media in motivating the consumer on a particular brand of cosmetics. Random sampling technique was used. Sample size was 200. Direct Interview method was adopted to collect data. Simple and bi-variate tables were prepared from information collected. Percentage Analysis was used for analyzing data. It found that reduction in price and attractive promotional schemes can attract more customers. The study concluded that cosmetics are not part of luxury. Manufacturers need to identify the need before marketing the cosmetic product.

Prof. Anute N., Dr. Deshmukh A. Prof. Khandagale A. (2015) studied consumer buying behaviour towards cosmetic products. The main aim of study was to study demographic profile of consumers and to find factors affecting consumer purchase decision. They also want to know the purchase pattern for cosmetic products. They found that majority of people use domestic cosmetic brand, television is most effective media to get information of cosmetics; quality of product is considered as most important factor for consumer purchase decision.

Dr. Nagananthi T., Mahalakshmi M. (2016) Studied consumers' brand preference and buying behavior of cosmetic products at Coimbatore city. The main aim of study was to identify consumers' brand preference towards cosmetic products and to determine the relationship of brand factors with demographic data. Primary data were collected from 200 samples through convenience sampling. Chi square test and one way ANOVA were used for data analysis. They found that personal care is one of the most important reasons for purchasing cosmetics. Himalaya herbals were the most important brand among consumers. Demographic factors influence consumer to purchase the cosmetics.

Banu Rekha M., Gokila K. (2015) studied consumer awareness, attitude and preference towards herbal cosmetic products with special reference to Coimbatore city. The main aim of study was to study consumer awareness towards herbal cosmetics, to identify the factors influencing the consumers to use herbal products. Descriptive research design was used with non-probability convenience sampling with 50 respondents of Coimbatore city. Karl Pearson's co-efficient of correlation, average ranking analysis and chi-square analysis were used for data analysis. They found that family income per month and spending for herbal products have positive correlation.

Quality was ranked as most important factor that influences consumers to purchase cosmetics. They concluded the research with a note that consumers believe that herbal cosmetics are not aluxury now and should be used by consumers.

Meremadi et al. 2013 deviced a model in which they studies the factors tha are considered by the consumer before buying of the personal care product. the aim was to build a mode that can increase the impact of advertising and can save the advertiser waste efforts and money. The model resulted n finding that major factors availability price quality and packaging mattered the most. The significant contribution of these factors was also found in the studies of Sakthivel, 2000. These factors were followed by genuineness and sales promotion technique.

## **CONSUMER BUYING BEHVAIOUR**

Consumer buying behavior is a decision process as well as an attitude of the people involved in purchasing and using products. Consumers make purchase decisions for buying small as well as large products. After recognizing a need or a want, consumers begin searching for products or services that fit their requirements.

Their decision depends upon many criteria. However, consumer purchases have happened much before their actual purchase. Marketing plays an important role in this. Marketing & Advertising have a strong positive impact on buying behavior of consumers, and they directly influence consumer buying a product from a company that she/he is well aware of. In ancient days, consumers were not bothered about the attributes before buying a product. But there comes a tremendous change in the consumer buying behavior of the 21st Century.

## **CUSTOMER PURCHASING DECISSION TOWARDS**

### **COSMETICS**

Before buying a product, Consumers walk or move through a series of steps. They emphasis the product in a way that it should satisfy their needs and have good quality with low or more affordable price, and should deliver them with value added features.

Consumer buying pattern differ when comes to the product quality, price, status, features, packaging. They mostly follow the rhythm of fashion and this changing preference affects their buying pattern. To identify and predict this changing behavior, marketers spend million rupees every year for market research. Currently the marketers are facing difficulties to understand and target the consumer's behaviour because they are flourished by the different varieties, affordable price and changing trend in the market of cosmetics. Consumer's preference is changing along with time.

Five stages of consumer buying behavior

There are mainly five steps/ stages in consumer decision process

#### **1. Recognition of problem**

Recognition of a problem starts when a customer realizes a problem or need. In all phases of life, humans are considered to be the customers of one company or another. And they have requirements and needs which have to be fulfilled at each phase. These requirements may be low or high involved ones. The first step of consumer buying behavior starts when the customer realizes that he needs or wants something.

#### **2. Search for information**

Once a customer identifies a problem, the next step is to adequate enough information to solve the problem. The extent of search for information depends on the customer's level of involvement in the purchase. The major source of information which influence the consumer's buying behavior are – Advertisements, Friends, Public, commercials and experience.

#### **3. Evaluation of alternatives**

Next stage of the consumer decision process is evaluating the alternatives. In this stage the Consumer will find the alternatives. They will compare and understand what they know about the alternative products and brands with what they considered the most.

#### 4. Purchase decision

After making a decision whether or not to purchase, a consumer might move through the first decision process as it plans and intends to purchase a particular brand or product.

#### 5. Outcome

In this step, after critically analyzing each stage in the decision process, final purchase is made.

### Suggestion and Conclusion

Cosmetic products are widely used by people now a days and hence the number of players enter into this business has increased considerably. Companies try to identify the consumer's attitude towards these cosmetic products so that they position their products to the particular category of people rather spending unnecessarily on non-targeted people. This study has provided a platform for the corporate to think on different dimensions what consumers prefer, which make them in deciding on Marketing Mix of different products, like modify the product or change in product design, fixing of price that better suit the targeted audience, appropriate promotion mix namely sales promotion, advertising, publicity and personal selling, and finally change in distribution channel.

The Indian cosmeceutical Industry is considered to be one of the fastest growing industries. The reason behind that might be the increase in the disposable income of the consumers and the increase in awareness towards their looks. In our study we discussed the skin care segment and within that our focus is on three types of cosmeceutical products and these are anti-aging products, anti-wrinkle products, anti-acne products, suns creams and fairness cream products. In the Indian market these products are popular and are growing with a healthy growth rate because of this reason more and more foreign players are also entering into the Indian market for this segment. Within the cosmeceutical product segment now a day it was observed that consumers preferences are going towards those cosmeceutical products which contain herbal ingredients or are made from the natural origin. Not only females but also males are concerned with this segment.

### Bibliography

- Dr. Anandrajan, S., Sivagami, T., (2016) Consumer Purchase Decision Behavior towards Cosmetics Marketing. Vol.I. Asia Pacific Journal of Research.
- Prof. Anute, N., Dr. Deshmukh, A., Prof. Khandagale, A., (2015) Consumer Buying Behaviour towards Cosmetics Products. Vol.03 Issue 07, International Journal in Management and Social Science.
- Dr. Nagananthi, T., Mahalaxmi, M., (2016) Consumers' Preference and Buying Behavior of Cosmetic Products at Coimbatore City. Vol 04 Issue 01. Inter-continental Journal of Marketing Research Review.
- Banu Rekha, M., Gokila, K., (2015) A study on Consumer Awareness, Attitude and Preference towards Herbal Cosmetics Products with special Reference to Coimbatore City. Vol 02 No-04, Page No. 96-100, International Journal of Interdisciplinary and multidisciplinary Studies.
- Meremadi, A., Sadeh, F., Borji, N., & Naji, S. (2013). Driving Factors and Effectiveness of Sales Promotion in Shopping Malls in Iran. In Proceedings of 6th International Business and Social Science Research Conference, Novotel Hotel World Trade Centre, Dubai, UAE.

# Decay properties of undetected superheavy nuclei with $Z > 110$

A. Jain<sup>1,2,3</sup>, P. K. Sharma<sup>4</sup>, S. K. Jain<sup>1</sup>, Dashty T. Akrawy<sup>5,6</sup>,  
and G. Saxena<sup>2,7,†</sup>

<sup>1</sup>Department of Physics, Manipal University Jaipur, Jaipur-303007, India

<sup>2</sup>Department of Physics (H&S), Govt. Women Engineering College, Ajmer-305002, India

<sup>3</sup>Department of Physics, S. S. Jain Subodh P.G.(Autonomous) College, Jaipur-302004, India

<sup>4</sup>Govt. Polytechnic College, Rajsamand-313324, India

<sup>5</sup>Physics Department, College of Science, Salahaddin University, Erbil 44001-Kurdistan, Iraq

<sup>6</sup>Becquerel Institute for Radiation Research and Measurements, Erbil, Kurdistan, Iraq

<sup>7</sup>Department of Physics, Faculty of Science, University of Zagreb, Bijenička c. 32, 10000 Zagreb, Croatia.

E-mail: †gauravphy@gmail.com

April 2023

**Abstract.** A comprehensive study of favoured and unfavoured  $\alpha$ -decay, cluster decay, weak-decay along with spontaneous fission in undetected superheavy nuclei within the range for proton number  $111 \leq Z \leq 118$  and neutron number  $161 \leq N \leq 192$  is performed. Half-lives for various mentioned decays are estimated with good accuracy on the basis of NUBASE2020 and are found in excellent match with the known half-lives.  $\alpha$ -decay mode is found most probable in this wide range and correspondingly potential  $\alpha$ -decay chains are reckoned. Peculiarly, the chances of cluster emission, as well as weak-decay, are also anticipated in this region of the periodic chart which open new pathways of detection of superheavy nuclei.

*Keywords:*  $\alpha$ -decay; Cluster decay; Weak-decay; Half-lives; Superheavy Nuclei.

## 1. Introduction

Nuclei with proton number  $Z > 104$ , referred as superheavy nuclei (SHN), manifest the most exciting and challenging arena in the field of nuclear physics. Experimental facilities like GSI, Darmstadt [1, 2] and RIKEN, Japan [3] are available to synthesize SHN by cold-fusion reactions of  $^{208}\text{Pb}$  or  $^{209}\text{Bi}$  by beams of nuclei with mass number  $A > 50$  [4]. In the other experimental facility like Dubna laboratory, Oganessian *et al* have successfully synthesized new SHN with  $Z = 112 - 118$  [5, 6] by the hot fusion

reaction with  $^{48}\text{Ca}$  beam and various actinide targets. The last synthesized element up to so far has proton number  $Z=118$  [7], nevertheless, many of the SHN are still undetected in the laboratory for which several experimental attempts have already been aimed [8–11]. In this connection, recently, few experiments have been performed for the future possibilities of synthesizing new elements with  $Z=119$  and  $Z=120$  [12].

The SHN are highly unstable and can break via various decays viz.  $\alpha$ -decay, spontaneous fission, cluster decay, weak-decay, etc. Among these decay modes,  $\alpha$ -decay plays a crucial role in the identification of SHN in the laboratories through  $\alpha$ -decay chains [13, 14]. To plan experiments related to the identification of SHN, various theoretical inputs are required out of which estimation of  $\alpha$ -decay half-lives is most pivotal. Various theoretical methods and models have been employed to estimate  $\alpha$ -decay half-lives such as Gamow-like model (GLM) [15], fission-like model [16], liquid drop model [17, 18] with its modifications [19–22], and Coulomb and proximity potential model (CPPM) [23, 24].

The half-lives for  $\alpha$ -transition can also be calculated from various empirical formulas based on Geiger-Nuttall law. There are several empirical or semi-empirical formulas [25–31] along with their refitted or modified versions [32–37] which are widely being used to estimate  $\alpha$ -decay half-lives in different regions of the periodic chart. In the present study, we have estimated  $\alpha$ -decay half-lives of 146 (even-even and odd-A) undetected SHN within the range  $111 \leq Z \leq 118$  and  $161 \leq N \leq 192$  by using one of the recent modified empirical formula, i.e. new modified Horoi formula (NMHF) [38], after testing its accuracy on the 424 experimental half-lives corresponding to ground to ground favoured and unfavoured  $\alpha$ -transitions. We have also compared our theoretical half-lives with that of the experimental half-lives of the known  $\alpha$ -decay chains [6, 39–43] in the above mentioned range. These estimates from NMHF are found in excellent match and therefore the formula is utilized to predict half-lives of the future potential SHN related to the already known or undetected decay chains.

Another decay mode, i.e. spontaneous fission (SF) which was firstly discussed by Bohr and Wheeler [44] and experimentally verified by Flerov and Petrjak [45], is also found to be equally decisive in  $Z \geq 90$  nuclei [46, 47]. The first theoretical try to estimate the half-lives of SF was done by Swiatecki in 1955 with liquid drop model [48] and uptill now many empirical formulas are proposed to compute half-life of SF [49–56]. Recently, the Bao formula [51] has been modified (modified Bao formula (MBF) [36]) using the latest evaluated nuclear properties table NUBASE2020 [43] and is used in the present work for the calculation of half-lives of SF.

The possibility of the heavy particle radioactivity (cluster decay) was also predicted in the heavy and superheavy nuclei [57–61]. Discussion of cluster decay started by Sandulescu *et al* in 1980 [62] and firstly observed by Rose and Jones [63]. Cluster decay refers to the decay of a fragment from the parent nucleus. Decay of fragments like  $^{20}\text{O}$ ,  $^{22,24-26}\text{Ne}$ ,  $^{28-30}\text{Mg}$ , and  $^{32,34}\text{Si}$  [64, 65] have been already observed experimentally for the nuclei with  $Z$  ranging from 87 to 96. The decay of such clusters is firmly connected to closed shell daughters as  $^{208}\text{Pb}$  or its neighbours, and therefore predominantly diverge



towards Pb isotopes. In superheavy nuclei, the probability of heavy clusters viz. Se, Br, Kr, Rb, Sr, Y, Zr, Nb, Mo etc. is already speculated in several Refs. [66–73]. To invoke the competition of various decay modes, we have comprehensively investigated cluster decay half-lives by using universal decay law (UDL) [74] for all the possible isotopes between  $111 \leq Z \leq 118$  and  $161 \leq N \leq 192$ . The clusters considered for these nuclei are chosen to result Pb isotopes ( $Z=82$ ) as possible daughter nuclei which lead to the emitting clusters ranging from  $Z=29$  to  $Z=36$ .

One more decay mode is the weak-decay ( $\beta^-/\beta^+$ /EC-decay) [75–80] which is a principal decay mode in a broad region of the periodic chart, however, is rarely found to exist in the superheavy region. Despite this fact, the possibility of weak-decay is also contemplated in the superheavy region by several Refs. [35, 81–83]. In the present study of SHN, we have also examined the weak-decay that is found somewhat apparent in few of the SHN consist of the isotopes of Rg, Cn, Nh, and Fl. The half-lives of weak-decay are calculated by using an empirical formula given by Fiset and Nix [84] and recently proven to be simple and successful in several SHN [35, 85, 86].

Finally, we have calculated half-lives and the competition of all probable decay modes considering them on equal footing, by using optimally chosen respective empirical formulas. The sensitivity of these half-lives on the uncertainties of  $Q$ -values are also evaluated by using available experimental uncertainties [6, 39–42, 87]. Since, the present work is focussed on superheavy nuclei where the role of uncertainties in  $Q$ -values becomes very crucial, therefore, we have evaluated theoretical uncertainties in  $Q$ -values of  $\alpha$ -decay taken from WS4 mass model [88] by using 69 experimental data [87] for  $Z \geq 106$ . Due to unavailability or sufficient experimental data of  $Q$ -values for  $\beta^-$ -decay, EC decay, and cluster decay, we have calculated the respective uncertainties in theoretical  $Q$ -values by using 113, 78, and 73 experimental data [64, 65, 87] for  $Z > 82$ . The results of half-lives of each decay are found in an excellent match with the available half-lives and hence utilised to estimate the half-lives of several unknown (undetected) nuclei within the range  $111 \leq Z \leq 118$  and  $161 \leq N \leq 192$ . This kind of contest of several decay modes after their accurate estimation of half-lives is an intriguing platform for the experiments eyeing up for the detection of new SHN.

## 2. Formalism

### 2.1. $\alpha$ -decay

For the selection of  $\alpha$ -decay half-lives formula, we have tested few recently fitted/modified empirical/semiempirical formulas [25, 34, 37, 38, 60, 89–98] and the comparison among these formulas is shown in Table 1. For the comparison, we use root mean square error (RMSE) and uncertainty ( $u$ ), which are calculated by using the following formulas:

$$RMSE = \sqrt{\frac{1}{N_{nucl}} \sum_{i=1}^{N_{nucl}} (\log T_{th}^i - \log T_{exp}^i)^2} \quad (1)$$

$$u = \sqrt{\frac{\sum(x_i - v)^2}{N_{nucl}(N_{nucl} - 1)}} \quad (2)$$

here,  $N_{nucl}$  is the total number of data.  $T_{th}^i$  and  $T_{exp}^i$  are the theoretical and experimental values of half-life for  $i^{th}$  data point, respectively.  $x_i$  is the  $i^{th}$  reading of data set,  $v$  is the mean of the data set. We found that NMHF has minimum RMSE (0.56) and uncertainties ( $\pm 0.09$  s) as tested it on 40 experimental data within the range  $111 \leq Z \leq 118$  and  $161 \leq N \leq 192$  while compared to other similar, latest fitted and known formulas such as Royer2020 [92], MYQZR2019 [91], Akrawy2018 [93], Modified RenB2019 [89], MRF2018 [95], DK2018 [95], Modified Budaca Formula (MBuF2022) [37], UF2022 [96], IUF2022 [97], ISEF2022 [98], new modified Sobiczewski formula (NMSF2021) [38] and new modified Manjunatha formula (NMMF2021) [38].

**Table 1.** Comparison of RMSE and uncertainties (in second) for the different tested formulae on 40 experimental data within the range  $111 \leq Z \leq 118$  and  $161 \leq N \leq 192$ .

Formula	RMSE	Uncertainty	Formula	RMSE	Uncertainty
NMHF2021 [38]	0.56	$\pm 0.09$	MUDL2019 [34]	1.03	$\pm 0.16$
QF2021 [25]	0.70	$\pm 0.11$	NMSF2021 [38]	1.12	$\pm 0.12$
IUF2022 [97]	0.76	$\pm 0.11$	MYQZR2019 [91]	1.20	$\pm 0.15$
MTNF2021 [25]	0.80	$\pm 0.12$	Soylu2021 [60]	1.25	$\pm 0.13$
NRenA2019 [89]	0.81	$\pm 0.12$	DK2018 [93]	1.33	$\pm 0.16$
IRF2022 [90]	0.84	$\pm 0.12$	MBuF2022 [37]	1.41	$\pm 0.17$
ISEF2022 [98]	0.95	$\pm 0.13$	NMMF2021 [38]	1.43	$\pm 0.15$
Royer2020 [92]	0.95	$\pm 0.14$	Akrawy2018 [94]	1.56	$\pm 0.19$
MSLB2019 [91]	0.95	$\pm 0.14$	MRenB2019 [89]	1.81	$\pm 0.23$
UF2022 [96]	1.00	$\pm 0.15$	MRF2018 [95]	1.88	$\pm 0.21$

Consequently, the present calculations of  $\alpha$ -decay half-lives are performed by using NMHF [38] which incorporates the terms related to (i) angular momentum taken away by the  $\alpha$ -particle and (ii) asymmetry of the parent nucleus. This formula is found to produce precise  $\alpha$ -decay half-lives for full periodic chart ranging from heavy to superheavy nuclei [38]. The formula is given by:

$$\log_{10} T_{1/2}^{NMHF}(s) = (a\sqrt{\mu} + b)[(Z_\alpha Z_d)^{0.6} Q_\alpha^{-1/2} - 7] + (c\sqrt{\mu} + d) + eI + fI^2 + gl(l + 1) \quad (3)$$

where the coefficients a, b, c, d, e, f, and g obtained by fitting are 107.0131, -206.5398, -160.6152, 309.6165, 19.7237, -31.1655, and 0.0238, respectively. Also,  $Z_d$  represents atomic number of daughter nucleus,  $\mu$  is the reduced mass which is given by  $A_d A_\alpha / (A_d + A_\alpha)$  where  $A_d$  and  $A_\alpha$  are the mass number of daughter nucleus and  $\alpha$ -particle, and  $I$  ( $= (N-Z)/A$ ) is the nuclear isospin asymmetry. For this work, if the  $Q_\alpha$  values are not available in atomic mass evaluation tables AME2020 [87] then the theoretical  $Q_\alpha$  values from WS4 mass model [88] are used which are found quite accurate in comparison to few other mass models [25]. The minimum angular momentum  $l$  of  $\alpha$ -particle, which distinguishes between favoured and unfavoured  $\alpha$ -transitions, can be

obtained by standard selection rules [99] using spin and parity values of the parent and daughter nuclei.

$$l = \begin{cases} \Delta_j & \text{for even } \Delta_j \text{ and } \pi_p = \pi_d \\ \Delta_j + 1 & \text{for even } \Delta_j \text{ and } \pi_p \neq \pi_d \\ \Delta_j & \text{for odd } \Delta_j \text{ and } \pi_p \neq \pi_d \\ \Delta_j + 1 & \text{for odd } \Delta_j \text{ and } \pi_p = \pi_d \end{cases} \quad (4)$$

where  $\Delta_j = |j_p - j_d|$  with  $j_p, \pi_p, j_d, \pi_d$ , being the spin and parity values of the parent and daughter nuclei, respectively. For the present paper, spin and parities are taken from Ref. [43], if available, otherwise taken theoretically from Ref. [100].

### 2.2. Spontaneous fission (SF)

In this part of the periodic chart, spontaneous fission (SF) is also found as probable as that of  $\alpha$ -decay, which eventually ascertained crucial for the planning of experiments towards the detection of new elements/isotopes through  $\alpha$ -decay chains. Therefore, the contest with SF has also accounted by testing several available empirical formulas on the experimentally known half-lives [43] of SF for the nuclei  $Z > 110$ . There are only 5 nuclei ( $^{281}\text{Rg}$ ,  $^{282,284}\text{Cn}$ , and  $^{284,286}\text{Fl}$ ) with known experimental half-lives of their SF and are used for probing the accuracy of RenA formula [49], formula by Xu *et al* [50], modified Swiatecki formula [51], semi-empirical formula proposed by Santhosh *et al* [52], Soylu formula [53], modified Santhosh formula [54] and Modified Bao formula (MBF) [36]. It is found that among the mentioned formulas, MBF estimates the half-lives more accurately as the RMSE values for available experimental 35 data (all) and 5 data (for the range  $111 \leq Z \leq 118$ ) [87] are found minimum i.e. 1.42 and 1.86, respectively. Therefore, the MBF formula is used in the present work which is expressed as below [36]:

$$\log_{10} T_{1/2}^{SF}(s) = c_1 + c_2 \left( \frac{Z^2}{(1 - kT^2)A} \right) + c_3 \left( \frac{Z^2}{(1 - kT^2)A} \right)^2 + c_4 E_{s+p} \quad (5)$$

here  $k=2.6$  and other coefficients are  $c_2 = -37.0510$ ,  $c_3 = 0.3740$ ,  $c_4 = 3.1105$ . The values of  $c_1$  for various sets of nuclei are  $c_1(\text{e-e}) = 893.2645$ ,  $c_1(\text{e-o}) = 895.4154$ ,  $c_1(\text{o-e}) = 896.8447$  and  $c_1(\text{o-o}) = 897.0194$ .

### 2.3. Cluster decay

To calculate the logarithmic half-lives of cluster emission, there are various available empirical formulas viz. Royer formula [101], the formula given by Balasubramaniam *et al* (BKAG) [102], Horoi formula [103], the formula by Ren *et al* [30], NRDX formula [104], universal decay law (UDL) [74], universal curve formula (UNIV) [105], Tavares-Medeiros formula (TM) [106], formula by Soylu [107], improved unified formula (IUF) [97], improved semi-empirical formula (ISEF) [98] and some recent modified formulas [108]. Considering the absence of experimental data of cluster radioactivity in superheavy region, only UDL formula among the above mentioned formulas demonstrates for the existence of a competitive relationship between  $\alpha$ -decay and cluster radioactivity in

superheavy region, due to its treatment as both the preformation model and the fission-like mechanisms [109], and henceforth justifies its use for further predictions. The UDL formula is represented by:

$$\log_{10}T_{1/2}^{UDL}(s) = aZ_cZ_d\sqrt{\frac{\mu}{Q}} + b[\mu Z_cZ_d(A_c^{1/3} + A_d^{1/3})]^{1/2} + c \quad (6)$$

where a, b and c are the fitting coefficients and the values of these coefficients are 0.3949, -0.3693 and -23.7615, respectively.  $\mu$  is reduced mass and calculated by the formula given as  $A_dA_c/(A_d + A_c)$  where d and c subscripts represent quantities related to daughter nucleus and emitted cluster, respectively.

#### 2.4. Weak-decay

To look into the possibility of weak-decay, we have picked up experimental half-lives of  $\beta^-$ -decay ( $\beta$ -decay) of 103 nuclei and  $\beta^+$ /EC decay of 99 nuclei, available for  $Z > 82$  in NUBASE2020 [43]. To estimate the precise half-lives of weak-decay, we have explored a few empirical formulas viz. Fiset and Nix formula [84], Zhang formula [77], Modified Zhang formula [78] and a recent formula modified by Sobhani *et al* [79] along with the results of half-lives obtained by using quasi-particle random-phase approximation (QRPA) [80]. After this analysis for the nuclei  $Z > 82$  the results of Fiset and Nix formula are found with minimum RMSE which endorse the use of this formula for the estimation of half-lives of weak-decay in superheavy nuclei, as has been demonstrated in Refs. [35, 85, 86]. The adopt formula is given by:

$$T_{\beta}(s) = \frac{540m_e^5}{\rho(W_{\beta}^6 - m_e^6)} \times 10^{5.0} \quad (7)$$

This Eqn. (7) is only logical for  $W_{\beta} \gg m_e$ . For the average density of states  $\rho$  in the daughter nucleus, we use the empirical results given by Seeger *et al* [110], from which  $\rho$  has values 2.73 for even-even, 15 for odd-odd nuclei and 8.6 for odd  $A$  (Mass number) nuclei, respectively. The formula for electron capture (EC) is given by:

$$T_{EC}(s) = \frac{9m_e^2}{2\pi(\alpha Z_K)^{2s+1}\rho [Q_{EC} - (1-s)m_e]^3} \left(\frac{2R_0}{\hbar c/m_e}\right)^{2-2s} \times \frac{\Gamma(2s+1)}{1+s} \times 10^{6.5} \quad (8)$$

In Eqn. (8),  $Z_K$  is the effective charge of the parent nucleus for an electron in the K-shell; it is approximately given by  $Z_K = Z_P - 0.35$ . The energy  $W_{\beta}$  is sum of energy of the emitted  $\beta$ -particle and its rest mass  $m_e$ , i.e.  $W_{\beta} = Q_{\beta} + m_e$ . Also, the quantity  $s$  is given by  $s = [1 - (\alpha Z_K)^2]^{\frac{1}{2}}$  and represents the rest mass of an electron minus its binding energy in the K-shell, in units of  $m_e$ . The quantity  $\alpha$  is the fine-structure constant, and  $R_0$  is the nuclear radius, which is taken to be  $R_0 = 1.2249A^{\frac{1}{3}} fm$ .

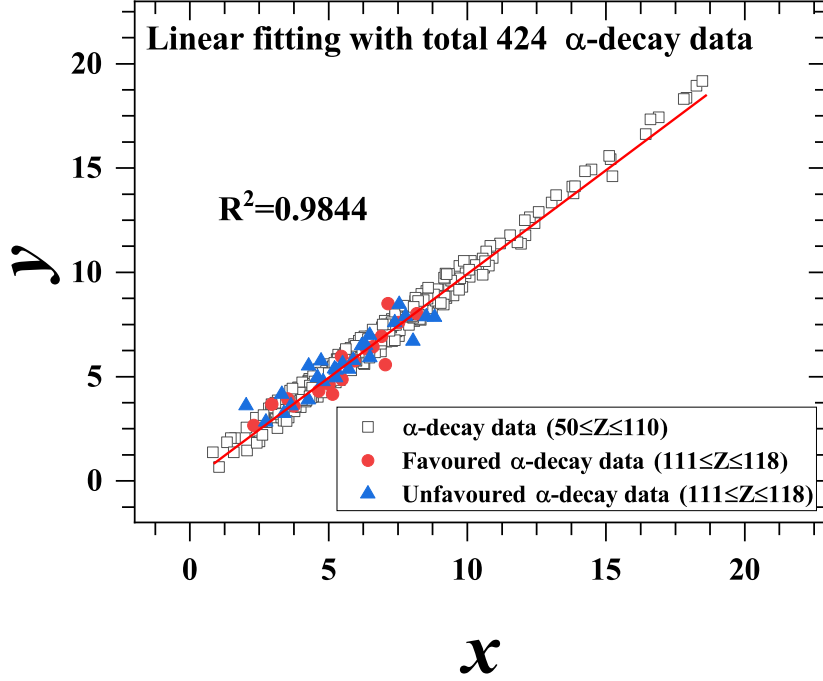


**Figure 1.** (Colour online) Linear fitting using 424 experimental data in which x-axis shows  $x=(a\sqrt{\mu}+b)[(Z_{\alpha}Z_d)^{0.6}Q_{\alpha}^{-1/2}-7]$  and y-axis is  $y=\log_{10}T_{1/2}^{Exp.}-(c\sqrt{\mu}+d)-eI-fI^2-gl(l+1)$ .

### 3. Result and discussion

#### 3.1. $\alpha$ -decay and decay chains

In the present work, firstly we have looked into the  $\alpha$ -decay half-lives using the recent proposed NMHF formula [38] mentioned in Eqn. (3) that has been found fairly accurate in the considered all the regions of periodic chart. We test this formula in considered superheavy region (with 17 favoured and 26 unfavoured available data for  $Z>110$ ) in Fig. 1, where we have plotted the variation in the quantity  $y=\log_{10}T_{1/2}^{Exp.}-(c\sqrt{\mu}+d)-eI-fI^2-gl(l+1)$  with the  $Q_{\alpha}$  dependent terms of the formula for a total of 424 favoured and unfavoured  $\alpha$ -decay data. Almost all the points are found very near to the straight line which lead to  $R^2=0.9844$  indicating a statistical measure of fit. It reflects an exemplary linear dependence of experimental  $\alpha$ -decay half-lives on  $Q_{\alpha}$  dependent terms for the NMHF formula and it is quite satisfactory to note from Fig. 1 that the estimated half-lives for the considered range (for the isotopes from Rg to Og) match reasonably well with the experimental known half-lives. The points which are quite off in Fig. 1 are due to the large uncertainties in half-lives for example:  $^{275,279}\text{Rg}$ ,  $^{284,288}\text{Cn}$ ,  $^{281,289}\text{Nh}$ ,  $^{295}\text{Og}$  etc. Hence, Fig. 1 vindicates the use of NMHF formula in this particular range of the nuclei ( $111\leq Z\leq 118$  and  $161\leq N\leq 192$ ).

In this connection, we have estimated half-lives for the ground to ground favoured  $\alpha$ -transition (for which  $l = 0$ ) from Cn isotopes to Og isotopes which are shown in

Table 2.  $Q_\alpha$ -values are taken from WS4 mass model [88] (mentioned in second and eighth column) due to its accuracy, judged over various other theories viz. relativistic mean-field theory (RMF) [85, 111–113], Finite Range Droplet Model (FRDM) [114], Relativistic continuum Hartree-Bogoliubov (RCHB) [115] etc. for almost 1500 nuclei in Ref. [25]. We have also calculated uncertainties in unknown  $Q_\alpha$ -values taken from WS4 mass model using Eqn. (2) with the help of 69 experimental data in superheavy region [87]. Remarkably, the uncertainties in  $Q_\alpha$ -values are found only  $\pm 0.04$  MeV using which the half-lives are tabulated in sixth and twelfth column of the table along with their respective uncertainties.

In a similar manner, the half-lives (including uncertainties) are estimated for ground to ground unfavoured  $\alpha$ -transition (for which  $l \neq 0$ ) which are mentioned in Table 3. The nuclei quoted in these tables (even-even and odd-A) are still undetected for which the theoretical spin parities for parent ( $j_p$ ) and daughter ( $j_d$ ) are taken from Ref. [100] From these Tables 2 and 3, it is noticeable that estimated half-lives are within the experimental reach and expected to be useful for the future experiments.

As mentioned above, detection of SHN is mainly governed by observation of  $\alpha$ -decay chains, therefore, matching of theoretical calculations with already observed decay chains is a prerequisite before estimating theoretical  $\alpha$ -decay chains for undetected nuclei. With this in view, in Fig. 2, we have compared  $\alpha$ -decay half-lives from the known decay chains [6, 39–42] of various nuclei in between Rg and Og elements. The theoretical half-lives from the NMHF formula are found in excellent match which once again demonstrate its accuracy. The error bars are also shown with the theoretical half-lives by using the uncertainties in experimental  $Q_\alpha$ -values [6, 39–42]. Additionally, in the each panel of Fig. 2 half-life of most probable nucleus adjacent to the known decay chains [6, 39–42] (shown by star symbols) or known nuclei as per NUBASE2020 [43] (shown by square symbols) is shown by connecting dotted lines. The SF half-life calculated by using Eqn. (5) for next probable nucleus is also depicted by blue circle which indicates quite larger value comparative to  $\alpha$ -decay half-life, and hence signifies the greater probability of  $\alpha$ -decay as comparison to SF in such nucleus. These predictions leading to the potential upper parts of known decay chains are also found consistent with the estimation by NUBASE2020 [43]. Therefore, most probable nuclei which are proposed here for the future detection in relation with known decay chains are:  $^{298}_{120}$ ,  $^{297}_{119}$ ,  $^{297,296,295}_{\text{Og}}$ ,  $^{295,291}_{\text{Ts}}$ ,  $^{295,294,289}_{\text{Lv}}$ ,  $^{293,285,283}_{\text{Mc}}$ ,  $^{283,282,281,280}_{\text{Fl}}$  and  $^{277}_{\text{Nh}}$ . Possible reactions resulting these probable candidates along with cross-section will be discussed in our subsequent article.

There is more possible expansion of regions belonging to  $\alpha$ -decay as well as potential  $\alpha$ -decay chains which can also be investigated within the same approach as mentioned above. With this in view, we have calculated  $\alpha$ -decay half-lives (using Eqn. (3)) in conjunction with SF half-lives (using Eqn. (5)) for the nuclei within  $111 \leq Z \leq 118$  and  $161 \leq N \leq 192$ . Both half-lives are calculated for various possible decay chains for the mentioned range and are tabulated in Appendix for the readers. The uncertainties in theoretical half-lives of  $\alpha$ -decay are calculated with the help of uncertainties in

**Table 2.**  $\alpha$ -decay half-lives for ground to ground favoured transitions in undetected nuclei in the range  $112 \leq Z \leq 118$ . These half-lives are calculated by NMHF formula for which the  $Q_\alpha$ -values and spin-parities are taken from Refs. [88] and [100], respectively. The uncertainties in  $Q_\alpha$ -values are  $\pm 0.04$  MeV.

Favoured $\alpha$ -Transition	$Q_\alpha$ (MeV)	$j_p$	$j_d$	$l$	$\log_{10}T_{1/2}$ (s)	Favoured $\alpha$ -Transition	$Q_\alpha$ (MeV)	$j_p$	$j_d$	$l$	$\log_{10}T_{1/2}$ (s)
$^{274}\text{Cn} \rightarrow ^{270}\text{Ds}$	11.55	$0^+$	$0^+$	0	$-3.83 \pm 0.08$	$^{296}\text{Cn} \rightarrow ^{292}\text{Ds}$	7.72	$0^+$	$0^+$	0	$6.53 \pm 0.14$
$^{289}\text{Cn} \rightarrow ^{285}\text{Ds}$	9.05	$1/2^+$	$1/2^+$	0	$2.22 \pm 0.11$	$^{297}\text{Cn} \rightarrow ^{293}\text{Ds}$	8.29	$1/2^+$	$1/2^+$	0	$4.61 \pm 0.13$
$^{290}\text{Cn} \rightarrow ^{286}\text{Ds}$	8.87	$0^+$	$0^+$	0	$2.72 \pm 0.12$	$^{298}\text{Cn} \rightarrow ^{294}\text{Ds}$	8.79	$0^+$	$0^+$	0	$3.07 \pm 0.12$
$^{291}\text{Cn} \rightarrow ^{287}\text{Ds}$	8.59	$1/2^+$	$1/2^+$	0	$3.59 \pm 0.12$	$^{300}\text{Cn} \rightarrow ^{296}\text{Ds}$	8.43	$0^+$	$0^+$	0	$4.18 \pm 0.13$
$^{292}\text{Cn} \rightarrow ^{288}\text{Ds}$	8.28	$0^+$	$0^+$	0	$4.55 \pm 0.13$	$^{302}\text{Cn} \rightarrow ^{298}\text{Ds}$	7.51	$0^+$	$0^+$	0	$7.39 \pm 0.15$
$^{294}\text{Cn} \rightarrow ^{290}\text{Ds}$	8.07	$0^+$	$0^+$	0	$5.27 \pm 0.13$	$^{304}\text{Cn} \rightarrow ^{300}\text{Ds}$	7.31	$0^+$	$0^+$	0	$8.17 \pm 0.16$
$^{275}\text{Nh} \rightarrow ^{271}\text{Rg}$	11.93	$9/2^-$	$9/2^-$	0	$-4.36 \pm 0.07$	$^{277}\text{Nh} \rightarrow ^{273}\text{Rg}$	12.20	$3/2^-$	$3/2^-$	0	$-4.80 \pm 0.07$
$^{276}\text{Fl} \rightarrow ^{272}\text{Cn}$	12.32	$0^+$	$0^+$	0	$-4.86 \pm 0.07$	$^{296}\text{Fl} \rightarrow ^{292}\text{Cn}$	8.56	$0^+$	$0^+$	0	$4.25 \pm 0.12$
$^{278}\text{Fl} \rightarrow ^{274}\text{Cn}$	12.52	$0^+$	$0^+$	0	$-5.17 \pm 0.07$	$^{298}\text{Fl} \rightarrow ^{294}\text{Cn}$	8.27	$0^+$	$0^+$	0	$5.21 \pm 0.13$
$^{280}\text{Fl} \rightarrow ^{276}\text{Cn}$	12.23	$0^+$	$0^+$	0	$-4.62 \pm 0.07$	$^{300}\text{Fl} \rightarrow ^{296}\text{Cn}$	9.56	$0^+$	$0^+$	0	$1.45 \pm 0.11$
$^{282}\text{Fl} \rightarrow ^{278}\text{Cn}$	11.38	$0^+$	$0^+$	0	$-2.98 \pm 0.08$	$^{302}\text{Fl} \rightarrow ^{298}\text{Cn}$	9.29	$0^+$	$0^+$	0	$2.20 \pm 0.11$
$^{292}\text{Fl} \rightarrow ^{288}\text{Cn}$	8.95	$0^+$	$0^+$	0	$3.01 \pm 0.12$	$^{304}\text{Fl} \rightarrow ^{300}\text{Cn}$	8.43	$0^+$	$0^+$	0	$4.77 \pm 0.13$
$^{293}\text{Fl} \rightarrow ^{289}\text{Cn}$	8.78	$1/2^+$	$1/2^+$	0	$3.52 \pm 0.12$	$^{306}\text{Fl} \rightarrow ^{302}\text{Cn}$	8.26	$0^+$	$0^+$	0	$5.35 \pm 0.13$
$^{294}\text{Fl} \rightarrow ^{290}\text{Cn}$	8.71	$0^+$	$0^+$	0	$3.75 \pm 0.12$	-	-	-	-	-	-
$^{297}\text{Mc} \rightarrow ^{293}\text{Nh}$	9.59	$5/2^-$	$5/2^-$	0	$1.56 \pm 0.11$	$^{303}\text{Mc} \rightarrow ^{299}\text{Nh}$	10.23	$5/2^-$	$5/2^-$	0	$0.02 \pm 0.10$
$^{299}\text{Mc} \rightarrow ^{295}\text{Nh}$	9.59	$5/2^-$	$5/2^-$	0	$1.60 \pm 0.11$	$^{305}\text{Mc} \rightarrow ^{301}\text{Nh}$	9.31	$5/2^-$	$5/2^-$	0	$2.40 \pm 0.11$
$^{301}\text{Mc} \rightarrow ^{297}\text{Nh}$	10.80	$5/2^-$	$5/2^-$	0	$-1.31 \pm 0.09$	-	-	-	-	-	-
$^{278}\text{Lv} \rightarrow ^{274}\text{Fl}$	12.96	$0^+$	$0^+$	0	$-5.58 \pm 0.07$	$^{296}\text{Lv} \rightarrow ^{292}\text{Fl}$	10.89	$0^+$	$0^+$	0	$-1.35 \pm 0.09$
$^{280}\text{Lv} \rightarrow ^{276}\text{Fl}$	12.95	$0^+$	$0^+$	0	$-5.52 \pm 0.07$	$^{298}\text{Lv} \rightarrow ^{294}\text{Fl}$	10.77	$0^+$	$0^+$	0	$-1.06 \pm 0.09$
$^{282}\text{Lv} \rightarrow ^{278}\text{Fl}$	12.37	$0^+$	$0^+$	0	$-4.50 \pm 0.07$	$^{300}\text{Lv} \rightarrow ^{296}\text{Fl}$	10.92	$0^+$	$0^+$	0	$-1.36 \pm 0.09$
$^{284}\text{Lv} \rightarrow ^{280}\text{Fl}$	11.83	$0^+$	$0^+$	0	$-3.46 \pm 0.08$	$^{301}\text{Lv} \rightarrow ^{297}\text{Fl}$	11.58	$1/2^+$	$1/2^+$	0	$-2.73 \pm 0.08$
$^{286}\text{Lv} \rightarrow ^{282}\text{Fl}$	11.31	$0^+$	$0^+$	0	$-2.40 \pm 0.08$	$^{302}\text{Lv} \rightarrow ^{298}\text{Fl}$	12.19	$0^+$	$0^+$	0	$-3.89 \pm 0.07$
$^{287}\text{Lv} \rightarrow ^{283}\text{Fl}$	11.28	$3/2^+$	$3/2^+$	0	$-2.32 \pm 0.08$	$^{304}\text{Lv} \rightarrow ^{300}\text{Fl}$	11.47	$0^+$	$0^+$	0	$-2.47 \pm 0.08$
$^{288}\text{Lv} \rightarrow ^{284}\text{Fl}$	11.29	$0^+$	$0^+$	0	$-2.32 \pm 0.08$	$^{306}\text{Lv} \rightarrow ^{302}\text{Fl}$	10.31	$0^+$	$0^+$	0	$0.10 \pm 0.10$
$^{294}\text{Lv} \rightarrow ^{290}\text{Fl}$	10.66	$0^+$	$0^+$	0	$-0.88 \pm 0.09$	$^{308}\text{Lv} \rightarrow ^{304}\text{Fl}$	9.53	$0^+$	$0^+$	0	$2.08 \pm 0.11$
$^{295}\text{Lv} \rightarrow ^{291}\text{Fl}$	10.77	$1/2^+$	$1/2^+$	0	$-1.10 \pm 0.09$	-	-	-	-	-	-
$^{280}\text{Og} \rightarrow ^{276}\text{Lv}$	13.71	$0^+$	$0^+$	0	$-6.43 \pm 0.06$	$^{296}\text{Og} \rightarrow ^{292}\text{Lv}$	11.75	$0^+$	$0^+$	0	$-2.73 \pm 0.08$
$^{282}\text{Og} \rightarrow ^{278}\text{Lv}$	13.49	$0^+$	$0^+$	0	$-6.05 \pm 0.06$	$^{297}\text{Og} \rightarrow ^{293}\text{Lv}$	12.10	$1/2^+$	$1/2^+$	0	$-3.40 \pm 0.08$
$^{284}\text{Og} \rightarrow ^{280}\text{Lv}$	13.23	$0^+$	$0^+$	0	$-5.58 \pm 0.07$	$^{298}\text{Og} \rightarrow ^{294}\text{Lv}$	12.18	$0^+$	$0^+$	0	$-3.53 \pm 0.07$
$^{285}\text{Og} \rightarrow ^{281}\text{Lv}$	13.07	$1/2^+$	$1/2^+$	0	$-5.31 \pm 0.07$	$^{300}\text{Og} \rightarrow ^{296}\text{Lv}$	11.96	$0^+$	$0^+$	0	$-3.08 \pm 0.08$
$^{286}\text{Og} \rightarrow ^{282}\text{Lv}$	12.92	$0^+$	$0^+$	0	$-5.03 \pm 0.07$	$^{302}\text{Og} \rightarrow ^{298}\text{Lv}$	12.04	$0^+$	$0^+$	0	$-3.21 \pm 0.08$
$^{287}\text{Og} \rightarrow ^{283}\text{Lv}$	12.80	$1/2^+$	$1/2^+$	0	$-4.81 \pm 0.07$	$^{304}\text{Og} \rightarrow ^{300}\text{Lv}$	13.12	$0^+$	$0^+$	0	$-5.13 \pm 0.07$
$^{288}\text{Og} \rightarrow ^{284}\text{Lv}$	12.62	$0^+$	$0^+$	0	$-4.47 \pm 0.07$	$^{306}\text{Og} \rightarrow ^{302}\text{Lv}$	12.48	$0^+$	$0^+$	0	$-3.99 \pm 0.07$
$^{289}\text{Og} \rightarrow ^{285}\text{Lv}$	12.59	$3/2^+$	$3/2^+$	0	$-4.41 \pm 0.07$	$^{308}\text{Og} \rightarrow ^{304}\text{Lv}$	11.20	$0^+$	$0^+$	0	$-1.47 \pm 0.09$
$^{290}\text{Og} \rightarrow ^{286}\text{Lv}$	12.60	$0^+$	$0^+$	0	$-4.41 \pm 0.07$	$^{310}\text{Og} \rightarrow ^{306}\text{Lv}$	10.43	$0^+$	$0^+$	0	$0.29 \pm 0.10$
$^{292}\text{Og} \rightarrow ^{288}\text{Lv}$	12.24	$0^+$	$0^+$	0	$-3.73 \pm 0.07$	-	-	-	-	-	-

**Table 3.** Same as Table 2 but for unfavoured transitions in the range  $111 \leq Z \leq 118$ .

Unfavoured $\alpha$ -Transition	$Q_\alpha$ (MeV)	$j_p$	$j_d$	$l$	$\log_{10}T_{1/2}$ (s)	Unfavoured $\alpha$ -Transition	$Q_\alpha$ (MeV)	$j_p$	$j_d$	$l$	$\log_{10}T_{1/2}$ (s)
$^{287}\text{Rg} \rightarrow ^{283}\text{Mt}$	8.44	13/2 <sup>+</sup>	9/2 <sup>-</sup>	3	4.02±0.12	$^{297}\text{Rg} \rightarrow ^{293}\text{Mt}$	8.38	3/2 <sup>-</sup>	1/2 <sup>-</sup>	2	4.20±0.13
$^{289}\text{Rg} \rightarrow ^{285}\text{Mt}$	8.30	3/2 <sup>-</sup>	9/2 <sup>-</sup>	4	4.68±0.13	$^{299}\text{Rg} \rightarrow ^{295}\text{Mt}$	7.85	3/2 <sup>+</sup>	5/2 <sup>+</sup>	2	5.96±0.14
$^{291}\text{Rg} \rightarrow ^{287}\text{Mt}$	7.87	3/2 <sup>-</sup>	1/2 <sup>+</sup>	1	5.71±0.14	$^{301}\text{Rg} \rightarrow ^{297}\text{Mt}$	7.15	3/2 <sup>+</sup>	5/2 <sup>+</sup>	2	8.61±0.16
$^{293}\text{Rg} \rightarrow ^{289}\text{Mt}$	7.75	3/2 <sup>-</sup>	5/2 <sup>-</sup>	2	6.23±0.14	$^{303}\text{Rg} \rightarrow ^{299}\text{Mt}$	6.85	3/2 <sup>+</sup>	5/2 <sup>+</sup>	2	9.87±0.17
$^{295}\text{Rg} \rightarrow ^{291}\text{Mt}$	7.40	3/2 <sup>-</sup>	1/2 <sup>-</sup>	2	7.56±0.15	-	-	-	-	-	-
$^{273}\text{Cn} \rightarrow ^{269}\text{Ds}$	11.64	3/2 <sup>+</sup>	1/2 <sup>+</sup>	2	-3.88±0.08	$^{299}\text{Cn} \rightarrow ^{295}\text{Ds}$	8.69	3/2 <sup>+</sup>	1/2 <sup>+</sup>	2	3.44 <sup>+0.02</sup> <sub>-0.22</sub>
$^{275}\text{Cn} \rightarrow ^{271}\text{Ds}$	11.74	13/2 <sup>-</sup>	3/2 <sup>+</sup>	5	-3.46±0.08	$^{301}\text{Cn} \rightarrow ^{297}\text{Ds}$	7.81	5/2 <sup>+</sup>	3/2 <sup>+</sup>	2	6.31 <sup>+0.05</sup> <sub>-0.24</sub>
$^{293}\text{Cn} \rightarrow ^{289}\text{Ds}$	8.19	3/2 <sup>+</sup>	1/2 <sup>+</sup>	2	5.02±0.13	$^{303}\text{Cn} \rightarrow ^{299}\text{Ds}$	7.44	7/2 <sup>+</sup>	5/2 <sup>+</sup>	2	7.71 <sup>+0.06</sup> <sub>-0.25</sub>
$^{295}\text{Cn} \rightarrow ^{291}\text{Ds}$	7.86	1/2 <sup>+</sup>	3/2 <sup>+</sup>	2	6.14±0.14	-	-	-	-	-	-
$^{291}\text{Nh} \rightarrow ^{287}\text{Rg}$	8.91	1/2 <sup>-</sup>	13/2 <sup>+</sup>	7	4.22±0.12	$^{299}\text{Nh} \rightarrow ^{295}\text{Rg}$	9.13	5/2 <sup>-</sup>	3/2 <sup>-</sup>	2	2.49±0.11
$^{293}\text{Nh} \rightarrow ^{289}\text{Rg}$	8.48	7/2 <sup>-</sup>	3/2 <sup>-</sup>	2	4.34±0.13	$^{301}\text{Nh} \rightarrow ^{297}\text{Rg}$	8.83	7/2 <sup>-</sup>	3/2 <sup>-</sup>	2	3.38±0.12
$^{295}\text{Nh} \rightarrow ^{291}\text{Rg}$	8.15	7/2 <sup>-</sup>	3/2 <sup>-</sup>	2	5.42±0.13	$^{303}\text{Nh} \rightarrow ^{299}\text{Rg}$	7.87	1/2 <sup>+</sup>	3/2 <sup>+</sup>	2	6.52±0.14
$^{297}\text{Nh} \rightarrow ^{293}\text{Rg}$	7.88	5/2 <sup>-</sup>	3/2 <sup>-</sup>	2	6.39±0.14	$^{305}\text{Nh} \rightarrow ^{301}\text{Rg}$	7.80	1/2 <sup>+</sup>	3/2 <sup>+</sup>	2	6.79±0.14
$^{275}\text{Fl} \rightarrow ^{271}\text{Cn}$	12.51	3/2 <sup>+</sup>	1/2 <sup>+</sup>	2	-5.06±0.07	$^{297}\text{Fl} \rightarrow ^{293}\text{Cn}$	8.35	1/2 <sup>+</sup>	3/2 <sup>+</sup>	2	5.05±0.13
$^{277}\text{Fl} \rightarrow ^{273}\text{Cn}$	12.40	13/2 <sup>-</sup>	3/2 <sup>+</sup>	5	-4.27±0.07	$^{299}\text{Fl} \rightarrow ^{295}\text{Cn}$	8.91	11/2 <sup>-</sup>	1/2 <sup>+</sup>	5	3.36 <sup>+0.48</sup> <sub>-0.71</sub>
$^{279}\text{Fl} \rightarrow ^{275}\text{Cn}$	12.43	5/2 <sup>+</sup>	13/2 <sup>-</sup>	5	-4.28±0.07	$^{301}\text{Fl} \rightarrow ^{297}\text{Cn}$	9.58	1/2 <sup>-</sup>	1/2 <sup>+</sup>	1	1.43 <sup>+0.08</sup> <sub>-0.13</sub>
$^{281}\text{Fl} \rightarrow ^{277}\text{Cn}$	11.82	1/2 <sup>+</sup>	3/2 <sup>+</sup>	2	-3.70±0.08	$^{303}\text{Fl} \rightarrow ^{299}\text{Cn}$	8.95	5/2 <sup>+</sup>	3/2 <sup>+</sup>	2	3.21 <sup>+0.02</sup> <sub>-0.21</sub>
$^{283}\text{Fl} \rightarrow ^{279}\text{Cn}$	10.88	3/2 <sup>+</sup>	11/2 <sup>+</sup>	4	-1.45±0.09	$^{305}\text{Fl} \rightarrow ^{301}\text{Cn}$	8.28	9/2 <sup>-</sup>	5/2 <sup>+</sup>	3	5.32 <sup>+0.08</sup> <sub>-0.35</sub>
$^{295}\text{Fl} \rightarrow ^{291}\text{Cn}$	8.61	3/2 <sup>+</sup>	1/2 <sup>+</sup>	2	4.23±0.12	-	-	-	-	-	-
$^{277}\text{Mc} \rightarrow ^{273}\text{Nh}$	12.64	1/2 <sup>-</sup>	3/2 <sup>-</sup>	2	-5.09±0.07	$^{285}\text{Mc} \rightarrow ^{281}\text{Nh}$	10.73	1/2 <sup>-</sup>	7/2 <sup>-</sup>	4	-0.90±0.09
$^{279}\text{Mc} \rightarrow ^{275}\text{Nh}$	12.65	1/2 <sup>-</sup>	9/2 <sup>-</sup>	4	-4.73±0.07	$^{293}\text{Mc} \rightarrow ^{289}\text{Nh}$	9.71	5/2 <sup>-</sup>	7/2 <sup>-</sup>	2	1.32 ±0.10
$^{281}\text{Mc} \rightarrow ^{277}\text{Nh}$	12.20	1/2 <sup>-</sup>	3/2 <sup>-</sup>	2	-4.24±0.07	$^{295}\text{Mc} \rightarrow ^{291}\text{Nh}$	9.72	5/2 <sup>-</sup>	1/2 <sup>-</sup>	2	1.33 ±0.10
$^{283}\text{Mc} \rightarrow ^{279}\text{Nh}$	11.32	1/2 <sup>-</sup>	3/2 <sup>-</sup>	2	-2.52±0.08	$^{307}\text{Mc} \rightarrow ^{303}\text{Nh}$	8.90	5/2 <sup>-</sup>	1/2 <sup>+</sup>	3	3.89±0.12
$^{277}\text{Lv} \rightarrow ^{273}\text{Fl}$	13.12	3/2 <sup>+</sup>	1/2 <sup>+</sup>	2	-5.72±0.07	$^{297}\text{Lv} \rightarrow ^{293}\text{Fl}$	10.84	3/2 <sup>+</sup>	1/2 <sup>+</sup>	2	-1.07±0.09
$^{279}\text{Lv} \rightarrow ^{275}\text{Fl}$	13.02	13/2 <sup>-</sup>	3/2 <sup>+</sup>	5	-4.95±0.07	$^{299}\text{Lv} \rightarrow ^{295}\text{Fl}$	10.84	1/2 <sup>+</sup>	3/2 <sup>+</sup>	2	-1.05±0.09
$^{281}\text{Lv} \rightarrow ^{277}\text{Fl}$	12.70	1/2 <sup>+</sup>	13/2 <sup>-</sup>	7	-3.76±0.07	$^{303}\text{Lv} \rightarrow ^{299}\text{Fl}$	11.93	3/2 <sup>+</sup>	11/2 <sup>-</sup>	5	-3.27 <sup>+0.52</sup> <sub>-0.67</sub>
$^{283}\text{Lv} \rightarrow ^{279}\text{Fl}$	12.11	1/2 <sup>+</sup>	5/2 <sup>+</sup>	2	-3.85±0.07	$^{305}\text{Lv} \rightarrow ^{301}\text{Fl}$	10.88	5/2 <sup>+</sup>	1/2 <sup>-</sup>	3	-1.15 <sup>+0.13</sup> <sub>-0.30</sub>
$^{285}\text{Lv} \rightarrow ^{281}\text{Fl}$	11.55	3/2 <sup>+</sup>	1/2 <sup>+</sup>	2	-2.75±0.08	$^{307}\text{Lv} \rightarrow ^{303}\text{Fl}$	9.84	7/2 <sup>+</sup>	5/2 <sup>+</sup>	2	1.30 <sup>+0.01</sup> <sub>-0.20</sub>
$^{279}\text{Ts} \rightarrow ^{275}\text{Mc}$	13.34	3/2 <sup>-</sup>	1/2 <sup>-</sup>	2	-5.88±0.06	$^{297}\text{Ts} \rightarrow ^{293}\text{Mc}$	11.62	3/2 <sup>-</sup>	5/2 <sup>-</sup>	2	-2.51±0.08
$^{281}\text{Ts} \rightarrow ^{277}\text{Mc}$	13.21	3/2 <sup>-</sup>	1/2 <sup>-</sup>	2	-5.64±0.06	$^{299}\text{Ts} \rightarrow ^{295}\text{Mc}$	11.46	1/2 <sup>-</sup>	5/2 <sup>-</sup>	2	-2.16±0.08
$^{283}\text{Ts} \rightarrow ^{279}\text{Mc}$	12.88	3/2 <sup>-</sup>	1/2 <sup>-</sup>	2	-5.05±0.07	$^{301}\text{Ts} \rightarrow ^{297}\text{Mc}$	11.61	1/2 <sup>-</sup>	5/2 <sup>-</sup>	2	-2.44±0.08
$^{285}\text{Ts} \rightarrow ^{281}\text{Mc}$	12.44	3/2 <sup>-</sup>	1/2 <sup>-</sup>	2	-4.25±0.07	$^{303}\text{Ts} \rightarrow ^{299}\text{Mc}$	12.78	1/2 <sup>-</sup>	5/2 <sup>-</sup>	2	-4.59±0.07
$^{287}\text{Ts} \rightarrow ^{283}\text{Mc}$	12.05	3/2 <sup>-</sup>	1/2 <sup>-</sup>	2	-3.50±0.07	$^{305}\text{Ts} \rightarrow ^{301}\text{Mc}$	12.08	1/2 <sup>-</sup>	5/2 <sup>-</sup>	2	-3.31±0.08
$^{289}\text{Ts} \rightarrow ^{285}\text{Mc}$	11.99	3/2 <sup>-</sup>	1/2 <sup>-</sup>	2	-3.34±0.08	$^{307}\text{Ts} \rightarrow ^{303}\text{Mc}$	10.92	5/2 <sup>+</sup>	5/2 <sup>-</sup>	1	-1.02±0.09
$^{295}\text{Ts} \rightarrow ^{291}\text{Mc}$	11.30	3/2 <sup>-</sup>	5/2 <sup>-</sup>	2	-1.88±0.08	$^{309}\text{Ts} \rightarrow ^{305}\text{Mc}$	10.01	9/2 <sup>+</sup>	5/2 <sup>-</sup>	3	1.38±0.10
$^{279}\text{Og} \rightarrow ^{275}\text{Lv}$	13.78	3/2 <sup>+</sup>	1/2 <sup>+</sup>	2	-6.42±0.06	$^{301}\text{Og} \rightarrow ^{297}\text{Lv}$	12.02	1/2 <sup>+</sup>	3/2 <sup>+</sup>	2	-3.04±0.08
$^{281}\text{Og} \rightarrow ^{277}\text{Lv}$	13.76	13/2 <sup>-</sup>	3/2 <sup>+</sup>	5	-5.78±0.06	$^{303}\text{Og} \rightarrow ^{299}\text{Lv}$	12.61	7/2 <sup>+</sup>	1/2 <sup>+</sup>	4	-4.15 <sup>+0.31</sup> <sub>-0.45</sub>
$^{283}\text{Og} \rightarrow ^{279}\text{Lv}$	13.33	1/2 <sup>+</sup>	13/2 <sup>-</sup>	7	-4.44±0.06	$^{305}\text{Og} \rightarrow ^{301}\text{Lv}$	12.91	5/2 <sup>+</sup>	1/2 <sup>+</sup>	2	-4.71 <sup>+0.03</sup> <sub>-0.16</sub>
$^{291}\text{Og} \rightarrow ^{287}\text{Lv}$	12.42	5/2 <sup>+</sup>	3/2 <sup>+</sup>	2	-3.93±0.07	$^{307}\text{Og} \rightarrow ^{303}\text{Lv}$	11.92	5/2 <sup>+</sup>	3/2 <sup>+</sup>	2	-2.89 <sup>+0.02</sup> <sub>-0.17</sub>
$^{293}\text{Og} \rightarrow ^{289}\text{Lv}$	12.24	1/2 <sup>+</sup>	5/2 <sup>+</sup>	2	-3.57±0.07	$^{309}\text{Og} \rightarrow ^{305}\text{Lv}$	10.72	7/2 <sup>+</sup>	5/2 <sup>+</sup>	2	-0.34 <sup>+0.01</sup> <sub>-0.19</sub>
$^{299}\text{Og} \rightarrow ^{295}\text{Lv}$	12.05	3/2 <sup>+</sup>	1/2 <sup>+</sup>	2	-3.12±0.08	-	-	-	-	-	-



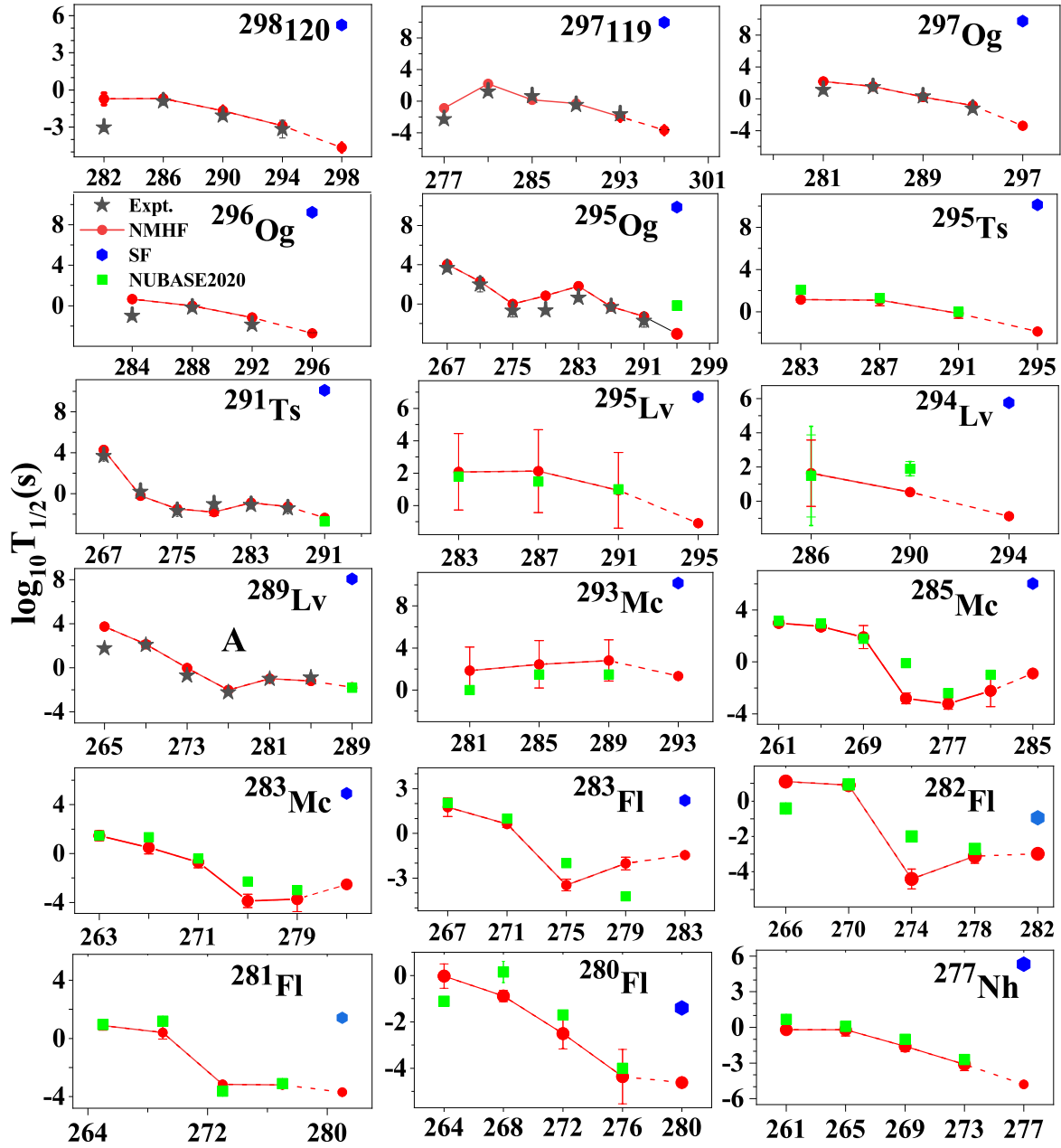


**Figure 2.** (Colour online)  $\alpha$ -decay half-lives for experimental decay chains calculated by the NMHF formula (red circles) are shown. Experimental data (black stars) are taken from Refs. [6, 39–42] whereas the latest evaluated data (green squares) are taken from NUBASE2020 [43]. Error bars are also mentioned in the graph: for both theoretical and experimental values. For the probable candidate (connected by dash lines), SF half-lives are depicted by blue hexagons.

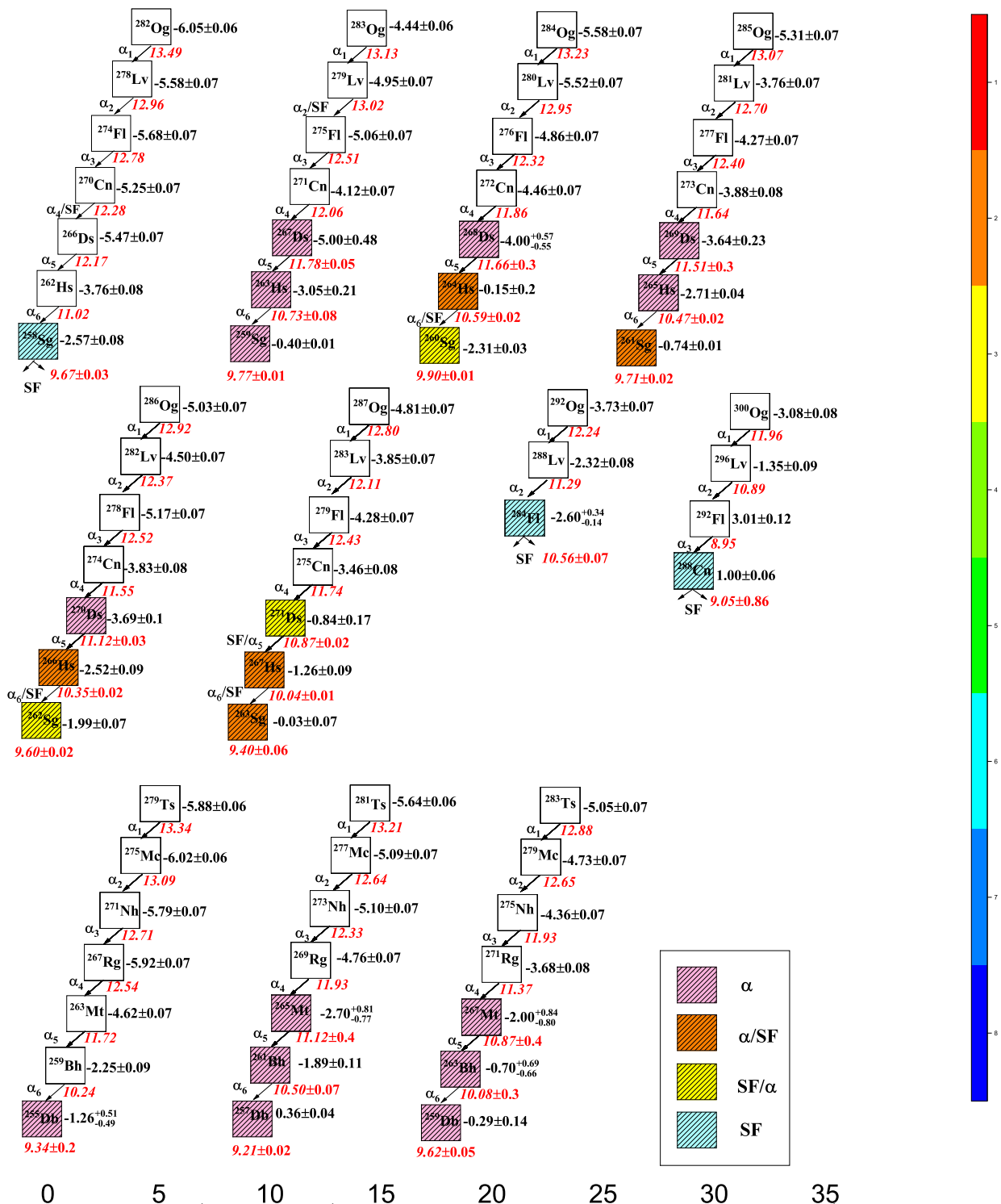


**Figure 3.** (Colour online) Theoretical decay chains by using NMHF formula (Black numbers indicate the logarithmic half-lives with uncertainties in second). Red numbers represent the  $Q_\alpha$ -values (in MeV) taken from WS4 mass model [88] or AME2020 [87]. The uncertainties in theoretical  $Q_\alpha$ -values is  $\pm 0.04$  MeV and the shaded blocks show the modes which are available in NUBASE2020 [43].

theoretical  $Q_\alpha$ -values of WS4 ( $\pm 0.04$  MeV). Many of the theoretical  $\alpha$ -decay chains are found with 3  $\alpha$ -transitions or more. Gratifyingly,  $\alpha$ -decay chain of  $^{281}\text{Og}$  is found with 6  $\alpha$ -transitions which leads to the adequate possibility of detection of these sets of nuclei in future experiments. Few selective decay chains in which one or more terminating nuclei are known as per NUBASE2020 [43], are shown in Fig. 3. These decay chains mainly consist of nuclei between Og ( $Z=118$ ) to Db ( $Z=105$ ). So, theoretical estimates lead to  $\alpha$ -decay chains of  $^{282-287,292,300}\text{Og}$  (rest others in between  $288 \leq A \leq 291$  and  $293 \leq A \leq 299$  are already part of Fig. 2) which are represented graphically in Fig. 3. In a similar way, the  $\alpha$ -decay chains of  $^{279-283}\text{Ts}$  (odd-A) are shown. In Fig. 3,  $Q_\alpha$ -values (red numbers) are taken from AME2020 [87] wherever available, otherwise from WS4 mass model [88]. The black numbers indicate logarithmic half-lives estimated by NMHF formula. The shaded blocks show the modes which are available in NUBASE2020 [43] and the colour of blocks corresponds to  $\alpha$ , SF,  $\alpha$ /SF or SF/ $\alpha$ . Most of the decay chains presented in Fig. 3 comprise several already known nuclei and, therefore, the nuclei with theoretical estimates in these decay chains are likely to be observed experimentally in future.

### 3.2. Cluster Decay

In the following, we have probed cluster decay from the mentioned SHN by calculating the logarithmic half-lives using UDL formula [74]. This formula is given in Eqn. (6) which mainly relies on  $Q$ -value calculated by using the following relation:

$$Q(\text{MeV}) = B.E.(d) + B.E.(c) - B.E.(p) + k[Z_p^\beta - Z_d^\beta] \quad (9)$$

The term  $k[Z_p^\epsilon - Z_d^\epsilon]$  indicates the screening effect caused by the surrounding electrons around the nucleus [116] where  $k=8.7$  eV [ $8.7 \times 10^{-6}$  MeV] and  $\epsilon=2.517$  for  $Z$  (proton number)  $\geq 60$  and  $k=13.6$  eV [ $13.6 \times 10^{-6}$  MeV] and  $\epsilon=2.408$  for  $Z < 60$  have been deducted from the data shown by Huang *et al* [117]. For this study, we have taken experimental binding energies (for daughter(d), cluster(c), and parent(p) nuclei) from AME2020 [87] to calculate  $Q$ -values for cluster emission, considering the fact that the validity of this mass model for the cluster emission in this superheavy region has already been verified in Refs. [67,68]. We have also calculated the uncertainties in these  $Q$ -values:  $\pm 0.05$  MeV, with the help of Eqn. (2) and using 73 experimental data of  $Q$ -values for cluster emission [64,65].

In Fig. 4, we have shown half-lives of cluster emission from experimentally known Rg to Og isotopes (with  $N=161-177$ ) in various panels, respectively. Considering  $Z_d = 82$  shell closure effect [118], i.e. the daughter as one of the isotopes of Pb, the isotopes of Cu, Zn, Ga, Ge, As, Se, Br, and Kr are taken into account as probable clusters from the parent isotopes of Rg, Cn, Nh, Fl, Mc, Lv, Ts and Og, respectively. From Fig. 4, parabolic trend is clearly seen where each parabola represents half-lives of one cluster from the corresponding chain of parent isotopes. Half-lives are shown up to  $\log_{10}T_c=30$  s considering the experimental limit of cluster emission [65]. From this extensive analysis, one can find a minima of each parabola which represents the potential cluster nucleus for a particular parent nucleus. From Fig. 4, one can notice that the half-life of minima

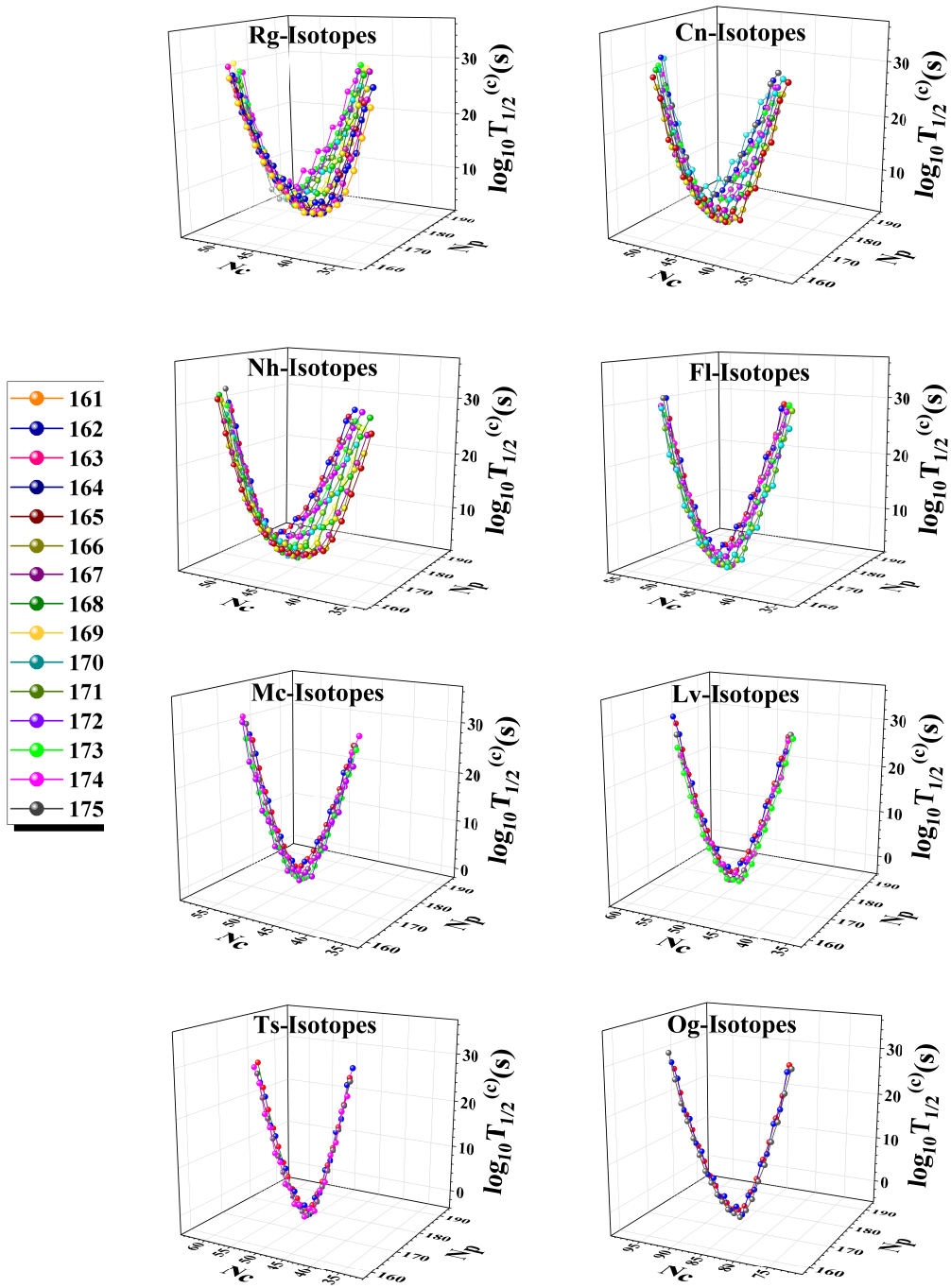


**Figure 4.** (Colour online) Half-lives of cluster emission (in second) from experimentally known Rg to Og isotopes (with  $N=161-177$ ) by using UDL formula [74].  $N_p$  and  $N_c$  represent neutron numbers of parent nuclei (Rg, Cn, Nh, Fl, Mc, Lv, Ts and Og) and respective clusters (Cu, Zn, Ga, Ge, As, Se, Br and Kr).

of each parabola lies somewhat close to the range of half-life of  $\alpha$ -decay as can be seen from Figs. 2, 3 and Tables 2, 3. Therefore, cluster decay is also found probable provided that it invariably competes with  $\alpha$  and SF decays in the superheavy region.

### 3.3. Competition among various decay-modes

In the preceding sections,  $\alpha$ -decay, spontaneous fission as well as cluster decay have been discussed for the considered range of nuclei. Competition among these decay modes is crucial to investigate the possibility of synthesis of new isotopes as well as to visualize prospects of other decay modes in known nuclei. Before probing the competition among mentioned decay modes, it will be worth to include weak-decay mode in this contest as it has already been conjectured as one of the possible decay modes in the superheavy region, though in an exceptional manner [35, 82, 83].

Table 4: Competition among various decay modes in the range  $111 \leq Z \leq 118$ . # values are the estimated from Trends in Neighboring Nuclei (TNN) in NUBASE2020 [43].

Nucleus	$\log_{10}T_{1/2}(s)$		Branching ratio				
	Exp.	Th.	$\alpha$	Cluster	SF	$\beta^-$	$\beta^+/\text{EC}$
$^{280}\text{Rg}$	$0.63 \pm 0.05$	-1.12	$69.07^{+1.13}_{-1.16}$	0.00	$30.91^{+1.13}_{-1.16}$	0.00	0.01
$^{281}\text{Rg}$	$1.23^{+0.16}_{-0.08}$	-0.20	$6.67^{+1.52}_{-1.26}$	0.00	$93.19^{+1.54}_{-1.27}$	0.07	$0.06 \pm 0.02$
$^{282}\text{Rg}$	$2.11 \pm 0.18$	0.31	$60.80^{+1.37}_{-1.39}$	0.00	$38.98^{+1.40}_{-1.42}$	0.00	$0.22 \pm 0.03$
$^{283}\text{Rg}$	2.08#	0.50	$22.12^{+2.14}_{-2.01}$	0.00	$77.65^{+2.19}_{-2.05}$	$0.07 \pm 0.01$	$0.16 \pm 0.05$
$^{284}\text{Rg}$	1.78#	1.74	$65.64^{+9.78}_{-11.54}$	0.00	$31.03^{+9.32}_{-11.25}$	0.00	$3.32^{+0.46}_{-0.29}$
$^{285}\text{Rg}$	1.48#	2.27	$66.89^{+10.21}_{-12.59}$	0.00	$30.50^{+10.25}_{-12.83}$	$0.45^{+0.18}_{-0.25}$	$2.15^{+0.22}_{-0.49}$
$^{286}\text{Rg}$	1.00#	3.00	$69.39^{+8.73}_{-10.49}$	0.00	$6.69^{+2.88}_{-4.67}$	0.00	$23.92^{+5.86}_{-5.83}$
$^{287}\text{Rg}$	-	3.02	$10.05^{+1.16}_{-5.84}$	0.00	$89.56^{+12.45}_{-6.17}$	$0.02 \pm 0.01$	$0.37^{+0.09}_{-0.03}$
$^{288}\text{Rg}$	-	3.43	$44.29^{+18.91}_{-18.27}$	0.00	$39.30^{+16.89}_{-19.72}$	$0.39^{+0.14}_{-0.13}$	$16.01^{+1.89}_{-1.58}$
$^{289}\text{Rg}$	-	1.26	$0.04 \pm 0.02$	0.00	$99.96^{+0.06}_{-0.02}$	0.00	0.00
$^{290}\text{Rg}$	-	2.64	$0.37 \pm 0.24$	0.00	$98.07^{+1.06}_{-0.51}$	$1.30^{+0.08}_{-0.09}$	$0.26 \pm 0.18$
$^{291}\text{Rg}$	-	1.76	0.01	0.00	$99.98^{+0.02}_{-0.01}$	0.01	0.00
$^{292}\text{Rg}$	-	2.66	$0.08 \pm 0.05$	0.00	$81.19^{+0.83}_{-0.75}$	$18.73^{+0.69}_{-0.70}$	0.00
$^{293}\text{Rg}$	-	1.45	0.00	0.00	$99.75 \pm 0.02$	$0.25 \pm 0.02$	0.00
$^{294}\text{Rg}$	-	1.92	0.00	0.00	$88.42^{+0.40}_{-0.39}$	$11.58^{+0.40}_{-0.39}$	0.00
$^{278}\text{Cn}$	-2.70#	-3.13	$95.46^{+0.38}_{-0.42}$	0.00	$4.53^{+0.38}_{-0.42}$	0.01	0.00
$^{279}\text{Cn}$	-4.22#	-2.05	$94.76^{+0.46}_{-0.50}$	0.00	$5.20^{+0.45}_{-0.50}$	0.04	0.00
$^{280}\text{Cn}$	-2.30#	-5.10	$0.08 \pm 0.01$	0.00	$99.92 \pm 0.01$	0.00	0.00
$^{282}\text{Cn}$	$-3.04^{+0.17}_{-0.09}$	-4.26	0.03	0.00	99.97	0.00	0.00
$^{284}\text{Cn}$	$-1.01^{+0.09}_{-0.06}$	-2.49	0.11	0.01	99.89	0.00	0.00
$^{285}\text{Cn}$	$1.45^{+0.12}_{-0.09}$	1.14	$59.49^{+15.60}_{-18.16}$	$0.04 \pm 0.01$	$38.34^{+14.86}_{-17.34}$	$1.56^{+0.65}_{-0.82}$	$0.57^{+0.08}_{-0.01}$
$^{287}\text{Cn}$	1.48#	2.09	$92.29^{+2.71}_{-4.40}$	$0.07^{+0.02}_{-0.03}$	$5.02^{+2.02}_{-3.28}$	$1.66^{+0.74}_{-0.13}$	$0.95^{+0.07}_{-0.20}$
$^{288}\text{Cn}$	1.00#	-0.16	0.44	0.00	$99.52 \pm 0.44$	0.04	0.00
$^{289}\text{Cn}$	-	1.91	$49.52^{+19.69}_{-19.95}$	0.01	$50.40^{+19.70}_{-19.93}$	$0.05^{+0.02}_{-0.03}$	0.01
$^{290}\text{Cn}$	-	0.09	$0.23 \pm 0.03$	0.00	$99.75^{+0.31}_{-0.14}$	0.01	0.00

Continued on next page

Table 4 – continued from previous page

	Exp.	Th.	$\alpha$	Cluster	SF	$\beta^-$	$\beta^+/\text{EC}$
$^{291}\text{Cn}$	-	3.20	$40.71^{+22.08}_{-19.23}$	0.00	$59.28^{+22.08}_{-19.23}$	0.00	0.00
$^{292}\text{Cn}$	-	0.63	0.01	0.00	$99.98^{+0.02}_{-0.01}$	0.00	0.00
$^{293}\text{Cn}$	-	3.67	$4.44^{+0.65}_{-0.27}$	0.00	$95.56^{+6.45}_{-2.74}$	0.00	0.00
$^{285}\text{Nh}$	$0.62^{+0.15}_{-0.08}$	0.16	$99.13^{+0.04}_{-0.03}$	0.06	0.04	$0.43 \pm 0.03$	$0.34^{+0.07}_{-0.06}$
$^{286}\text{Nh}$	$1.08 \pm 0.19$	0.43	$99.42 \pm 0.08$	$0.08^{+0.01}_{-0.02}$	0.00	0.00	$0.50^{+0.06}_{-0.07}$
$^{287}\text{Nh}$	1.30#	1.07	$97.22^{+0.05}_{-0.02}$	$0.78 \pm 0.01$	0.01	$0.89^{+0.14}_{-0.16}$	$1.11 \pm 0.19$
$^{288}\text{Nh}$	1.30#	0.99	$98.88^{+1.11}_{-6.84}$	0.21	0.00	0.00	0.90
$^{289}\text{Nh}$	1.48#	2.69	$74.40^{+2.51}_{-7.22}$	$8.65^{+8.51}_{-2.92}$	$0.12^{+0.11}_{-0.05}$	$3.86^{+3.81}_{-1.64}$	$12.97^{+1.27}_{-2.61}$
$^{290}\text{Nh}$	$0.90 \pm 0.42$	1.55	$98.48^{+0.46}_{-0.63}$	$0.05^{+0.02}_{-0.03}$	0.00	0.00	$1.48^{+0.44}_{-0.60}$
$^{291}\text{Nh}$	-	4.02	$30.73^{+3.70}_{-2.47}$	$2.40^{+1.19}_{-0.26}$	$0.18^{+0.10}_{-0.02}$	$4.31^{+2.60}_{-0.69}$	$62.37^{+0.19}_{-7.24}$
$^{292}\text{Nh}$	-	3.31	$66.38^{+11.03}_{-12.62}$	$0.03^{+0.01}_{-0.02}$	0.00	$0.05^{+0.02}_{-0.04}$	$33.54^{+10.99}_{-12.56}$
$^{293}\text{Nh}$	-	4.34	$99.80^{+0.12}_{-0.30}$	$0.05 \pm 0.03$	$0.15 \pm 0.09$	0.00	0.00
$^{294}\text{Nh}$	-	4.28	$45.78^{+3.36}_{-1.92}$	0.00	0.03	$12.87^{+2.83}_{-4.78}$	$41.32^{+0.81}_{-0.67}$
$^{295}\text{Nh}$	-	5.38	$91.84^{+1.07}_{-1.13}$	0.01	$8.15^{+1.07}_{-1.22}$	0.00	0.00
$^{296}\text{Nh}$	-	4.12	$1.13^{+0.15}_{-0.13}$	0.00	$0.19 \pm 0.01$	$98.67^{+0.18}_{-0.14}$	0.01
$^{297}\text{Nh}$	-	4.57	$1.53^{+0.22}_{-0.20}$	0.00	$57.27^{+1.38}_{-1.37}$	$41.21^{+1.15}_{-1.17}$	0.00
$^{298}\text{Nh}$	-	1.97	$0.71^{+0.11}_{-0.09}$	0.00	$78.09^{+0.38}_{-0.37}$	$21.20 \pm 0.27$	0.00
$^{282}\text{Fl}$	-	-3.44	$99.06^{+0.42}_{-0.77}$	0.00	$0.93^{+0.41}_{-0.76}$	0.00	0.00
$^{283}\text{Fl}$	-	-1.80	$99.68^{+0.17}_{-0.37}$	0.00	0.01	0.27	0.03
$^{285}\text{Fl}$	$-0.88^{+0.10}_{-0.22}$	-1.20	$99.71^{+0.03}_{-0.04}$	0.05	0.00	$0.21^{+0.04}_{-0.05}$	0.03
$^{286}\text{Fl}$	$-0.92^{+0.15}_{-0.07}$	-0.74	$97.77^{+0.10}_{-0.12}$	$0.26 \pm 0.02$	$1.26 \pm 0.02$	$0.71 \pm 0.12$	0.00
$^{287}\text{Fl}$	$-0.32^{+0.13}_{-0.08}$	-0.28	$97.43^{+0.01}_{-0.05}$	$1.69^{+0.14}_{-0.13}$	0.00	$0.77 \pm 0.03$	0.11
$^{288}\text{Fl}$	$-0.18^{+0.09}_{-0.07}$	-0.05	$94.04^{+0.25}_{-0.35}$	$3.89 \pm 0.14$	$0.34^{+0.02}_{-0.03}$	$1.73^{+0.14}_{-0.15}$	0.00
$^{289}\text{Fl}$	$0.28^{+0.17}_{-0.09}$	0.28	$95.15^{+0.13}_{-0.03}$	$3.76^{+0.30}_{-0.28}$	0.00	$0.93 \pm 0.05$	0.15
$^{290}\text{Fl}$	$1.90 \pm 0.42$	0.48	$86.73^{+1.29}_{-1.59}$	$10.68^{+0.56}_{-0.58}$	0.02	$2.57^{+0.41}_{-0.49}$	0.00
$^{291}\text{Fl}$	1.00#	0.92	$96.05^{+3.94}_{-9.19}$	$2.35^{+2.34}_{-0.52}$	0.00	$1.40^{+1.39}_{-0.35}$	$0.20^{+0.20}_{-0.45}$
$^{292}\text{Fl}$	-	2.32	$20.52^{+2.42}_{-2.24}$	$4.13^{+0.04}_{-0.65}$	0.04	$75.31^{+2.23}_{-1.14}$	0.00
$^{293}\text{Fl}$	-	3.21	$48.68^{+2.44}_{-2.69}$	$2.50^{+0.76}_{-0.04}$	0.00	$45.59^{+2.72}_{-2.97}$	$3.23 \pm 0.36$
$^{294}\text{Fl}$	-	2.91	$14.41^{+2.06}_{-1.85}$	$0.21 \pm 0.02$	0.16	$85.22^{+2.09}_{-1.87}$	0.00
$^{295}\text{Fl}$	-	3.97	$55.14^{+4.43}_{-4.52}$	$0.23 \pm 0.01$	0.01	$44.61^{+4.44}_{-4.53}$	0.00
$^{296}\text{Fl}$	-	3.42	$14.91^{+2.24}_{-2.00}$	0.01	1.87	$83.21^{+2.23}_{-2.00}$	0.00
$^{297}\text{Fl}$	-	4.94	$77.40^{+3.54}_{-3.97}$	0.04	$0.34 \pm 0.03$	$22.22^{+3.50}_{-3.94}$	0.00
$^{298}\text{Fl}$	-	3.34	$1.37^{+0.22}_{-0.19}$	0.00	$86.34^{+0.15}_{-0.19}$	$12.29 \pm 0.38$	0.00
$^{299}\text{Fl}$	-	2.52	$14.49^{+9.80}_{-10.87}$	0.00	$85.51^{+9.80}_{-10.87}$	0.00	0.00
$^{289}\text{Mc}$	$-0.48^{+0.17}_{-0.12}$	-0.36	$85.27^{+0.88}_{-0.79}$	$13.86^{+0.96}_{-0.91}$	0.00	$0.63 \pm 0.03$	0.24
$^{290}\text{Mc}$	$-0.08 \pm 0.20$	-0.61	$90.14^{+0.91}_{-1.00}$	$9.76^{+0.90}_{-0.99}$	0.00	0.00	0.09
$^{291}\text{Mc}$	0.00#	-0.39	$57.15^{+2.16}_{-2.12}$	$42.49^{+2.19}_{-2.16}$	0.00	$0.22^{+0.06}_{-0.08}$	0.14
$^{292}\text{Mc}$	0.70#	-0.10	$93.07^{+6.88}_{-8.89}$	$6.72^{+6.67}_{-0.86}$	0.00	0.00	$0.21^{+0.20}_{-0.28}$
$^{293}\text{Mc}$	-	1.19	$73.35^{+1.09}_{-1.58}$	$21.65^{+0.07}_{-0.06}$	0.00	$2.66^{+0.33}_{-0.38}$	$2.34^{+0.13}_{-0.14}$
$^{294}\text{Mc}$	-	1.22	$95.65^{+1.86}_{-3.81}$	$1.94 \pm 0.02$	0.00	0.00	$2.41^{+0.19}_{-0.20}$
$^{295}\text{Mc}$	-	1.32	$97.40^{+1.07}_{-2.27}$	0.46	0.00	$0.68^{+0.09}_{-0.11}$	$1.46 \pm 0.07$
$^{296}\text{Mc}$	-	1.49	$97.36^{+0.19}_{-0.20}$	0.04	0.00	0.00	$2.60^{+0.19}_{-0.20}$
$^{297}\text{Mc}$	-	1.55	$99.01^{+0.25}_{-0.53}$	0.01	0.00	$0.19 \pm 0.03$	$0.79 \pm 0.01$
$^{298}\text{Mc}$	-	1.70	$98.03^{+0.66}_{-0.88}$	0.00	0.00	0.00	$1.97^{+0.12}_{-0.13}$

Continued on next page

Table 4 – continued from previous page

	Exp.	Th.	$\alpha$	Cluster	SF	$\beta^-$	$\beta^+/\text{EC}$
$^{302}\text{Mc}$	-	-1.26	$54.38^{+2.55}_{-2.58}$	0.00	$45.62^{+2.55}_{-2.58}$	0.00	0.00
$^{278}\text{Lv}$	-	-5.91	$56.60^{+1.84}_{-1.86}$	0.00	$45.40^{+1.84}_{-1.86}$	0.00	0.00
$^{281}\text{Lv}$	-	-3.76	$99.97^{+0.01}_{-0.02}$	0.01	0.00	0.02	0.00
$^{288}\text{Lv}$	-	-2.35	$93.69^{+2.42}_{-3.87}$	$6.24 \pm 0.04$	0.00	$0.07 \pm 0.01$	0.00
$^{289}\text{Lv}$	-1.80#	-1.87	$78.49^{+1.49}_{-1.41}$	$21.37^{+1.50}_{-1.43}$	0.00	$0.12 \pm 0.01$	$0.01 \pm 0.01$
$^{290}\text{Lv}$	$-2.08^{+0.20}_{-0.10}$	-2.01	$46.28^{+1.68}_{-1.69}$	$53.63^{+1.69}_{-1.70}$	0.00	$0.08 \pm 0.01$	0.00
$^{291}\text{Lv}$	$-1.72^{+0.63}_{-0.14}$	-2.18	$12.45^{+0.82}_{-0.87}$	$87.53^{+0.82}_{-0.87}$	0.00	0.02	0.00
$^{292}\text{Lv}$	$-1.89^{+0.26}_{-0.14}$	-2.31	$7.49 \pm 0.18$	$92.49 \pm 0.19$	0.00	0.02	0.00
$^{293}\text{Lv}$	$-1.24^{+0.43}_{-0.13}$	-1.39	$24.82^{+1.42}_{-1.48}$	$75.09^{+1.43}_{-1.49}$	0.00	0.08	0.02
$^{294}\text{Lv}$	-	-1.21	$46.01^{+0.03}_{-0.02}$	$53.85^{+0.04}_{-0.03}$	0.00	$0.13^{+0.01}_{-0.02}$	0.00
$^{295}\text{Lv}$	-	-1.14	$92.78^{+2.94}_{-4.83}$	$7.17 \pm 0.02$	0.00	0.04	0.01
$^{302}\text{Lv}$	-	-3.90	$98.34^{+0.70}_{-1.21}$	0.00	$1.66^{+0.34}_{-0.42}$	0.00	0.00
$^{303}\text{Lv}$	-	-3.67	$39.25^{+5.11}_{-5.78}$	0.00	$60.75^{+1.68}_{-3.08}$	0.00	0.00
$^{289}\text{Ts}$	-	-3.37	$93.31^{+2.36}_{-3.59}$	$6.68 \pm 0.09$	0.00	0.01	0.00
$^{290}\text{Ts}$	-	-3.24	$89.00^{+3.83}_{-5.65}$	$11.00 \pm 0.12$	0.00	0.00	0.00
$^{291}\text{Ts}$	-2.70#	-2.96	$22.81^{+1.42}_{-1.48}$	$77.18^{+1.42}_{-1.48}$	0.00	0.01	0.00
$^{292}\text{Ts}$	-2.00#	-3.07	$29.81^{+4.01}_{-2.32}$	$70.19^{+4.01}_{-2.32}$	0.00	0.00	0.00
$^{293}\text{Ts}$	$-1.66^{+0.17}_{-0.08}$	-3.03	$8.53^{+0.58}_{-0.62}$	$91.47^{+0.59}_{-0.62}$	0.00	0.00	0.00
$^{294}\text{Ts}$	$-1.15 \pm 0.20$	-2.48	$20.49^{+1.53}_{-1.46}$	$79.50^{+1.53}_{-1.46}$	0.00	0.00	0.00
$^{295}\text{Ts}$	-	-2.37	$32.12 \pm 0.16$	$67.87^{+12.02}_{-10.22}$	0.00	0.01	0.00
$^{296}\text{Ts}$	-	-2.48	$90.22^{+3.59}_{-5.46}$	$9.78 \pm 0.10$	0.00	0.00	0.00
$^{297}\text{Ts}$	-	-2.52	$96.54^{+1.30}_{-2.10}$	$3.45 \pm 0.04$	0.00	0.00	0.00
$^{305}\text{Ts}$	-	-4.22	$12.14^{+0.96}_{-0.90}$	0.00	$87.86^{+7.37}_{-4.90}$	0.00	0.00
$^{283}\text{Og}$	-	-4.46	$94.08^{+1.80}_{-2.57}$	$5.92 \pm 0.13$	0.00	0.01	0.00
$^{287}\text{Og}$	-	-4.86	$89.77^{+3.21}_{-4.45}$	$10.23^{+0.32}_{-0.44}$	0.00	0.00	0.00
$^{288}\text{Og}$	-	-4.61	$72.42^{+7.62}_{-9.38}$	$27.58^{+0.76}_{-0.94}$	0.00	0.00	0.00
$^{289}\text{Og}$	-	-4.59	$66.16^{+8.78}_{-10.26}$	$33.84^{+0.88}_{-1.03}$	0.00	0.00	0.00
$^{290}\text{Og}$	-	-4.65	$57.16^{+9.95}_{-10.77}$	$42.84^{+9.95}_{-10.77}$	0.00	0.00	0.00
$^{291}\text{Og}$	-	-4.51	$26.27^{+0.93}_{-0.77}$	$73.73^{+9.27}_{-7.63}$	0.00	0.00	0.00
$^{292}\text{Og}$	-	-4.64	$12.27 \pm 0.15$	$87.73^{+5.70}_{-4.14}$	0.00	0.00	0.00
$^{293}\text{Og}$	-3.00#	-4.69	$7.62^{+0.38}_{-0.26}$	$92.38^{+3.82}_{-2.66}$	0.00	0.00	0.00
$^{294}\text{Og}$	$-3.16^{+0.71}_{-0.14}$	-4.50	$3.12^{+0.22}_{-0.24}$	$96.88^{+0.22}_{-0.24}$	0.00	0.00	0.00
$^{295}\text{Og}$	$-0.17 \pm 0.47$	-4.09	$3.61^{+0.41}_{-0.20}$	$96.39^{+4.08}_{-1.99}$	0.00	0.00	0.00
$^{296}\text{Og}$	-	-4.13	$4.06 \pm 0.04$	$95.94^{+2.36}_{-1.54}$	0.00	0.00	0.00
$^{297}\text{Og}$	-	-3.77	$42.49^{+11.37}_{-10.83}$	$57.50^{+0.37}_{-0.36}$	0.00	0.00	0.00
$^{298}\text{Og}$	-	-3.81	$53.23^{+10.91}_{-11.44}$	$46.77^{+0.41}_{-0.40}$	0.00	0.00	0.00
$^{299}\text{Og}$	-	-3.20	$82.76^{+5.63}_{-7.77}$	$17.24 \pm 0.22$	0.00	0.00	0.00
$^{300}\text{Og}$	-	-3.10	$94.20^{+2.08}_{-3.22}$	$5.80 \pm 0.09$	0.00	0.00	0.00
$^{301}\text{Og}$	-	-3.05	$98.78^{+0.45}_{-0.72}$	$1.22 \pm 0.02$	0.00	0.00	0.00
$^{304}\text{Og}$	-	-5.13	$98.70^{+0.51}_{-0.84}$	0.00	$1.30 \pm 0.10$	0.00	0.00
$^{305}\text{Og}$	-	-5.01	$49.38^{+0.73}_{-1.76}$	0.00	$50.62^{+0.73}_{-1.75}$	0.00	0.00
$^{307}\text{Og}$	-	-3.42	29.58	0.00	70.42	0.00	0.00

In this paper, we follow Eqn. (7) to calculate half-lives for  $\beta^-$ -decay, whereas, Eqn.

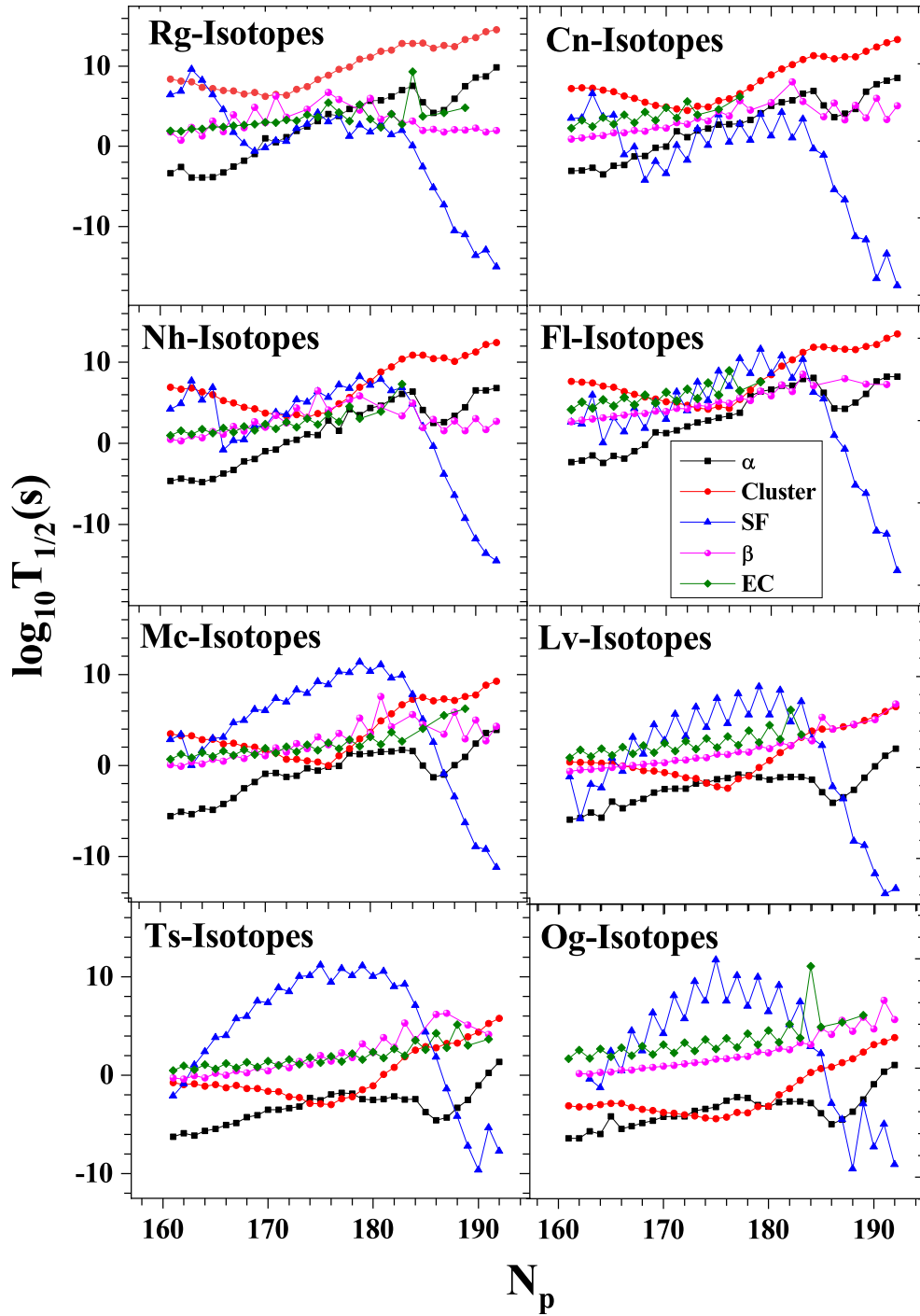


**Figure 5.** (Colour online) Competition among the various decay modes in the range  $111 \leq Z \leq 118$ . Half-lives for these decay modes are shown as a function of the neutron number for isotopes from Rg to Og.



(8) is used to calculate half-lives for electron capture (EC). These half-lives are plotted in Fig. 5 along with half-lives of  $\alpha$ -decay from NMHF formula (Eqn. (3)) and half-lives of spontaneous fission from MBF formula (Eqn. (5)) for the considered range of nuclei. Half-lives of cluster emission calculated by UDL formula (Eqn. (6)) are also plotted for each isotope. It is important to point out here that each point of cluster decay half-life in Fig. 5 corresponds to the minima of each parabola in Fig. 4 for a given isotope. Therefore, the clusters participating in this contest are the clusters which are found most probable for a particular parent isotope. To analyze the half-lives of weak-decay microscopically, sensitivity to the unknown  $Q$ -energies is crucial [119–121]. For this, we have calculated the uncertainties in theoretical  $Q$ -values of  $\beta^-$ -decay and EC by using 113 and 78 experimental data in region  $Z>82$  [87], which are found to be  $\pm 0.02$  MeV and  $\pm 0.20$  MeV, respectively. We have estimated the weak-decay half-lives using these uncertainties, however, to make Figs. 4 and 5 unclutter, we have not displayed the error bars.

From Fig. 5 the competition among  $\alpha$ , cluster, SF,  $\beta^-$  and EC decay modes is clearly evident. In principle, the decay mode which has the lowest half-life among others becomes most probable. In view of this, for the neutron rich isotopes, spontaneous fission is found to dominate while  $\alpha$ -decay prevails on the neutron deficient side for all the considered nuclei. In the middle region, however, the other decay modes begin to compete with  $\alpha$  and SF. As an example, cluster decay (red line) is ascertained to be more probable than  $\alpha$ -decay for  $N\sim 178$  for Mc, Lv, Ts and Og isotopes. For Rg, Cn, Nh and Fl isotopes, weak-decay (pink and green lines) is observed to meet closely to the half-lives of other decay modes. To quantify this competition, we have calculated the branching ratios for respective decay modes as:

$$b = \frac{T_{1/2}^{Th.}}{T_{1/2}^{\alpha/Cluster/SF/\beta/EC}} \quad (10)$$

where,  $T_{1/2}^{Th.}$  is the total half-life calculated by considering half-lives of all decay modes and the relation is given by:

$$\frac{1}{T_{1/2}^{Th.}} = \frac{1}{T_{1/2}^{\alpha}} + \frac{1}{T_{1/2}^{Cluster}} + \frac{1}{T_{1/2}^{SF}} + \frac{1}{T_{1/2}^{\beta}} + \frac{1}{T_{1/2}^{EC}} \quad (11)$$

where the superscripts refer to the half-lives of concerned decay modes. Respective branching ratios for considered decay modes (from Eqn. (10)) are mentioned in percentage form with uncertainty in the Table 4. Experimental half-lives taken from NUBASE2020 [43] are mentioned along with the logarithm of total half-lives calculated by using Eqn. (11). These half-lives are found in a reasonable match which supports the approach of combining half-lives of various decay modes. From the close inspection of Table 4, chances of weak-decay are observed for Rg, Nh and Fl isotopes. Particularly,  $^{294,296}\text{Fl}$  is found with  $\sim 90\%$  probability of  $\beta$ -decay besides the  $\gtrsim 50\%$  probability of EC-decay in  $^{291,294}\text{Nh}$ . The chances of weak-decay, however, are found negligible for the nuclei with  $Z>114$ . Contrarily, cluster decay is found more probable in  $Z>114$

which reaches up to 95% for the case of  $^{294,295,296}\text{Og}$ . At various other places this decay competes with  $\alpha$ -decay and becomes more significant. As a result,  $^{83}\text{As}$ ,  $^{84-86}\text{Se}$ ,  $^{85-87}\text{Br}$ ,  $^{86,88,89}\text{Kr}$  clusters are found noteworthy to decay from  $^{291}\text{Mc}$ ,  $^{290-294}\text{Lv}$ ,  $^{291-295}\text{Ts}$ ,  $^{291-297}\text{Og}$  nuclei, respectively. This important outcome has been summarized in Fig. 6 as a periodic chart of the considered range. Most probable decay modes are mentioned by different colours in the diagram. Known decay modes as per NUBASE2020 [43] are pictured by shaded squares.

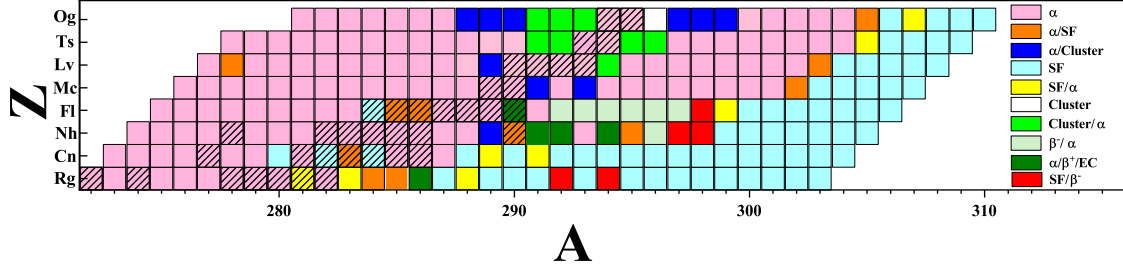


**Figure 6.** (Colour online) Chart of considered nuclei with their probable decay modes. Shaded blocks show experimental decay modes taken from Ref. [43].

#### 4. Conclusions

Theoretical calculations of half-lives of  $\alpha$ -decay, spontaneous fission, heavy-cluster decay and  $\beta$ -decay have been brought forward by using NMHF, MBF, UDL and Fiset & Nix formulas, respectively. The  $\alpha$ -decay half-lives of synthesized SHN ( $Z > 110$ ) are successfully reproduced by employing the NMHF formula which demonstrates the predictability of this formula in the superheavy region. NMHF formula has been used to calculate the favoured and unfavoured  $\alpha$ -decay half-lives of undetected SHN ranging from Rg to Og isotopes ( $161 \leq N \leq 192$ ). In addition to the  $\alpha$ -decay half-lives, spontaneous fission half-lives (using MBF formula) are also calculated for various possible decay chains in the mentioned range, which are consequently utilized to predict various unknown  $\alpha$ -transitions and probable decay chains of SHN as well.

The cluster decay modes are also investigated in the mentioned range using UDL formula through the study and as a result  $^{83}\text{As}$ ,  $^{84-86}\text{Se}$ ,  $^{85-87}\text{Br}$ ,  $^{86,88,89}\text{Kr}$  cluster emissions from  $^{291}\text{Mc}$ ,  $^{290-294}\text{Lv}$ ,  $^{291-295}\text{Ts}$ ,  $^{291-297}\text{Og}$  nuclei, respectively, are reported. Finally, a comparison among  $\alpha$ -decay, spontaneous fission, heavy-cluster decay and weak-decay modes is encased which establishes  $\alpha$ -decay and SF modes as the commanding mode of SHN, however, in few cases cluster decay mode is also found presiding over the  $\alpha$  or SF decay modes. Additionally, chances of weak-decay modes are found equally probable in some nuclei and hence requires more detailed attention in this region of periodic chart too. Conclusively, we have done a comprehensive and combined study of various types of decay viz.  $\alpha$ -decay, SF-decay including rarely found weak-decay (in superheavy region) and the cluster decay in the above mentioned range with their accurate estimation of half-lives together with uncertainties and different

branching ratios. This theoretical study may provide a useful impetus for the detection of superheavy elements in the near future.

## 5. Acknowledgement

AJ and GS acknowledge the support provided by SERB (DST), Govt. of India under CRG/2019/001851 and SIR/2022/000566, respectively.

## References

- [1] Hofmann S and Münzenberg G 2000 *Rev. Mod. Phys.* **72** 733.
- [2] Hofmann S 2011 *Radiochim. Acta* **99** 405.
- [3] Morita K *et al* 2007 *J. Phys. Soc. Japan* **76** 045001.
- [4] Hamilton J, Hofmann S and Oganessian Y T 2013 *Annu. Rev. Nucl. Part. Sci.* **63** 383.
- [5] Oganessian Y T *et al* 2010 *Phys. Rev. Lett.* **104** 142502.
- [6] Oganessian Y T and Utyonkov V 2015 *Nucl. Phys. A* **944** 62.
- [7] Oganessian Y T *et al* 2006 *Phys. Rev. C* **74** 044602.
- [8] Düllmann C E 2014 T. collaboration in *Fission and Properties of Neutron-Rich Nuclei* (World Scientific) pp. 271–277.
- [9] Heinz S 2012 in *EPJ Web of Conferences*, Vol. 38 (EDP Sciences) p. 01002.
- [10] Oganessian Y T *et al* 2009 *Phys. Rev. C* **79** 024603.
- [11] Hofmann S *et al* 2016 *Eur. Phys. J. A* **52** 1.
- [12] Voinov A *et al* 2020 *Bull. Russ. Acad. Sci.: Phys.* **84** 351.
- [13] Cheng J -H *et al* 2019 *Nucl. Phys. A* **987** 350.
- [14] Hofmann S, Münzenberg G, Hesseberger F and Schött H 1984 *Nucl. Instrum. Methods Phys. Res. B* **223** 312.
- [15] Zdeb A, Warda M and Pomorski K 2013 *Phys. Rev. C* **87** 024308.
- [16] Yong-Jia W, Hong-Fei Z, Wei Z and Jun-Qing L 2010 *Chin. Phys. Lett.* **27** 062103.
- [17] Poenaru D, Ivascu M and Sandulescu A 1979 *J. Phys. G: Nucl. Part. Phys.* **5** L169.
- [18] Royer G 2000 *J. Phys. G: Nucl. Part. Phys.* **26** 1149.
- [19] Cui J *et al* 2018 *Phys. Rev. C* **97** 014316.
- [20] Bao X, Zhang H, Zhang H, Royer G and Li J 2014 *Nucl. Phys. A* **921** 85.
- [21] Royer G and Zhang H 2008 *Phys. Rev. C* **77** 037602.
- [22] Santhosh K P, Akrawy D T, Hassanabadi H, Ahmed A H and Jose T A 2020 *Phys. Rev. C* **101** 064610.
- [23] Zanganah V, Akrawy D T, Hassanabadi H, Hosseini S and Thakur S 2020 *Nucl. Phys. A* **997** 121714.
- [24] Santhosh K P, Sahadevan S, Priyanka B and Unnikrishnan M 2012 *Nucl. Phys. A* **882** 49.
- [25] Saxena G, Jain A and Sharma P K 2021 *Phys. Scr.* **96** 125304.
- [26] Viola Jr V E and Seaborg G T 1966 *J. Inorg. Nucl. Chem.* **28** 741.
- [27] Sobiczewski A, Patyk Z and Cwiok S 1989 *Phys. Lett. B* **224** 1.
- [28] Parkhomenko A and Sobiczewski A 2005 *Acta Phys. Pol. B* **36** 3095.
- [29] Brown B A 1992 *Phys. Rev. C* **46** 811.
- [30] Ren Z, Xu C and Wang Z 2004 *Phys. Rev. C* **70** 034304.
- [31] Qi C, Xu F, Liotta R J and Wyss R 2009 *Phys. Rev. Lett.* **103** 072501.
- [32] Xu Y -Y *et al* 2022 *Eur. Phys. J. A* **58** 1.
- [33] Akrawy D T and Poenaru D N 2017 *J. Phys. G: Nucl. Part. Phys.* **44** 105105.
- [34] Akrawy D T, Hassanabadi H, Hosseini S S and Santhosh K P 2019 *Int. J. Mod. Phys. E* **28** 1950075.

- [35] Singh U K, Sharma P K, Kaushik M, Jain S K, Akrawy D T and Saxena G 2020 *Nucl. Phys. A* **1004** 122035.
- [36] Saxena G, Sharma P K and Saxena P 2021 *J. Phys. G: Nucl. Part. Phys.* **48** 055103.
- [37] Akrawy D T, Budaca A I, Saxena G and Ahmed A H 2022 *Eur. Phys. J. A* **58** 145.
- [38] Sharma P K, Jain A and Saxena G 2021 *Nucl. Phys. A* **1016** 122318.
- [39] Oganessian Y T, Sobiczewski A and Ter-Akopian G 2017 *Phy. Scr.* **92** 023003.
- [40] Oganessian Y T *et al* 1999 *Nature* **400** 242.
- [41] Forsberg U *et al* 2016 *Nucl. Phys. A* **953** 117.
- [42] Oganessian Y T *et al* 2000 *Phys. Rev. C* **62** 041604.
- [43] Kondev F G, Wang M, Huang W, Naimi S and Audi G 2020 *Chin. Phys. C* **45** 030001.
- [44] Bohr N and Wheeler J A 1939 *Phys. Rev.* **56** 426.
- [45] Flerov G N and Petrzhak K 1940 *Phys. Rev.* **58** 275.
- [46] Dvorak J *et al* 2006 *Phys. Rev. Lett.* **97** 242501.
- [47] Oganessian Y T *et al* 2005 *Phys. Rev. C* **72** 034611.
- [48] Swiatecki W 1955 *Phys. Rev.* **100** 937.
- [49] Ren Z and Xu C 2005 *Nucl. Phys. A* **759** 64.
- [50] Xu C, Ren Z and Guo Y 2008 *Phys. Rev. C* **78** 044329.
- [51] Bao X, Guo S, Zhang H, Xing Y, Dong J and Li J 2015 *J. Phys. G: Nucl. Part. Phys.* **42** 085101.
- [52] Santhosh K P and Nithya C 2016 *Phys. Rev. C* **94** 054621.
- [53] Soylu A 2019 *Chin. Phys. C* **43** 074102.
- [54] Santhosh K P, Tinu Ann Jose and Deepak N K 2021 *Phys. Rev. C* **103** 064612.
- [55] Heßberger F P 2017 *Eur. Phys. J. A* **53** 75.
- [56] Reinhard P G 2018 *Eur. Phys. J. A* **54** 13.
- [57] Poenaru D, Gherghescu R and Greiner W 2012 *Phys. Rev. C* **85** 034615.
- [58] Santhosh K P and Jose T A 2021 *Pramana* **95** 162.
- [59] Santhosh K P and Jose T A 2019 *Phys. Rev. C* **99** 064604.
- [60] Soylu A and Qi C 2021 *Nucl. Phys. A* **1013** 122221.
- [61] Sowmya N, Manjunatha H, Gupta P D and Dhananjaya N 2021 *Braz. J. Phys.* **51** 99.
- [62] Sandulescu A, Poenaru D and Greiner W 1980 *Sov. J. Part. Nucl. II* **11** 528.
- [63] Rose H and Jones G 1984 *Nature* **307** 245.
- [64] Barwick S, Price P, Ravn H, Hourani E and Hussonnois M 1986 *Phys. Rev. C* **34** 362.
- [65] Bonetti R and Guglielmetti A 2007 *Rom. Rep. Phys.* **59** 301.
- [66] Zhang Y, Wang Y *et al* 2018 *Phys. Rev. C* **97** 014318.
- [67] Soylu A, Koyuncu F 2019 *Eur. Phys. J A* **55** 118.
- [68] Santhosh K P and Nithya C 2018 *Phys. Rev. C* **97** 064616.
- [69] Poenaru D and Gherghescu R 2018 *Phys. Rev. C* **97**, 044621.
- [70] Poenaru D, Stöcker H and Gherghescu R 2018 *Eur. Phys. J. A* **54** 14.
- [71] Matheson Z, Giuliani S A and Nazarewicz W, Sadhukhan J, Schunck N 2018 *Phys. Rev. C* **99** 041304.
- [72] Warda M, Zdeb A, and Robledo L M 2018 *Phys. Rev. C* **98** 941602(R).
- [73] Jain A, Sharma R, Jain S K, Sharma P K and Saxena G 2021 *Hyperfine Interact.* **242** 1.
- [74] Qi C, Xu F, Liotta R J and Wyss R 2009 *Phys. Rev. Lett.* **103** 072501.
- [75] Oganessian Y T *et al* 2011 *Phys. Rev. C* **83** 054315.
- [76] Karpov A *et al* 2012 *Int. J. Mod. Phys. E* **21** 1250013.
- [77] Zhang X and Ren Z 2006 *Phys. Rev. C* **73** 014305.
- [78] Zhang X, Ren Z, Qijun Zhi and Qiang Zheng 2007 *J. Phys. G: Nucl. Part. Phys.* **73** 2611.
- [79] Sobhani H and Khalafi H 2022 *Chin. J. of Phys.* <https://doi.org/10.1016/j.cjph.2022.10.011>.
- [80] Möller P, Mumpower M R, Kawano T and Myers W D 2019 *At. Data Nucl. Data Tables* **125** 1.
- [81] Hirsch M, Staudt A, Muto K and Klapdorkleingrothaus H 1993 *At. Data Nucl. Data Tables* **53** 165.
- [82] Sarriguren P 2019 *Phys. Rev. C* **100** 014309.

- [83] Sarriguren P, Algora A, Kiss G 2018 *Phys. Rev. C* **98** 024311.
- [84] Fiset E and Nix J 1972 *Nucl. Phys. A* **193** 647.
- [85] Saxena G, Kumawat M, Singh S S and Aggarwal M 2019 *Int. J. Mod. Phys. E* **28** 1950008.
- [86] Sharma R, Jain A, Sharma P K, Jain S K and Saxena G 2022 *Phys. Scr.* **97** 045307.
- [87] Wang M, Huang W, Kondev F, Audi G Naimi S 2020 *Chin. Phys. C* **45** 030003.
- [88] Wang N, Liu M, Wu X and Meng J 2014 *Phys. Lett. B* **734** 215.
- [89] Akrawy D T, Hassanabadi H, Qian Y and Santhosh K P 2019 *Nucl. Phys. A* **983** 310.
- [90] Ismail Y, Ellithi A Y, Adel A and Abbas M A 2022 *Phys. Scr.* **97** 075303.
- [91] Akrawy D T and Ahmed A H 2019 *Phys. Rev. C* **100** 044618.
- [92] Deng J -G, Zhang H -F and Royer G 2020 *Phys. Rev. C* **101** 034307.
- [93] Akrawy D T, Hassanabadi H, Hosseini S and Santhosh K P 2018 *Nucl. Phys. A* **971** 130.
- [94] Akrawy D T, Ahmed Ali H 2018 *Int. J. Mod. Phys. E* **27** 1850068.
- [95] Akrawy D T, Hassanabadi H, Hosseini S and Santhosh K P 2018 *Nucl. Phys. A* **975** 19.
- [96] Yang-Yang Xu *et al* 2022 *Eur. Phys. J. A* **58** 163.
- [97] Ismail M, Ellithi A Y, Adela A and Abbas M A 2022 *Eur. Phys. J. A* **58** 225.
- [98] Cheng S, Wu W, Cao L and Zhang F S 2022 *Eur. Phys. J. A* **58** 168.
- [99] Denisov V Y and Khudenko A 2009 *At. Data Nucl. Data Tables* **95** 815.
- [100] <https://t2.lanl.gov/nis/data/astro/molnix96/spidat.html>
- [101] Royer G and Moustabchir R, 2001 *Nucl. Phys. A* **683** 182.
- [102] Balasubramaniam M *et al* 2004 *Phys. Rev. C* **70** 017301.
- [103] Horoi M 2004 *J. Phys. G: Nucl. Part. Phys.* **30** 945.
- [104] Ni D, Ren Z, Dong T, Xu C 2008 *Phys. Rev. C* **78** 044310.
- [105] Poenaru D N, Gherghescu R A and Greiner W 2011 *Phys. Rev. C* **83** 014601.
- [106] Tavares O A P and Medeiros E L 2018 *Eur. Phys. J. A* **54** 65.
- [107] Soylu A and Qi C 2021 *Nucl. Phys. A* **1013** 122221.
- [108] Jain A, Sharma P K, Jain S K, Deegwal J K and Saxena G, 2023 *Nucl. Phys. A* **1031** 122597.
- [109] Zhang Y L and Wang Y Z 2018 *Phys. Rev. C* **97** 014318.
- [110] Seeger P A, Fowler W A, Clayton D D 1965 *The AstroPhys. J* suppl. no. 97 **XI** 121.
- [111] Yadav H, Kaushik M, Toki H 2004 *Int. J. Mod. Phys. E* **13** 647.
- [112] Saxena G, Kumawat M, Kaushik M, Jain S K, Aggarwal M 2017 *Phys. Lett. B* **775** 126.
- [113] Saxena G, Singh U K, Kumawat M, Kaushik M, Jain S K and Aggarwal M 2018 *Int. J. Mod. Phys. E* **27** 1850074.
- [114] Möller P, Sierk A, Ichikawa T, *et al* 2019 *At. Data Nucl. Data Tables* **125** 1.
- [115] Xia X *et al* 2018 *At. Data Nucl. Data Tables* **121** 1.
- [116] Denisov V Y and Khudenko A A 2009 *Phys. Rev. C* **79** 054614.
- [117] Huang K -N, Aoyagi M, Chen, Crasemann B, Mark H 1976 *At. Data Nucl. Data Tables* **18** 243.
- [118] Andreyev A N *et al* 2013 *Phys. Rev. Lett.* **110** 242502.
- [119] Sarriguren P 2020 *J. Phys. G: Nucl. Part. Phys.* **47** 125107.
- [120] Sarriguren P 2021 *Phys. Lett. B* **815** 136149.
- [121] Sarriguren P 2022 *Phys. Rev. C* **105** 014312.

## 6. Appendix

**Table 5.**  $\alpha$ -decay half-lives and prediction of decay chains of  $^{281,301-305}\text{Og}$ ,  $^{299,301,303}\text{Ts}$  and  $^{275}\text{Lv}$  and their decay modes using NMHF formula.  $Q_\alpha$ -values (with uncertainties  $\pm 0.04$  MeV) are taken from WS4 mass model [88] and spin-parities are taken from Ref. [100]. Spontaneous Fission (SF) half-lives are calculated by MBF formula [36].

Nucleus	$Q_\alpha$ (MeV)	$j_p^\pi$	$j_d^\pi$	$l$	$\log_{10}T_{1/2}(\text{s})$		Predicted Decay Mode	Nucleus	$Q_\alpha$ (MeV)	$j_p^\pi$	$j_d^\pi$	$l$	$\log_{10}T_{1/2}(\text{s})$		Predicted Decay Mode
					NMHF	MBF							NMHF	MBF	
					( $\alpha$ )	(SF)							( $\alpha$ )	(SF)	
$^{305}\text{Og}$	12.91	5/2 <sup>+</sup>	1/2 <sup>+</sup>	2	-4.71 $\pm$ 0.07	-4.72	$\alpha$	$^{304}\text{Og}$	13.12	0 <sup>+</sup>	0 <sup>+</sup>	0	-5.13 $\pm$ 0.07	-3.25	$\alpha$
$^{301}\text{Lv}$	11.58	1/2 <sup>+</sup>	1/2 <sup>+</sup>	0	-2.73 $\pm$ 0.08	2.41	$\alpha$	$^{300}\text{Lv}$	10.92	0 <sup>+</sup>	0 <sup>+</sup>	0	-1.36 $\pm$ 0.09	3.16	$\alpha$
$^{297}\text{Fl}$	8.35	1/2 <sup>+</sup>	3/2 <sup>+</sup>	2	5.05 $^{+0.22}_{-0.03}$	7.41	$\alpha$	$^{296}\text{Fl}$	8.56	0 <sup>+</sup>	0 <sup>+</sup>	0	4.25 $\pm$ 0.12	5.15	$\alpha$
$^{293}\text{Cn}$	8.19	3/2 <sup>+</sup>	1/2 <sup>+</sup>	2	5.02 $^{+0.23}_{-0.04}$	3.69	SF	$^{292}\text{Cn}$	8.28	0 <sup>+</sup>	0 <sup>+</sup>	0	4.55 $\pm$ 0.13	0.63	SF
$^{303}\text{Og}$	12.61	7/2 <sup>+</sup>	1/2 <sup>+</sup>	4	-4.15 $\pm$ 0.07	1.32	$\alpha$	$^{302}\text{Og}$	12.04	0 <sup>+</sup>	0 <sup>+</sup>	0	-3.21 $\pm$ 0.08	1.96	$\alpha$
$^{299}\text{Lv}$	10.84	1/2 <sup>+</sup>	3/2 <sup>+</sup>	2	-1.05 $^{+0.18}_{-0.01}$	7.23	$\alpha$	$^{298}\text{Lv}$	10.77	0 <sup>+</sup>	0 <sup>+</sup>	0	-1.06 $\pm$ 0.09	5.01	$\alpha$
$^{295}\text{Fl}$	8.61	3/2 <sup>+</sup>	1/2 <sup>+</sup>	2	4.23 $^{+0.22}_{-0.03}$	8.54	$\alpha$	$^{294}\text{Fl}$	8.71	0 <sup>+</sup>	0 <sup>+</sup>	0	3.75 $\pm$ 0.12	5.69	$\alpha$
$^{291}\text{Cn}$	8.59	1/2 <sup>+</sup>	1/2 <sup>+</sup>	0	3.59 $\pm$ 0.12	3.43	SF/ $\alpha$	$^{290}\text{Cn}$	8.87	0 <sup>+</sup>	0 <sup>+</sup>	0	2.72 $\pm$ 0.12	0.09	SF
$^{287}\text{Ds}$	7.77	1/2 <sup>+</sup>	1/2 <sup>+</sup>	0	5.66 $\pm$ 0.14	-0.16	SF	-	-	-	-	-	-	-	
$^{301}\text{Og}$	12.02	1/2 <sup>+</sup>	3/2 <sup>+</sup>	2	-3.04 $^{+0.17}_{-0.02}$	6.06	$\alpha$	$^{281}\text{Og}$	13.76	13/2 <sup>-</sup>	3/2 <sup>+</sup>	5	-5.78 $^{+0.66}_{-0.53}$	-1.02	$\alpha$
$^{297}\text{Lv}$	10.84	3/2 <sup>+</sup>	1/2 <sup>+</sup>	2	-1.07 $^{+0.18}_{-0.01}$	8.49	$\alpha$	$^{277}\text{Lv}$	13.12	3/2 <sup>+</sup>	1/2 <sup>+</sup>	2	-5.72 $^{+0.16}_{-0.03}$	-1.04	$\alpha$
$^{293}\text{Fl}$	8.78	1/2 <sup>+</sup>	1/2 <sup>+</sup>	0	3.52 $^{+0.12}_{-0.12}$	8.68	$\alpha$	$^{273}\text{Fl}$	12.97	1/2 <sup>+</sup>	11/2 <sup>-</sup>	5	-5.30 $^{+0.66}_{-0.53}$	-3.51	$\alpha$
$^{289}\text{Cn}$	9.05	1/2 <sup>+</sup>	1/2 <sup>+</sup>	0	2.22 $^{+0.11}_{-0.11}$	2.21	SF/ $\alpha$	$^{269}\text{Cn}$	12.57	11/2 <sup>-</sup>	7/2 <sup>+</sup>	3	-5.47 $^{+0.28}_{-0.15}$	-4.71	$\alpha$
$^{285}\text{Ds}$	7.80	1/2 <sup>+</sup>	5/2 <sup>+</sup>	2	5.67 $^{+0.23}_{-0.04}$	1.34	SF	$^{265}\text{Ds}$	12.33	7/2 <sup>+</sup>	11/2 <sup>-</sup>	3	-5.49 $^{+0.28}_{-0.15}$	-2.70	$\alpha$
-	-	-	-	-	-	-	-	$^{261}\text{Hs}$	10.96	11/2 <sup>-</sup>	9/2 <sup>-</sup>	2	-3.51 $^{+0.18}_{-0.01}$	-0.80	$\alpha$
-	-	-	-	-	-	-	-	$^{257}\text{Sg}$	9.71	9/2 <sup>-</sup>	7/2 <sup>+</sup>	1	-1.37 $^{+0.12}_{-0.07}$	-0.44	$\alpha$ /SF
$^{303}\text{Ts}$	12.78	1/2 <sup>-</sup>	5/2 <sup>-</sup>	2	-4.59 $^{+0.16}_{-0.03}$	1.85	$\alpha$	$^{301}\text{Ts}$	11.61	1/2 <sup>-</sup>	5/2 <sup>-</sup>	2	-2.44 $^{+0.18}_{-0.02}$	7.11	$\alpha$
$^{299}\text{Mc}$	9.59	5/2 <sup>-</sup>	5/2 <sup>-</sup>	0	1.60 $\pm$ 0.11	7.80	$\alpha$	$^{297}\text{Mc}$	9.59	5/2 <sup>-</sup>	5/2 <sup>-</sup>	0	1.56 $^{+0.10}_{-0.11}$	9.58	$\alpha$
$^{295}\text{Nh}$	8.15	7/2 <sup>-</sup>	3/2 <sup>-</sup>	2	5.42 $^{+0.23}_{-0.04}$	6.47	$\alpha$	$^{293}\text{Nh}$	8.48	7/2 <sup>-</sup>	3/2 <sup>-</sup>	2	4.34 $^{+0.22}_{-0.03}$	7.17	$\alpha$
$^{291}\text{Rg}$	7.87	3/2 <sup>-</sup>	1/2 <sup>+</sup>	1	5.71 $^{+0.16}_{-0.11}$	1.76	SF	$^{289}\text{Rg}$	8.30	3/2 <sup>-</sup>	9/2 <sup>-</sup>	4	4.68 $^{+0.51}_{-0.25}$	1.26	SF
$^{299}\text{Ts}$	11.46	1/2 <sup>-</sup>	5/2 <sup>-</sup>	2	-2.16 $^{+0.18}_{-0.01}$	9.02	$\alpha$	$^{275}\text{Lv}$	13.51	1/2 <sup>+</sup>	11/2 <sup>-</sup>	5	-5.82 $^{+0.47}_{-0.34}$	-5.24	$\alpha$ /SF
$^{295}\text{Mc}$	9.72	5/2 <sup>-</sup>	1/2 <sup>-</sup>	2	1.33 $^{+0.20}_{-0.01}$	10.31	$\alpha$	$^{271}\text{Fl}$	13.40	11/2 <sup>-</sup>	9/2 <sup>+</sup>	1	-6.70 $^{+0.56}_{-0.68}$	-7.19	$\alpha$ /SF
$^{291}\text{Nh}$	8.91	1/2 <sup>-</sup>	13/2 <sup>+</sup>	7	4.22 $^{+1.28}_{-1.05}$	6.75	$\alpha$	$^{267}\text{Cn}$	13.05	9/2 <sup>+</sup>	11/2 <sup>-</sup>	1	-6.55 $^{+0.60}_{-0.72}$	-6.58	$\alpha$ /SF
$^{287}\text{Rg}$	8.44	13/2 <sup>+</sup>	9/2 <sup>-</sup>	3	4.02 $^{+0.34}_{-0.09}$	3.07	SF	$^{263}\text{Ds}$	12.34	11/2 <sup>-</sup>	9/2 <sup>-</sup>	2	-5.68 $^{+0.38}_{-0.51}$	-4.02	$\alpha$
-	-	-	-	-	-	-	-	$^{259}\text{Hs}$	10.79	9/2 <sup>-</sup>	5/2 <sup>+</sup>	3	-3.08 $^{+0.25}_{-0.09}$	-2.79	$\alpha$ /SF
-	-	-	-	-	-	-	-	$^{255}\text{Sg}$	9.90	5/2 <sup>+</sup>	5/2 <sup>+</sup>	0	-1.92 $\pm$ 0.09	-3.97	SF

# Deformation dependence of 2p-radioactivity half-lives: Probe with a new formula across the mass region with $Z < 82$

G. Saxena<sup>1,§</sup>, Mamta Aggarwal<sup>2,†</sup>, D. Singh<sup>3</sup>, A. Jain<sup>1,4</sup>, P. K. Sharma<sup>5</sup> and H. L. Yadav<sup>6</sup>

<sup>1</sup>Department of Physics (H&S), Govt. Women Engineering College, Ajmer-305002, India

<sup>2</sup>Department of Physics, University of Mumbai, Kalina, Mumbai-400098, India

<sup>3</sup>Department of Physics, University of Rajasthan, Jaipur-302002, India

<sup>4</sup>Department of Physics, Manipal University Jaipur, Jaipur-303007, India

<sup>5</sup>Govt. Polytechnic College, Rajsamand-313324, India

<sup>6</sup>Physics Department, Banaras Hindu University, Varanasi-221005, India.

E-mail: <sup>†</sup>mamta.a4@gmail.com, <sup>§</sup>gauravphy@gmail.com

July 2022

**Abstract.** Effect of deformation on half-life of two-proton (2p) radioactivity is investigated across the periodic chart for nuclei with  $Z < 82$ . 2p-decay half-lives are estimated by employing our newly proposed semi-empirical formula wherein the nuclear deformation has been incorporated in a phenomenological way. Robustness of the formula is demonstrated as it estimates the measured values quite accurately and, hence, reliably applied to predict the other possible 2p-emitters. For many proton rich nuclei for which experimental data on the decay energies are not available, we have used the theoretical values obtained from our calculations using the relativistic mean-field (RMF) approach. The uncertainties in the theoretical decay energy values are minimised by machine learning (ML) technique. Correlation of 2p-radioactivity with 2p-halo and deformation is probed. Our calculations show the phenomenon of shape coexistence in several 2p-emitters, wherein the prolate shape is found to be more predominant for the ground state.

*Keywords:* 2p-decay; Half-lives; Deformation; Shape-coexistence; Empirical formula.

Submitted to: *J. Phys. G: Nucl. Phys.*

## 1. Introduction

Two-proton radioactivity is a rare and lesser known exotic charged-particle decay mode, in which the valence protons are no longer bound by the strong nuclear forces and where the Coulomb and centrifugal barriers along with the structural effects prevent the proton emission and slow down the decay process that enables the life-times to

be long enough to probe the atomic structure [1–3]. The prediction of two-proton emission half-lives is generally difficult for the unknown nuclei as they crucially depend upon the accurate estimate of 2p-decay energy ( $Q_{2p}$ ) evaluated with high precision which itself is quite a challenging task in exotic nuclei. The deformation effects that increase the number of particles in the classically forbidden region below the continuum threshold and also contribute to pairing, influence the decay modes and the decay energy as well. Some recent works have speculated the phenomenon of shape coexistence, arising out of the competing shapes, to bring about the structural changes in the exotic nuclei and to affect the half-lives [4, 5], which has significant implications in the phenomena like r-process in nuclear astrophysics. In view of this possible significance of deformation in the stability of nuclear systems [6, 7],  $Q_{2p}$  and consequently the life-times, the structural effects must be incorporated in the evaluation of accurate  $Q_{2p}$  and half-life values. The nuclei with  $Q_{2p} > 0$  and  $Q_p < 0$  define 2p-radioactivity [8–20], where the simultaneous emission of p-p subsystem of valence protons [1] is allowed after the tunneling through the barrier, but the sequential emission or 1p-decay is strongly suppressed by diproton correlations indicating the sensitivity of 2p-decay on pairing between the valence protons. The diproton weakly bound system in the decay channel might form a halo like structure [21–23] and support the enhanced probability of direct 2p-decay as shown by us [20] or may have deformed states [24] that are expected to impact the Q-values and consequently the decay modes of such diproton systems in competition with the  $\beta$ -decay and 1p-decay which needs investigation.

2p-decay life-time measurements have become a thrust area of research in recent times primarily due to the access to 2p-emitters, which has so far reached up to the light mass nuclei  $^{45}\text{Fe}$ ,  $^{54}\text{Zn}$ ,  $^{48}\text{Ni}$ ,  $^{19,20,22}\text{Mg}$ ,  $^{30,31}\text{Ar}$ ,  $^{22}\text{Si}$  and  $^{67}\text{Kr}$  [8, 9, 25–36]. Recent measurement of 2p-decay life-time of  $^{67}\text{Kr}$  has indicated the impact of shape deformation on 2p-radioactivity [24] and its sensitivity to the orbital configuration ( $l$ ) and proton-proton interaction. 2p-decay life-time is sensitive to  $l$  value as the centrifugal potential energy can reduce the tunneling probability and increase the half-life. The deformation dependency of 2p-radioactivity first speculated by Mukha *et al.* [37] and then theoretically investigated by us [7, 19, 20, 38, 39] and more recently by Santhosh [40] is expected to impact 2p-decay life-times, but it still remains a lesser explored area of research and is precisely the main objective of this work.

To explore the deformation effects on 2p-radioactivity, we first propose a semi-empirical relation to estimate 2p-decay half-lives by incorporating the quadrupole deformation in addition to the Q-value and angular momentum ( $l$ ) sensitivity. The parameters of this relation are obtained in a way as to provide a best fit to the half-lives of experimentally known 2p-radioactive nuclei. As most of these proton rich nuclei lie close to the proton drip line, their measured values of deformations are not as yet available. Thus for our purpose we have instead utilized the theoretical values obtained from the relativistic mean-field (RMF) calculations [18, 41, 42]. The formula thus obtained is found to perform much better than the other existing formulae [43, 44] and theories [40, 45–51] for the 2p-decay life-times. Encouraged by this we have employed it to investigate and



predict the possible candidates of 2p-emitters across the entire mass region with  $Z < 82$ .

For many nuclei near the proton drip line even the accurate experimental Q-values are not available. Again we have taken recourse to using the theoretical RMF [18,41,42] values for the 2p-decay energy  $Q_{2p}$ . However, 2p-decay half-lives being sensitive to the  $Q_{2p}$ , we have used the machine learning technique to minimize the uncertainties in theoretical  $Q_{2p}$  values. Furthermore, 2p-emitters, being located near the drip line are expected to exhibit shape coexistence and possible halo formations. These two aspects have been demonstrated here by carrying out quadrupole constrained RMF calculations [18,41,42] for the 2p-emitters which are experimentally known as well as those predicted by our formula.

## 2. Formula for half-life

The already existing semi-empirical formulae [43,44] to evaluate the 2p-decay half-life consider the linear dependency of  $\log_{10}T_{1/2}$  on  $Z_d^{0.8}/\sqrt{Q}$  in a similar way as done for  $\alpha$ -decay and 1p-decay. The  $\alpha$ -emission half-lives have shown significant improvement by including the deformation effects [52] which is also speculated for  $\beta$ -decay [5], proton emission [53] as well as two-proton emission [40,53]. In fact, the proton and  $\alpha$ -emission both may be described by similar formulas with different parameters as both the decay modes are quantum tunneling effect. However, studies have shown [54] that the half-life is more sensitive to the Q-value for proton emission than that for the  $\alpha$ -decay, due to smaller reduced mass and also due to high centrifugal barrier. This implies that it is difficult to predict the half-life of proton emission for nuclei for which  $l$  and Q-values are not available with good accuracy. Despite these difficulties, here we attempt to study the 2p-decay half-lives of nuclei across the mass region for  $Z < 82$  employing a semi-empirical relation which includes its explicit dependence on the Q-value, the reduced mass  $\mu$ , angular momentum  $l$  carried by the emitted particles, and the quadrupole deformation  $\beta$ . This is expressed by

$$\log_{10}T_{1/2} = a + b\sqrt{\mu}\sqrt{Z_d A^{1/3}} + c\sqrt{\mu}\left(\frac{Z_d}{\sqrt{Q}}\right) + d\sqrt{l(l+1)} + e|\beta|^p \quad (1)$$

where the symbols a, b, c, d, e, and p represent the parameters to be determined in a least square fit to the experimental data. Here, the half-life is in the unit of seconds,  $Z_d$  is the proton number of the daughter nucleus, and  $A$  denotes the mass number of the parent nucleus. The form of the first three terms is basically similar to that obtained in the semi-classical treatment for the evaluation of the expression for the transmission coefficient of an  $\alpha$ -particle through a Coulomb barrier [55,56]. The term  $\sqrt{l(l+1)}$  reflects the hindrance effect of the centrifugal barrier [57]. The form of the last term represents in a phenomenological way the effect of quadrupole deformation motivated by the detailed studies of Ref. [58] in which  $\alpha$  emission probability has been found to increase by an exponential factor with increasing  $\beta$ . Since the nuclei being studied in this work lie at or beyond the proton drip line, the experimental values of  $\beta$  for all these nuclei are not available as yet. Hence for our purpose in Eqn. (1), we use

the  $\beta$  values obtained from the RMF theory [18, 41, 42]. The  $\beta$  deformation computed using the RMF approach are known to be in good agreement with those obtained using other theories, for example, Hartree-Fock-Bogoliubov (HFB) [59], Finite Range Droplet Model (FRDM) [60], and Weizsaecker-Skyrme-4 model (WS4) [61]. Also, so far there are no experimental data available for the 2p-radioactivity with  $l \neq 0$ . However, as in Refs. [43, 44], we have used 2p-radioactivity half-lives of 7 nuclei with  $l \neq 0$  extracted from [46] for our database, which are mentioned separately in Table 1 wherein these have been indicated as 'other data'. The purpose of inclusion of such data for the fitting procedure is to test and also elucidate the quality of results obtained with the present approach for the  $l \neq 0$  cases. Thus together we have used a set of 24 measured radioactive 2p-decay cases with experimental  $Q_{2p}$  and  $\log_{10}T_{1/2}$  values as shown in Table 1 for the fitting of Eqn. (1) as described briefly below.

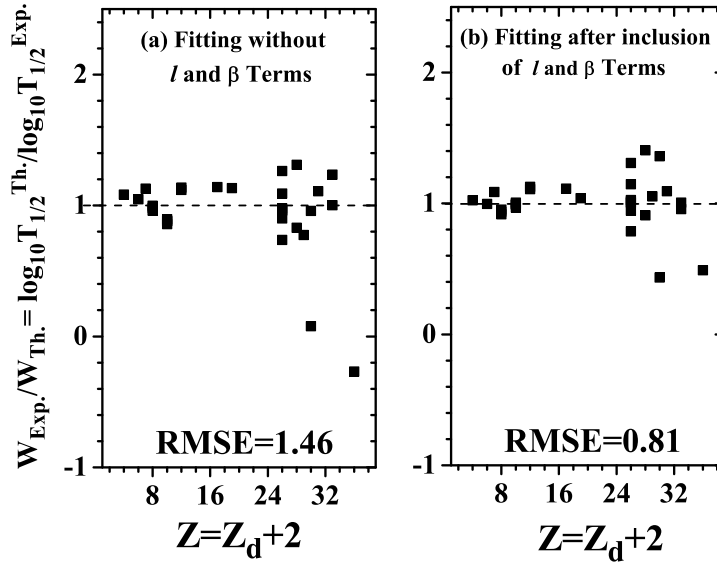


**Figure 1.** Ratio of experimental to theoretical decay widths  $W_{Exp.}/W_{Th.} = \log_{10}T_{1/2}^{Th.}/\log_{10}T_{1/2}^{Exp.}$  for a best fit of our formula given by Eqn. (1) (a) without the angular momentum and deformation dependent terms, and (b) including the angular momentum and deformation dependent terms.

**Table 1.** Comparison of present results (column 6) for the logarithmic half-lives  $\log_{10}T_{1/2}$  of 2p-emitters (column 1) with the experimental values (column 5) and other theoretical predictions (columns 7-16) [40,43–51]. For the experimental  $Q_{2p}$ ,  $l$  and half-life values the respective references are mentioned in the table. As the measured values for deformation  $\beta$  are not available, we have used the values computed from the RMF theory (see text for details). Here abbreviations GLDM and ELDM denote the generalized and effective liquid drop models; GLM stands for the Gamow- like model; SEB for the screened electrostatic barrier; UFM for the unified fission model; CPPM for the Coulomb and proximity potential model whereas CPPMDN refers to the CPPM for the deformed nuclei.

2p Emitter	$Q_{2p}$ (MeV)	$l$	$\beta$	$\log_{10}T_{1/2}$ (sec.)											
				Data	Present Formula	Sreeja [43]	Liu [44]	GLDM [45]	ELDM [46]	Taveres [47]	GLM [48]	SEB [49]	UFM [50]	CPPMDN [40]	CPPM [51]
Experimental Data															
${}^6\text{Be}$	$1.37 \pm 0.005$	0	0.00	$-20.30^{+0.04}_{-0.02}$ [62]	$-21.04 \pm 0.09$	-21.95	-23.81	$-19.37^{+0.01}_{-0.01}$	-19.97		-19.70	-19.86	$-19.41^{+0.003}_{-0.003}$	-21.91	
${}^{12}\text{O}$	$1.64 \pm 0.024$	0	0.00	$> -20.20$ [63]	$-19.16 \pm 0.11$	-18.47	-20.17	$-19.17^{+0.13}_{-0.08}$	-18.27		-18.04	-17.70	$-18.45^{+0.04}_{-0.03}$	-20.90	
${}^{12}\text{O}$	$1.82 \pm 0.12$	0	0.00	$-20.94^{+0.41}_{-0.19}$ [64]	$-19.43 \pm 0.11$		-20.52	$-19.46^{+0.13}_{-0.07}$			-18.30	-18.03	$-18.69^{+0.15}_{-0.14}$	-21.22	
${}^{12}\text{O}$	$1.79 \pm 0.04$	0	0.00	$-20.10^{+0.18}_{-0.13}$ [65]	$-19.39 \pm 0.11$		-20.46	$-19.43^{+0.04}_{-0.03}$			-18.26	-17.98	$-18.65^{+0.05}_{-0.05}$	-21.17	
${}^{12}\text{O}$	$1.80 \pm 0.40$	0	0.00	$-20.12^{+0.75}_{-0.26}$ [66]	$-19.40 \pm 0.11$		-20.48	$-19.44^{+0.30}_{-0.20}$			-18.27	-18.00	$-18.66^{+0.62}_{-0.41}$	-21.19	
${}^{16}\text{Ne}$	$1.33 \pm 0.80$	0	0.44	$-20.64^{+0.30}_{-0.18}$ [64]	$-20.23 \pm 0.22$	-15.94	-17.53	$-16.45^{+0.23}_{-0.21}$			-16.23	-15.47	$-16.49^{+0.24}_{-0.22}$	-18.01	
${}^{16}\text{Ne}$	$1.40 \pm 0.20$	0	0.44	$-20.38^{+0.20}_{-0.13}$ [67]	$-20.43 \pm 0.22$	-16.16	-17.77	$-16.63^{+0.05}_{-0.05}$	-16.60		-16.43	-15.71	$-16.68^{+0.05}_{-0.05}$	-18.25	
${}^{19}\text{Mg}$	$0.75 \pm 0.05$	0	-0.24	$-11.40^{+0.15}_{-0.35}$ [68]	$-12.88 \pm 0.16$	-10.66	-12.03	$-11.79^{+0.47}_{-0.42}$	-11.72		-11.46	-10.92	$-11.77^{+0.47}_{-0.43}$	-11.96	-12.17
${}^{45}\text{Fe}$	$1.10 \pm 0.10$	0	0.00	$-2.40^{+0.24}_{-0.15}$ [25]	$-2.08 \pm 0.20$		-2.21	$-2.23^{+1.34}_{-1.17}$			-2.09	-2.30	$-1.94^{+1.34}_{-1.18}$	-2.76	-2.07
${}^{45}\text{Fe}$	$1.14 \pm 0.04$	0	0.00	$-2.07^{+0.24}_{-0.21}$ [26]	$-2.57 \pm 0.20$	-1.66	-2.64	$-2.71^{+0.61}_{-0.57}$			-2.58	-2.66	$-2.43^{+0.61}_{-0.58}$	-2.36	-2.55
${}^{45}\text{Fe}$	$1.21 \pm 0.05$	0	0.00	$-2.42 \pm 0.03$ [69]	$-3.36 \pm 0.20$	-2.34	-3.35	$-3.50^{+0.56}_{-0.52}$			-3.37	-3.27	$-3.23^{+0.56}_{-0.52}$	-3.15	-3.33
${}^{45}\text{Fe}$	$1.154 \pm 0.016$	0	0.00	$-2.52^{+0.12}_{-0.09}$ [28]	$-2.73 \pm 0.20$	-1.81	-2.79	$-2.87^{+0.19}_{-0.18}$	-2.43		-2.74	-2.79	$-2.60^{+0.19}_{-0.18}$	-2.53	-2.71
${}^{48}\text{Ni}$	$1.35 \pm 0.02$	0	0.00	$-2.08^{+0.34}_{-0.52}$ [28]	$-3.10 \pm 0.21$	-2.13	-3.13	$-3.24^{+0.2}_{-0.2}$			-3.21	-3.02	$-2.91^{+0.21}_{-0.19}$	-2.79	-3.03
${}^{48}\text{Ni}$	$1.29 \pm 0.04$	0	0.00	$-2.52^{+0.41}_{-0.18}$ [70]	$-2.48 \pm 0.21$	-1.61	-2.59	$-2.62^{+0.44}_{-0.42}$			-2.59	-2.54	$-2.29^{+0.44}_{-0.41}$	-2.17	-2.41
${}^{54}\text{Zn}$	$1.48 \pm 0.02$	0	0.27	$-2.43^{+0.26}_{-0.12}$ [27]	$-3.48 \pm 0.23$	-1.83	-2.81	$-2.95^{+0.19}_{-0.19}$	-2.52		-3.01	-2.82	$-2.61^{+0.19}_{-0.19}$	-2.59	-2.79
${}^{54}\text{Zn}$	$1.28 \pm 0.21$	0	0.27	$-2.76^{+0.19}_{-0.12}$ [8]	$-1.39 \pm 0.24$	-0.10	-1.01	$-0.87^{+0.25}_{-0.24}$			-0.93	-1.24	$-0.52^{+2.80}_{-2.18}$	-1.45	-0.71
${}^{67}\text{Kr}$	$1.69 \pm 0.017$	0	-0.27	$-1.70 \pm 0.18$ [71]	$-0.99 \pm 0.26$	0.31	-0.58	$-1.25^{+0.16}_{-0.16}$	-0.06		-0.76	-0.87	$-0.54^{+0.16}_{-0.16}$	-1.06	-0.22
'Other Data' ‡ [46]															
${}^{10}\text{N}$	1.30	1	0.25	-17.64	$-18.77 \pm 0.14$	-20.04	-18.59		-17.64		-17.36	-17.30	-18.07		
${}^{28}\text{Cl}$	1.97	2	0.30	-12.95	$-13.86 \pm 0.21$	-14.52	-12.46		-12.95	$-11.19^{+0.31}_{-0.29}$	-13.11	-12.16			
${}^{32}\text{K}$	2.08	2	-0.12	-12.25	$-12.16 \pm 0.19$	-13.46	-11.55		-12.25	$-10.62^{+0.32}_{-0.30}$	-12.49	-11.49			
${}^{52}\text{Cu}$	0.77	4	0.19	9.36	$9.57 \pm 0.28$	8.62	8.74		9.36		8.94				
${}^{57}\text{Ga}$	2.05	2	0.25	-5.30	$-5.18 \pm 0.26$	-5.22	-4.14		-5.30	$-5.80^{+0.51}_{-0.49}$	-5.91	-5.04			
${}^{60}\text{As}$	3.49	4	0.22	-8.68	$-8.46 \pm 0.27$	-10.84	-8.33		-8.68	$-10.95^{+0.42}_{-0.45}$	-9.40	-8.10			
${}^{62}\text{As}$	0.69	2	0.22	14.52	$15.10 \pm 0.29$	13.83	14.18		14.52		14.06				
RMSE					0.81	1.93	1.29	1.61	1.73	1.67	1.61	1.90	1.71	1.10	0.96

‡ Since there are no experimental data available for the 2p-decay with  $l \neq 0$ , following Refs. [43,44] we have included the half-lives of 7 nuclei with  $l \neq 0$  extracted from Ref. [46] in our database for the purpose of elucidation of the quality of results obtained using our present formula for the  $l \neq 0$  cases. ↻

In our least square fit to the experimental data we obtain the root mean square error (RMSE) using the expression

$$RMSE = \sqrt{\frac{1}{N_{nucl}} \sum_{i=1}^{N_{nucl}} (x_i)^2} \quad (2)$$

where  $N_{nucl}$  is the total number of data used for the calculations. Here we use  $x = (\log T_{Th} - \log T_{Exp})$ , and  $x = (Q_{Th} - Q_{Exp})$  for the RMSE evaluation of the half-lives and that of the Q-value, respectively. In order to elucidate the effect of deformation and centrifugal terms in Eqn. (1), first we have fitted our set of data by keeping only the first three terms. It yields the RMSE of 1.48 as also indicated in Fig. 1 (a) where we have plotted the result of this fitting in the form of ratio of experimental to calculated decay widths  $W_{Exp}/W_{Th} = \log_{10} T_{1/2}^{Th} / \log_{10} T_{1/2}^{Exp}$  as a function of  $Z = Z_d + 2$ . The obtained values of the coefficients a, b and c corresponding to this fitting are  $-22.3520 \pm 0.0646$ ,  $-0.5323 \pm 0.0058$  and  $0.8667 \pm 0.0011$ , respectively. The RMSE obtained above reduces to a value of 1.14 when the fitting is done by including the fourth term related to the centrifugal potential. Thereafter, we apply the same procedure by including the last term related to the quadrupole deformation  $\beta$  in Eqn. (1). The power  $p$  in the  $\beta$  dependent term has been determined by varying its value and repeating the same fitting procedure to obtain a minimum of RMSE. The variation in the RMSE value has not been found significant for  $2.5 \leq p \leq 3.5$ , and therefore, we have chosen  $p = 3$  for the formula. Finally, this procedure when all the five terms in Eqn. (1) are included yields a much reduced RMSE of 0.81. The results of the best fit have been shown in Fig. 1 (b). It is gratifying to note that the inclusion of deformation ( $\beta$ ) dependence in Eqn. (1) reduces the RMSE significantly. Somewhat larger deviation for a few points in Fig. 1 (b) for  $Z > 24$  suggests the need of more precise estimation from their particular experiments as our predictions are found in a good agreement for some other points of the same nuclei. The values for the coefficients corresponding to the best fit are found to be  $a = -21.3232 \pm 0.0719$ ,  $b = -0.6491 \pm 0.0069$ ,  $c = 0.8703 \pm 0.0013$ ,  $d = 0.6909 \pm 0.0114$ , and  $e = -36.1448 \pm 1.1700$ , respectively. Evidently, the parameters a, b, d, and e are in units of sec. while c has the unit of  $\text{sec} \cdot (\text{MeV})^{1/2}$ . Clearly a positive value of the coefficient 'd' indicates the hindrance effect of the centrifugal barrier, which can delay the transition thereby increasing the half-life. Contrary to this, the negative value of the coefficient 'e' points out towards a greater transition probability for the deformed decaying nuclei as compared to the spherical case.

Table 1 shows the results for the 2p-decay half-life, in the form of  $\log_{10} T_{1/2}$ , for the known 2p-emitters [8, 25–28, 46, 62–71] calculated using our newly proposed formula given by Eqn. (1). It also lists the measured values of  $\log_{10} T_{1/2}$ ,  $Q_{2p}$ , and  $l$  values used to set up the formula given by Eqn. (1). There are also given the deformation values  $\beta$  used for these 2p-emitters, which in the absence of measurements are taken to be those obtained from the RMF theory [18, 41, 42] as described above. It is seen from the table that the calculated results are in excellent agreement with the experimental data. This agreement is especially found to be remarkable for the deformed cases.

Table 1 also provides the calculated results for the half-lives along with the RMSE values obtained in other theoretical models for the purpose of comparison. It is readily seen that our proposed formula gives the least RMSE among all the available theoretical approaches [40,43–51]. A closer comparison of calculated results with experimental data in Table 1 as well as in Fig. 2 further shows the ability of present formula to provide a more satisfactory description of the experimental data as compared to those obtained from other theoretical approaches [40,43–51]. However, it is pointed out that the effect of deformation has very recently been taken into account by Santhosh [40] within the framework of Proximity Potential Model for the deformed nuclei. The calculated results for the half-lives in Ref. [40] are seen to compare well with the experimental data, and comparatively are similar in quality to the predictions of the present approach.

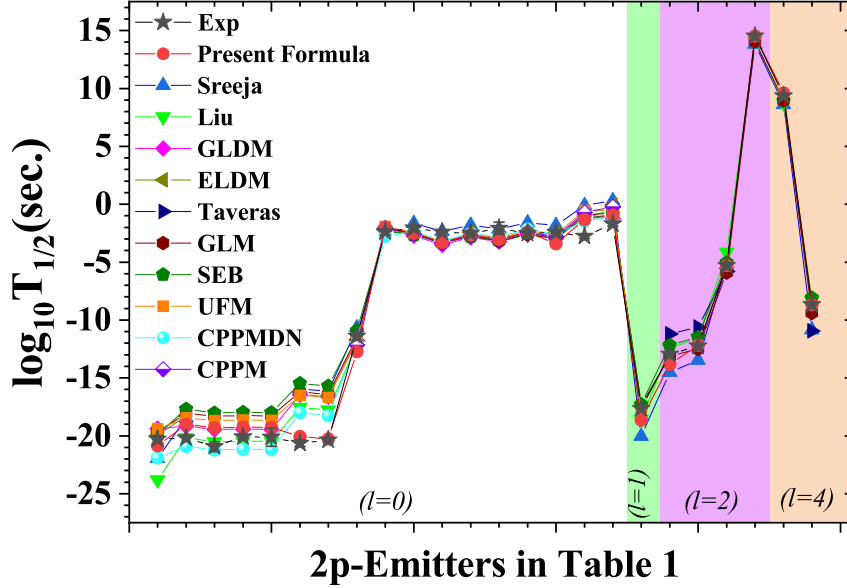


**Figure 2.** (Colour online) Comparison of  $\log_{10}T_{1/2}$  values obtained using the present formula with the experimental data and the results obtained in other theoretical descriptions [40,43–51]. The results for  $l \neq 0$  have been separated from those with  $l = 0$  by the vertical lines in the figure. X-axis refers to the 2p-emitters of Table 1 for which the half-lives have been displayed.

### 3. Prediction of 2p-emitters

The success of our theoretical approach described above encourages us to extend our study to look for the possible existence of other presently unknown 2p-emitters. For this purpose we have treated the following two cases separately.

(1) From amongst the proton rich nuclei across the mass region below  $Z < 82$  for which,

**Table 2.** 2p-decay half-lives calculated by using present formula for new potential candidates as per experimental systematics. The  $Q_{2p}$  values are taken from the latest evaluated nuclear properties table NUBASE2020 [72]. The angular momentum ( $l$ ) is calculated from selection rules based on parity and spin of parent and daughter nuclei, which are also taken from NUBASE2020 [72]. As described in the text, deformation values  $\beta$  have been taken from the RMF theory [18, 41, 42].

2p Emitter	$Q_{2p}$ (MeV) [72]	$l$	$\beta$	$\log_{10}T_{1/2}$ (sec.) (Present Formula)
$^{22}\text{Si}$	$1.58\pm 0.50$	0	0.00	$-15.20\pm 0.14$
$^{39}\text{Ti}$	$1.06\pm 0.02$	0	-0.15	$-5.51\pm 0.19$
$^{42}\text{Cr}$	$1.48\pm 0.31$	0	-0.17	$-7.61\pm 0.19$
$^{49}\text{Ni}$	$1.08\pm 0.78$	0	-0.06	$0.06 \pm 0.21$
$^{55}\text{Zn}$	$0.78\pm 0.40$	2	0.25	$8.80 \pm 0.27$
$^{59}\text{Ge}$	$1.60\pm 0.45$	0	0.21	$-2.72\pm 0.23$
$^{64}\text{Se}$	$0.70\pm 0.52$	0	0.24	$14.26\pm 0.27$
$^{68}\text{Kr}$	$1.46\pm 0.54$	0	-0.29	$1.22 \pm 0.27$
$^{77}\text{Zr}$	$0.44\pm 0.46$	0	0.48	$32.87\pm 0.42$
$^{81}\text{Mo}$	$0.73\pm 0.58$	0	0.57	$16.96\pm 0.50$
$^{85}\text{Ru}$	$1.13\pm 0.64$	0	-0.22	$14.03\pm 0.29$
$^{104}\text{Te}$	$0.73\pm 0.33$	0	0.14	$35.97\pm 0.33$
$^{108}\text{Xe}$	$1.01\pm 0.39$	0	0.17	$27.28\pm 0.32$
$^{165}\text{Pt}$	$1.44\pm 0.50$	0	0.10	$37.49\pm 0.39$
$^{170}\text{Hg}$	$1.85\pm 0.34$	0	0.00	$29.87\pm 0.38$

the experimental data on  $Q_{2p}$  and  $Q_p$  are available in the latest database NUBASE2020 [72], we identify the nuclei satisfying the criteria  $Q_{2p} > 0$  and  $Q_p < 0$  as the potential 2p-emitters and evaluate their half-lives using Eqn. (1). The results thus obtained for the logarithmic half-life have been listed in Table 2.

(2) The proton rich nuclei for which experimental data on  $Q_{2p}$  and  $Q_p$  values are not available as yet, we take recourse to using the theoretically computed results. In order to avoid the sensitivity and uncertainties of theoretical models we have used the following procedure. We have selected only those nuclei as possible potential 2p-emitter candidates for which, in addition to the RMF [18, 41, 42] results for the  $Q_{2p}$  and  $Q_p$  values, other widely used theoretical models including NSM [7, 19], HFB [59], WS4 [61], FRDM [73], RCHB [74], KTUY05 [75], and INM [76] fulfill the criteria of two-proton emission. This ensures that the results of the RMF theory, for  $Q_{2p}$ ,  $l$  and  $\beta$  we employ in Eqn. (1) to compute half-life, are consistent with those from other theoretical models.

In recent times the use of machine learning techniques have been applied for the estimation of various data related to nuclear physics [78]. These techniques can be utilized to bring down the possible theoretical uncertainties in our RMF computed  $Q_{2p}$  values. With this in view, we apply one of the machine learning techniques by employing XGBoost algorithm, which was found to be effective in our earlier work on  $\alpha$ -emission [78]. For our purpose, we determine the possible errors in  $Q_{2p}$  and  $Q_p$  values from RMF theory using  $Q_{2p}$  data for 2467 nuclei and  $Q_p$  data for 2635 nuclei taken

from the database NUBASE2020 [72] as the training data to machine learning. The estimation of errors from the machine algorithm has been found to qualify to a good accuracy which was validated by the test data of 529 and 531 nuclei, respectively, for  $Q_{2p}$  and  $Q_p$  values shown in Fig. 3. Hence the  $Q_{2p}$  and  $Q_p$  values from RMF theory

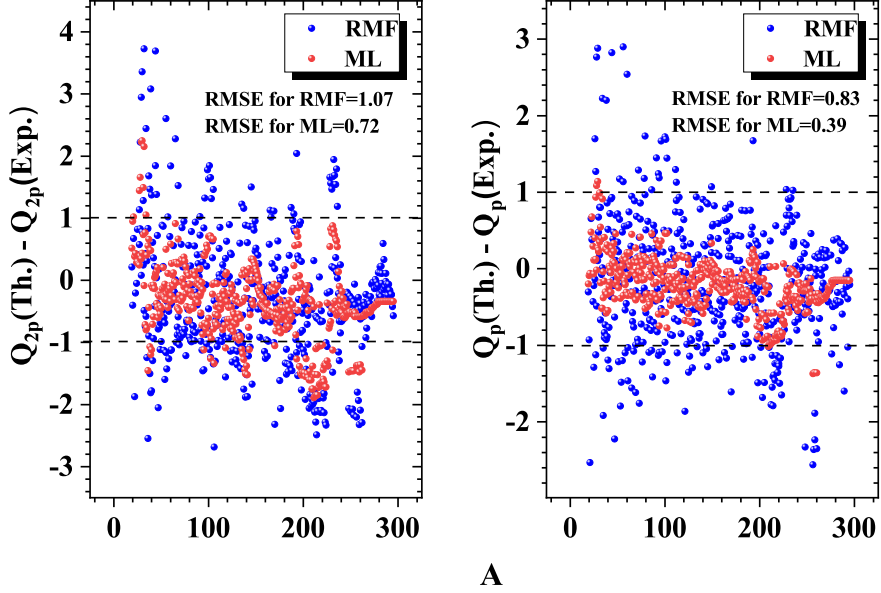


**Figure 3.** (Colour online) Differences between theoretical and experimental  $Q_{2p}$  and  $Q_p$  values for the 529 and 531 nuclei, respectively. The blue dots denote the RMF error whereas that for the machine modified results are depicted using red dots. The RMS values for the errors corresponding to the RMF theory and that from the machine learning (ML) technique are also mentioned.

for the potential nuclei are modified by including their possible errors obtained by the above-mentioned procedure. The modified  $Q_{2p}$  and  $Q_p$  values thus obtained are hereafter denoted by  $Q_{2p}^{ML}$  and  $Q_p^{ML}$ , respectively. This set of  $Q^{ML}$  values is now used to identify the possible new 2p-emitters by applying the criteria  $Q_{2p}^{ML} > 0$  and  $Q_p^{ML} < 0$ . These have been listed in Table 3 along with their calculated logarithmic half-life using Eqn. (1). Table 3 also shows the  $Q_{2p}$  and modified  $Q_{2p}^{ML}$  values to illustrate how the machine learning technique affects the theoretically obtained RMF  $Q$ -values. In addition, the  $l$  and  $\beta$  values employed in the half-life calculations have also been given in the table. The results for the half-life show that apart from the nuclei  $^{38}\text{Ti}$ ,  $^{72}\text{Sr}$ ,  $^{76}\text{Zr}$ , and  $^{84}\text{Ru}$ , the other heavier possible candidates have relatively long life-time. For such nuclei in the heavy mass region, in addition to the 2p-decay, there always exist other possible dominant modes including  $\alpha$ ,  $\beta^+$ , cluster decays as well as spontaneous fission.

**Table 3.** Half-life of theoretical true 2p-emitter candidates obtained using the present formula where  $Q_{2p}$  is taken equals the modified  $Q_{2p}^{ML}$  (the disintegration energy which is modified by machine learning). The angular momentum ( $l$ ) is calculated by using parity and spin of parent and daughter nuclei, which are taken from NUBASE2020 [72] and from Ref. [77]. (see the text for detail).

Potential 2p-Emitter	RMF		$Q_{2p}^{ML}$ (MeV)	$l$	$\log_{10} T_{1/2}$ (sec.) (Present Formula)
	$\beta$	$Q_{2p}$ (MeV)			
$^{38}\text{Ti}$	0.22	1.86	2.57	0	$-14.11 \pm 0.19$
$^{72}\text{Sr}$	-0.27	0.38	0.86	0	$14.02 \pm 0.28$
$^{76}\text{Zr}$	-0.33	1.00	1.40	0	$4.87 \pm 0.30$
$^{84}\text{Ru}$	-0.22	0.60	1.20	0	$12.63 \pm 0.28$
$^{105}\text{Te}$	0.12	0.24	0.58	2	$46.37 \pm 0.37$
$^{120}\text{Nd}$	0.42	0.33	0.66	0	$47.74 \pm 0.45$
$^{126}\text{Sm}$	0.40	0.24	1.07	0	$31.48 \pm 0.42$
$^{150}\text{Hf}$	0.18	1.16	1.38	0	$33.74 \pm 0.37$
$^{154}\text{W}$	-0.11	1.25	1.65	0	$29.25 \pm 0.37$
$^{159}\text{Os}$	-0.04	0.79	1.25	0	$41.36 \pm 0.39$

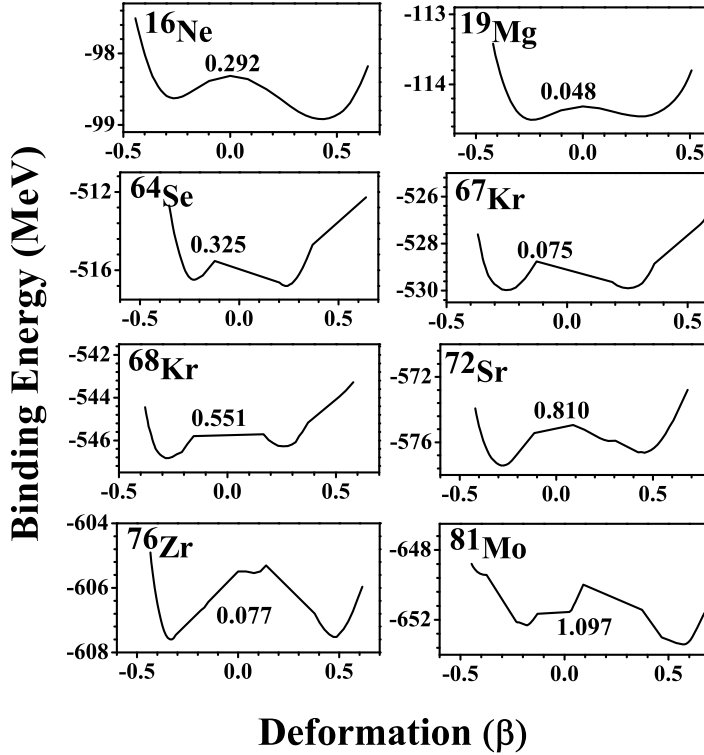


**Figure 4.** Potential energy surfaces for 2p-emitters showing shape coexistence. The energy difference between prolate and oblate states are mentioned by numbers in the respective panels.



#### 4. Shape-coexistence and Halos

The neutron and proton rich nuclei in different regions of the nuclear chart are known to exhibit shape coexistence [79,80], wherein one or more states lying close to the ground state having different deformation ranging from oblate to spherical to prolate are found to exist. The shape coexistence in nuclei is known to provide a good evidence for the crucial role of interplay between the shell effects and the collective degrees of freedom in the structure and stability of nuclei. This has been amply demonstrated in several studies of nuclear decay and fission processes [6,81,82]. Thus in order to understand the influence of deformation on the process of 2p-radioactivity and the life-time of 2p-emitters, we have performed the quadrupole constrained RMF calculations [18,41,42] for all the known 2p-emitters described in Table 1, and also of those predicted to be potential candidates as listed in Tables 2 and 3. The results of our calculations show that out of 33 deformed cases considered altogether from the three tables, 17 nuclei exhibit shape coexistence with energy difference  $\Delta E$  between the two minima being small and having a range given by  $40 \text{ keV} \leq \Delta E \leq 1 \text{ MeV}$ . Typical potential energy surfaces obtained in such calculations for a few representative nuclei have been plotted in Fig. 4 for the purpose of illustration. In several cases of the 2p-emitters shown in Fig. 4 we observe two well separated minima having prolate and oblate shapes. Strikingly the additional minima lying higher than the ground state have similar energy but very different shapes. Thus in such cases the nucleus may exist in a state corresponding to the energy and shape of this additional close lying minimum. The life-time of this state will depend on the extent of overlap between its wave function with that of the ground state, its excitation energy and the height of saddle separating it from the ground state. A long life-time may give rise to a meta-stable state or even a shape isomer. We have also carried out the deformation constraint calculations for the daughter nuclei of the 2p-emitters. It is found that several of these daughter nuclei also have an additional minimum close to the ground state minimum but having different shapes as in the case of parent nuclei described above. Evidently, in a 2p-decay the transition from the parent to the daughter nuclei, apart from being strongly dependent on the  $Q_{2p}$  energy, are expected to be influenced by their shapes. Thus 2p-decays involving different shapes for the parent and daughter nuclei are likely to be hindered resulting in longer half-lives. This in turn is expected to better facilitate the experimental probe of very short lived nuclei away from the drip lines. In view of the fact that the nuclei  $^{16}\text{Ne}$ ,  $^{19}\text{Mg}$ , and  $^{67}\text{Kr}$  (shown in Fig. 4) along with  $^{28}\text{Cl}$ ,  $^{32}\text{K}$ , and  $^{60,62}\text{As}$  being amongst the experimentally known 2p-emitters (see Table 1) exhibit shape coexistence, the other nuclei in our study showing shape coexistence, viz.,  $^{38,39}\text{Ti}$ ,  $^{59}\text{Ge}$ ,  $^{64}\text{Se}$ ,  $^{68}\text{Kr}$ ,  $^{72}\text{Sr}$ ,  $^{76}\text{Zr}$ , and  $^{81}\text{Mo}$  may be considered as possible 2p-emitters to be probed in the near future. It is observed that for these nuclei the half-lives obtained by using our present formula (Eqn. (1)) as listed in Tables 2 and 3 fall in the range of values similar to those of the experimentally known 2p-emitters.

As mentioned earlier, the ground states of the 2p-emitters studied here differ in

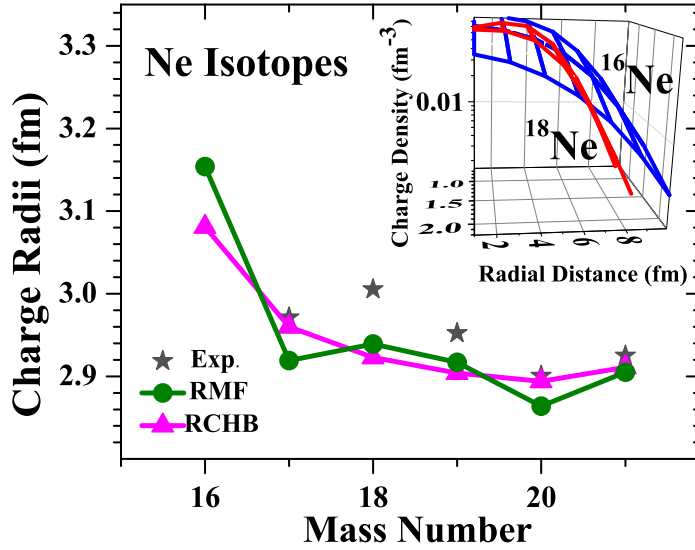


**Figure 5.** (Colour Online) Calculated charge radii of Ne isotopes plotted as a function of mass number. One finds a sudden increase in the radius of  $^{16}\text{Ne}$  at the proton drip line indicating a halo formation. In the inset we compare the charge density distribution of  $^{16}\text{Ne}$  with that of the neighbouring isotope  $^{18}\text{Ne}$ . Again a much wider distribution for the  $^{16}\text{Ne}$  isotope is seen.

shapes ranging from a deformed prolate or oblate to a spherical one. However, prolate shape in the ground state is found to be more prevalent. This predominance reaffirms the significance of prolate deformation in the 2p-radioactivity as observed by Mukha *et al.* [37]. Additionally, in the case of deformed nuclei, the occupancy in Nilsson orbital with the mixing of states near the Fermi level and the scattering of valence particles due to pairing correlations may contribute to a halo formation [83,84] with loosely bound pair of protons. With this in view, we look for the possible imprints of halo in the deformed nuclei listed in Tables 1, 2, 3 by studying their charge radii and density profiles. The charge radii  $r_c = (\langle r_c^2 \rangle)^{1/2}$  is calculated from the charge density distributions using the following relation,

$$\langle r_c^2 \rangle = \frac{\int \rho_c r^2 d\tau}{\int \rho_c d\tau} \quad (3)$$

Our results show that the light nuclei having proton number  $Z < 20$ , for example,  $^{16}\text{Ne}$ ,  $^{19}\text{Mg}$ ,  $^{22}\text{Si}$  etc. indeed display a sudden increase in their charge radii with respect to the neighbouring isotopes while approaching the proton drip line indicating thereby the halo like formation. The corresponding charge density profiles of such nuclei also show significant spatial spread as compared to the neighbouring isotopes. This has been illustrated for the case of  $^{16}\text{Ne}$  in Fig. 5 which shows the charge radii of Ne isotopes as a function of mass number. A sudden increase in the charge radius for the proton drip line isotope  $^{16}\text{Ne}$  is seen. The inset in Fig. 5 shows the density profile of  $^{16}\text{Ne}$  in comparison with that of its neighbouring isotope  $^{18}\text{Ne}$  to highlight the spread of charge density in the case of isotope  $^{16}\text{Ne}$  with a halo. Here the occurrence of halo formation is

found only for the lighter nuclei with  $Z < 20$  which is in accord with our earlier prediction of 2p-halo in the light mass region [20].

## 5. Conclusion

Deformation dependence of the two-proton (2p) emission half-lives for nuclei has been studied within the framework of a semi-empirical formula akin to that used for the alpha radioactivity treated as quantum tunnelling phenomenon. Apart from the usual Q-value and angular momentum dependence, it incorporates the quadrupole deformation in a phenomenological way. The method is found to be robust and performs quite well in comparison to other descriptions [40, 43–51] for the 2p-radioactivity half-lives. The results for the identified potential 2p-emitters have been listed in Tables 2 and 3. It is expected that some of these predicted 2p-radioactive nuclei would be accessible in the near future for measurements and possible verification providing a new impetus to the field of radioactivity.

Furthermore, we have shown that many of the 2p-emitters being located close to the proton drip-line exhibit shape coexistence with a small energy difference between the oblate and prolate shapes. However, for the ground state the prolate shape is found to be more prevalent. In addition, it is found that the lighter 2p-emitters with  $Z < 20$  being excessively proton rich ( $Z/N > 1.4$ ) tend to have halo formation due to the loosely bound protons.

## 6. Acknowledgements

Authors would like to thank M. Kaushik and Prafulla Saxena for their help for the calculations using machine learning techniques. Authors G. Saxena and M. Aggarwal gratefully acknowledge the support provided by Science and Engineering Research Board (SERB)-DST, Govt. of India under CRG/2019/001851 and WOS-A scheme, respectively.

## References

- [1] Goldansky V I 1960 *Nucl. Phys.* **19** 482.
- [2] Woods P J and Davids C N 1997 *Annu. Rev. Nucl. Part. Sci.* **47** 541.
- [3] Blank B and Ploszajczak M 2008 *Rept. Prog. Phys.* **71** 046301.
- [4] Crider B P 2016 *Phys. Lett. B* **763** 108.
- [5] Sarriguren P, Algora A and Pereira J 2014 *Phys. Rev. C* **89** 034311.
- [6] Strutinsky V M 1967 *Nucl. Phys. A* **95** 420.
- [7] Aggarwal M 2014 *Phys. Rev. C* **89** 024325.
- [8] Ascher P *et al* 2011 *Phys. Rev. Lett.* **107** 102502.
- [9] Mukha I *et al* 2007 *Phys. Rev. Lett.* **99** 182501.
- [10] Brown B A 1991 *Phys. Rev. C* **43** 1513(R).
- [11] Nazarewicz W *et al* 1996 *Phys. Rev. C* **53** 740.
- [12] Cole B J 1996 *Phys. Rev. C* **54** 1240.

- [13] Ormand W E 1996 *Phys. Rev. C* **53** 214.  
Ormand W E 1997 *Phys. Rev. C* **55** 2407.
- [14] Grigorenko L V *et al* 2009 *Phys. Lett. B* **677** 30.
- [15] Zhao Q, Dong J M, Song J L and Long W H 2014 *Phys. Rev. C* **90** 054326.
- [16] Lim Y, Xia X and Kim Y 2016 *Phys. Rev. C* **93** 014314.
- [17] Delion D S, Liotta R J and Wyss R 2013 *Phys. Rev. C* **87** 034328.
- [18] Singh D, Saxena G, Kaushik M, Yadav H L and Toki H 2012 *Int. Jour. Mod. Phys. E* **21** 1250076.
- [19] Aggarwal M 2010 *Phys. Lett. B* **693** 489.
- [20] Saxena G, Kumawat M, Kaushik M, Jain S K and Aggarwal M 2017 *Phys. Lett. B* **775** 126.
- [21] Xu X X *et al* 2013 *Phys. Lett. B* **727** 126.
- [22] Lin C J *et al* 2009 *Phys. Rev. C* **80** 014310.
- [23] Xu X X *et al* 2010 *Phys. Rev. C* **81** 054317.
- [24] Wang S M and Nazarewicz W 2018 *Phys. Rev. Lett.* **120** 212502.
- [25] Pfützner M *et al* 2002 *Eur. Phys. J A* **14** 279.
- [26] Giovinazzo J *et al* 2002 *Phys. Rev. Lett.* **89** 102501.
- [27] Blank B *et al* 2005 *Phys. Rev. Lett.* **94** 232501.
- [28] Dossat C *et al* 2005 *Phys. Rev. C* **72** 054315.
- [29] Pomorski M *et al* 2011 *Phys. Rev. C* **83** 061303.
- [30] Mukha I *et al* 2015 *Phys. Rev. Lett.* **115** 202501.
- [31] Koldste G T *et al* 2014 *Phys. Lett. B* **737** 383.
- [32] Lis A A *et al* 2015 *Phys. Rev. C* **91** 064309.
- [33] Wallace J P *et al* 2012 *Phys. Lett. B* **712** 59.
- [34] Lund M V *et al* 2016 *Eur. Phys. J. A* **52** 304.
- [35] Sun L J *et al* 2017 *Phys. Rev. C* **95** 014314.
- [36] Xu X X *et al* 2016 arXiv:1610.08291v1.
- [37] Mukha I *et al* 2006 *Nature* **439** 298.
- [38] Aggarwal M 2014 *Phys. Rev. C* **90** 064322.
- [39] Aggarwal M 2006 *Phys. Scr.* **2006** 178.
- [40] Santhosh K P 2021 *Phys. Rev. C* **104** 064613.
- [41] Geng L S, Toki H, Sugimoto S and Meng J 2003 *Prog. Theor. Phys.* **110** 921.
- [42] Geng L S [http : //www.rcnp.osaka - u.ac.jp/Divisions/np2/old/Research/Thesis/PhD\\_Geng.pdf](http://www.rcnp.osaka-u.ac.jp/Divisions/np2/old/Research/Thesis/PhD_Geng.pdf)  
(Ph.D. thesis).
- [43] Sreeja I and Balasubramaniam M 2019 *Eur. Phys. J. A* **55** 33.
- [44] Liu H-M *et al* 2021 *Chin. Phys. C* **45** 024108.
- [45] Cui J P, Gao Y H, Wang Y Z and Gu J Z 2020 *Phys. Rev. C* **101** 014301.
- [46] Goncalves M, Teruya N, Tavares O and Duarte S 2017 *Phys. Lett. B* **774** 14.
- [47] Tavares O A P and Medeiros E L 2018 *Eur. Phys. J. A* **54** 65.
- [48] Liu H-M *et al* 2021 *Chin. Phys. C* **45** 044110.
- [49] Zou Y-T *et al* 2021 *Chin. Phys. C* **45** 104101.
- [50] Xing F *et al* 2021 *Chin. Phys. C* **45** 124105.
- [51] Zhu D-X *et al* 2022 *Chin. Phys. C* **46** 4.
- [52] Coban A, Bayrak O, Soylyu A and Boztosun I 2021 *Phys. Rev. C* **85** 044324.
- [53] Budaca R and Budaca A I 2022 *Nucl. Phys. A* **1017** 122355.
- [54] Dong J M, Zhang H F and Royer G 2009 *Phys. Rev. C* **79** 054330.
- [55] Gamow G, 1928 *Z. Phys.* **51** 204.
- [56] Segre E, 1964 'Nuclei and Particles', W. A. Benjamin, Inc., New York.
- [57] Deng J-G and Zhang H-F 2021 *Phys. Lett. B* **816** 136247.
- [58] Fröman P O 1957 *Mat.-Fys. Skr.* **1** 1.
- [59] Xu Y, Goriely S, Jorissen A, Chen G L and Arnould M 2013 *Astronomy & Astrophysics* **549** A106.
- [60] Möller P, Sierk A J, Ichikawa T and Sagawa H 2016 *At. Data Nucl. Data Tables* **109–110** 1.
- [61] Wang N, Liu M, Wu X and Meng J 2014 *Phys. Lett. B* **734** 215.

- [62] Whaling W 1966 *Phys. Rev.* **150** 836.
- [63] Jager M F *et al* 2012 *Phys. Rev. C* **86** 011304(R) (2012).
- [64] KeKelis G J *et al* 1978 *Phys. Rev. C* **17** 1929.
- [65] Kryger R A *et al* 1995 *Phys. Rev. Lett.* **74** 860.
- [66] Suzuki D *et al* 2009 *Phys. Rev. Lett.* **103** 152503.
- [67] Woodward C J, Tribble R E and Tanner D M 1983 *Phys. Rev. C* **27** 27.
- [68] S271 Collaboration Mukha I 2009 *Eur. Phys. J. A* **42** 421.
- [69] Audirac L *et al* 2012 *Eur. Phys. J. A* **48** 179.
- [70] Pomorski M *et al* 2014 *Phys. Rev. C* **90** 014311.
- [71] Goigoux T *et al* 2016 *Phys. Rev. Lett.* **117** 162501.
- [72] Wang M, Huang W J, Kondev F G, Audi G and Naimi S 2021 *Chin. Phys. C* **45** 030003.
- [73] Möller P, Mumpower M R, Kawano T and Myers W D 2019 *At. Data Nucl. Data Tables* **125** 1.
- [74] Xia X W *et al* 2018 *At. Data Nucl. Data Tables* **121–122** 1.
- [75] Koura H, Tachibana T, Uno M and Yamada M 2005 *Progr. Theor. Phys.* **113** 305.
- [76] Nayak R C and Satpathy L 2012 *At. Data Nucl. Data Tables* **98** 616.
- [77] <https://t2.lanl.gov/nis/data/astro/molnix96/spidat.html>.
- [78] Saxena G, Sharma P K and Saxena P 2021 *J. Phys. G: Nucl. Part. Phys.* **48** 055103.
- [79] Wood J L and Heyde K 2016 *J. Phys. G: Nucl. Part. Phys.* **43** 020402.
- [80] Wood J L, Heyde K, Nazarewicz W, Huyse M and Duppen P-V 1992 *Phys. Rep. C* **215** 101.
- [81] Nilsson S G *et al* 1969 *Nucl. Phys. A* **131** 1.
- [82] Möller P and Nix J R 1994 *J. Phys. G: Nucl. Part. Phys.* **20** 1681.
- [83] Saxena G, Kumawat M, Sharma R and Aggarwal M 2021 *J. Phys. G: Nucl. Part. Phys.* **48** 125102.
- [84] Yadav H L, Kaushik M and Toki H 2004 *Int. Jour. Mod. Phys. E* **13** 647.



# EFFECT OF ADVERTISING IN RURAL AREAS

**JAIDEEP SHARMA**

**Assistant Professor**

## **ABSTRACT**

In a nation of more than one billion individuals, over 80% live in provincial regions. This outright number of the country people requires the advertisers to contact them for the showcasing of different products and administrations. The fundamental target of the review is to comprehend the crash of promotions in acquisition of labor and products in Nithar is an inside town of tehsil-Bhusawar in Bharatpur locale. The more youthful ages are presented to innovative turn of events and are liable to move from the openness from customary media to the new and advancing on the web and computerized notices. This paper expects to concentrate on Effect of advertising in rural areas and standpoint concerning new age commercials. Factual instruments utilized are KMO Bartlett's Test, Factor Analysis, Regression investigation, 't' - test and ANOVA. The outcomes are investigated and summed up in like manner.

## **Introduction**

The word "advertising" is derived from a Latin word "advertere" which means to turn people's attention to a specific thing. If you want to be successful in the Indian market, it is impossible to overlook the rural markets. Rural markets absorb a big chunk of the market in India, and there has been an impressive increase in the rural market potential owing to tremendous economic growth in India.

Advertising in rural markets is a quite a challenge because of lack of standard opportunities; there exists a sense of solidarity and complexity in the rural markets. Hence, creating an advertising campaign for rural India is often considered a tough responsibility. Rural marketing is a different ballgame that drives marketing gurus to unlearn the traditional concepts. Every facet and feature of marketing demands a refashion when the focus is shifted to rural marketing.

India is a country of about one billion people where more than 80% of the humankind inhabits in rural areas. The untempered number of the rural population demands market research for marketing various goods and services. Although almost about 30% of the Indian population is considered to be improvised, there exists a great opportunity for essential marketing articles in rural India.

Rural market has been creating consistently in the course of the most recent couple of years and is presently much greater than the metropolitan market. According to evaluation report, 70 percent of individuals live in towns. In excess of 800 million individuals stay in towns of India. 'Go rural' is the advertiser's new motto. Indian advertisers, as well as worldwide organizations like Colgate-Palmolive, Godrej, and Hindustan Lever have fixated on provincial business sectors. Subsequently, looking for the valuable open doors, which provincial business sectors deal to the advertisers, it tends to be expressed that the predetermination would be able to be extremely encouraging for people that can comprehend the elements of provincial markets and exploit them to their fine advantage. Rustic promoting isn't like publicizing in metropolitan regions. Not just because of the aspects of the populace, and furthermore the

need of normalized open doors – not to say the impression of local area, the experience of solidarity and the intricacy of rural networks. Making a promoting showcasing crusade for a rural place is as often as possible troublesome. Besides, generally rustic promoting efforts aren't predetermined for a solitary local area; all things considered, they reason to make a close by presence in different regions. An accomplished and confirmed aggregator will smooth out the technique, improve normalization, also, predict capacity challenges sooner than they arise as moment obstructions, helping to make the most of provincial promoting valuable open doors. Promoting in rustic India represents a few challenges, aside from the geological distance and distance of various towns. Nonetheless, the multiplication of the media, particularly the developing accomplish of the electronic media in rural India, has provided exposure to various product and administrations, which have been up until recently taken into thought the area of metropolitan clients. Promoting plays out a prominently more noteworthy job in getting alterations society and providing new item realities to the clients. It moreover upgrades efficiency in view of mass utilization. Great promoting ought to produce consideration, blast inside the dependability of privilege, be smooth to be perceived and recalled. The three fundamental objectives of publicizing and promoting are to offer a sensible cost, persuade clients to purchase and go about as a suggestion to the crowd. From those 3 basic objectives arise different summed up targets, such affirmation of new items, broadening of the market to new shoppers, the declaration of item changes, making an extraordinary offer, the declaration of the district of stockiest and dealers, instruction of clients, reminding clients, appealing stockiest, and making logo want. Other fundamental objectives of publicizing are to exchange the outlook of somebody without a doubt nearer to the logo. It is basic for the sponsor to perceive the method for making people move at the adaptation of order impacts hypothesis of verbal trade. In this manner, it is sanitized that the metropolitan rustic gap keeps existing and the business sectors, which need to win in the rural market. This is a awesome sign and a marker for the industry. Notwithstanding, nothing is accessible on a platter and tapping the horticultural commercial center. Yet, all things considered, the predetermination of outright certainty lies inside the rural markets.

## REVIEW OF LITERATURE

This examination adds to the writing by zeroing in on the viability of promoting particularly in provincial showcasing and its effect through explicit associations or producers to hold onto the undiscovered capacity market of India, which is finished with open doors. The aim of writing evaluates is to legitimize, the explanation of a guaranteeing exploration to look, gives an outline of antiquated sees and convey to the gentle investigations attributes and issues. Arun Kant Painoli (2017) observed that there are various factors impacting the shopping conduct of the customer while they buy the novel symbol of cleanser powder and cake. Retailer proposal and promotion are the greatest significant factors in building unwavering quality inside the brain of the clients. Dev Narayan Sarkar's (2016) concentrate on recognized that country advertising can be improved by naming neighborhood populace as merchants, wholesalers and retailers of their items; or via utilizing neighborhood labor supply in different tasks along with exchange promoting, acquirement of crude substances and selling and spreading records on the advertiser's items quickly to rustic clients. Katke, K. (2007) The impacts of this exploration demonstrate that thereexists a powerless connection among ecological reaction with the shopper looking for conduct along with the attitudinal notwithstanding social parts of the buyers purchasing conduct. Passionate response then againintroduced hearty relationship with the buyer looking for conduct.

## Statement of the Problem

1. Denied individuals and denied markets: The quantity of individuals beneath the destitution line has not diminished in any considerable way. In this way, destitute individuals and thus underdeveloped markets describe rustic business sectors. A greater part of provincial individuals is custom bound, and they additionally deal with issues like conflicting electrical power, scant foundation and untrustworthy phone framework, and politico-business affiliations that upset improvement endeavors.
2. Absence of correspondence offices: Even today, most towns in the nation are difficult to reach during the storms. Countless towns in the nation have no entrance to phones. Other correspondence framework is additionally profoundly immature.

3. Transport: Many country regions are not associated by rail transport. Numerous streets have been ineffectively surfaced and got seriously harmed during rainstorm. The utilization of bullock trucks is inescapable even today. Camel trucks are utilized in Rajasthan and Gujarat in both provincial and metropolitan areas.

4. Numerous dialects and vernaculars: The dialects and tongues fluctuate from one state to another, locale to locale and presumably from one area to another. Since messages must be conveyed in the neighborhood language, it is challenging for the advertisers to plan special techniques for each of these regions. Offices, for example, telephone, message and fax are less evolved in towns adding to the communication issues looked by the advertisers.

5. Scattered markets: Rural populace is dissipated over a huge land region. Also, it is nearly impossible to guarantee the accessibility of a brand all around the country. Region fairs are intermittent and occasional in nature. Makers and retailers lean toward such events, as they permit more noteworthy perceivability and catch the consideration of the interest group for bigger ranges of time. Promoting in such a profoundly heterogeneous market is likewise over the top expensive.

6. Low per capita Income: The per capita pay of rustic individuals is low when contrasted with the metropolitan individuals. Additionally, request in rustic business sectors relies upon the rural circumstance, which thusly relies upon the storms. Hence, the interest isn't steady or ordinary. Subsequently, the per-capita pay is low in towns contrasted and metropolitan regions.

7. Low degrees of proficiency: The degree of education is lower contrasted and metropolitan regions. This again prompts an issue of correspondence in these provincial regions. Print medium becomes insufficient and to a degree superfluous, since its compass is poor.

## Scope of the study

At present, information about the advertisements being broadcast in the rural area and the impact of those advertisements on the rural people, as well as to know whether the people are able to understand the advertisements being broadcast in the rural areas or not. Whether the correct information about the said Vastu is accessible to them. Correct selection of advertising medium in rural areas. And broadcasting advertisements according to the educational qualification of the rural area.

## Objectives

1. To arrangement and encourage measures to evaluate publicizing feasibility in countrymarkets.
2. To review the development and advancement of TV promotions and provincial business sectors in India.
3. To see the secret factors of publicizing practicality in provincial business sectors

## Methodology

The review was exploratory and illustrative in nature. Both essential and optional information were tapped together, the essential information was gathered through overview technique and connections between segment factors were assessed by utilizing measurable devices.

## Data Collection

In this study, going to the rural area did personal interview and also obtained data from advertising agency, as well as the place and medium where the advertisements are broadcast.

## Area of the Study

Nithar is a interior village of tehsil-Bhusawar in Bharatpur district. It is a historical village which has a number of ancient monuments such as CHATARIS , BAWALI'S ( step well ), PALACES , TEMPLES and ruins of FORTS above the hills of Aravalis. The village is inhabited in the lap of Aravalis Hills. The place was ruled by the king 'REETH PAAL' , the brother of king VIJAY PAAL of Bayana in early mideval age. The village came under the rule of jat king SURAJMAL in medival age and durring this period 7 Bawalis ,number of Chataris and Temples along with gardens owned by various communities



such as Meenas, Jatav, Vaish, Brahmans, priest, etc. were constructed. The remains of these historical structures can still be seen in the village. The pal king Reethpal after whose name the name of this village kept, constructed a fort on the hill and also the temple of MAA HINGLAJ and BHARRON to keep watch on the activities of the enemies to provide robust safety to his kingdom. It is believed that this particular village was earlier inhabited by Gujjar community who had given shelter to a Meena Lady, who was forced to leave her native place by Rajput community after killing all her clan members in the early medieval age. The said lady gave birth to two sons who by their wisdom and intelligence along with the help of local deity (GRAM DEVTA) inhabited the village by their own clan. The village is now

Particulars	Total	Male	Female
Total No. of Houses	1,078	-	-
Population	6,296	3,363	2,933
Child (0-6)	920	491	429
Schedule Caste	1,486	808	678
Schedule Tribe	3,568	1,885	1,683
Literacy	69.64 %	86.04 %	50.84 %
Total Workers	2,914	1,496	1,418
Main Worker	2,105	-	-
Marginal Worker	809	159	650

dominated by MEENA community who are successors of those two brothers. Later on another group of Meena's joined the clan of these two brothers which made Meena as the largest population of this village. Beside Meena's the village also inhabited by Brahmins, Baniyas, Jatav, Khatis, Luhar, Sunar, Khtek etc. The total population of the village is around 12000 in 2011.

Recently a lot of development activities have taken place which inter alia includes construction of a major district road connecting to Jaipur via Mahaua, Kasturba Gandhi Balika

Vidhyalaya boarding school up to class 6-12, a senior secondary school for girls and a senior secondary school of girls and boys. The village is also a Primary Health Centre and a Veterinary Hospital for Livestock.

The village is situated in MADA AREAS and is facing acute shortage of water that is for irrigation as well as drinking water. Some steps have been taken by government to provide drinking water but these are not sufficient to meet the need of all the people. An integrated approach is needed to provide drinking water facility to the village. Beside this panchayat should also construct ANI-CUT and Band etc. to conserve water to improve water level in the irrigation well. Now these days Nithar is known as "AADARSH GRAM NITHAR"

## Data Collection Tools

A particularly coordinated interview plan was guided in this survey to move data from the model client. The gathering plan was pretested with fifty respondents and taking into account the results got, it was to some degree changed.

## Population of the Study

The population of the review establishes all the client in the review region, The Nithar town seeing notices. There is no positive source to get the size of the population. Thus, the population of the review is endless one.

## Sources of Data

The List accessible in the Village Panchayat Office was utilized as the source to choose the Record of Households in the Village Administrative Office was utilized as the source to choose the example clients.

## Conclusion

Giving the vision is a never - following through with responsibility. Business gives the vision and mission of things and organizations. The delayed consequence of the assessment has revealed that a huge piece of the promotions are restricted to making awareness of their things and organizations. One can't have his vision declaration illustrated and hung in the entrance and consider the errand wrapped up. From a correspondence perspective, all advancements must should tell the truth about their things and organizations. Such notification could help the customers in handling issues, and guide them in settling on the best decision. The course of decisive reasoning is to be seen by the marketing specialists. The pieces of decisive reasoning are to be completely seen preceding making an advancement. Enough composition on decisive reasoning is to be completely seen before getting ready advertisement. It is seen that as the promotion by and large didn't help people with having adequate data about the things and organizations. This shortfall of data on the thing stays an obstruction while picking a brand for a particular thing. Dealing with this issue of clients is to be noted by the people who are related with the course of plugs have carried out colossal enhancements for the social characters of common people like dietary examples, dressing styles, walking styles, buying conduct, standard and social characteristics. Regardless, it has acquired least changes the financial conditions of the natural people. The authentic improvement of a nation depends upon progress in the money related conditions of the natural people. It will assist the advertiser with working on the deals in country regions and the everyday environments of the rustic individuals.

## Reference

- <https://studiousguy.com/rural-advertising/>
- <http://www.onefivenine.com/india/villages/Bharatpur/Weir/Nithar>
- Painoli, A. K. (2017). Factors Influencing the Purchase of FMCG by Rural Consumers: An Empirical Study with Reference to Detergent Powder and Cake in the Uttarakhand State (India. Elk Asia Pacific Journal of Marketing and Retail Management,11-18.
- Katke, K. (2007). The Impact of Television Advertising on Child Health & Family Spending. International Marketing Conference on Marketing & Society, 30-37
- Sarkar, D. N. (2016). Conceptual Expansion of the Discipline of Rural Marketing: An Objective Analysis. Vision 20(3),1-15.



## Effect of different plant hormones on *in vitro* plant regeneration via somatic embryogenesis in *Cajanus cajan* L. millsp.

Manisha Sharma

St Wilfred's P.G. College, Mansarovar, Jaipur, Rajasthan, India

### Abstract

In the present study, regeneration of Pigeon pea (*Cajanus cajan* L. Millsp), belongs to family Fabaceae was achieved via somatic embryogenesis. Mature cotyledons were cultured on MS, B<sub>5</sub> and modified MS media (MSB<sub>5</sub>). The media were supplemented with different concentrations of various auxins, viz, IAA/IBA/NAA/2, 4-D (1.0 to 6.0 mg/L) and cytokinins, viz, BAP/kn (1.0 to 6.0 mg/L) alone as well as in various combinations. Besides auxins and cytokinins, adenine sulphate was also incorporated into the media at various levels (50 to 150 mg/L). Embryogenic callus was induced on modified MS media augmented with 2, 4-D (3.0 mg/l) BAP (5.0 mg/l) and adenine sulphate (100 mg/l). At this particular combination, nodular embryogenic callus was obtained within 2-3 weeks. Further proliferation and maturation of these somatic embryos was achieved on MSB<sub>5</sub> medium containing reduced concentrations of hormones, i.e. 2, 4-D (1.5 mg/l), BAP (2.5 mg/l) and adenine sulphate (50 mg/l). In about 20-30 days, the somatic embryos depicted typical stages of embryo development. Germinating embryos showed well developed shoot, but meager root initiation. Therefore, these were further transferred on ½ MS media devoid of phytohormones, containing activated charcoal (5%). After 10-15 days, rooting was achieved. *In vitro* regenerated shoots (5-6 cm long) with well-developed roots were transferred to pots containing vermiculite and soil (1:3) and maintained at high humidity.

**Keywords:** pigeon pea, somatic embryogenesis, modified ms media etc

### Introduction

Development of plants via tissue culture methods are based on hypothesis of totipotency. It is believed that each cell of plants has ability to differentiate, proliferate, and regenerate to produce a perfect plant (Feher A, 2019; Thorpe TA, 2007; Sugimoto L *et al.*, 2011) [4, 28, 27]. Generally, plants show regenerative capacity due to presence of high level of developmental plasticity in cells (Pulianmackal AJ *et al.*, 2014; Ikeuchi M *et al.*, 2016) [16, 10]. Regeneration of plants in *in vitro* conditions can be achieved either by organogenesis or somatic embryogenesis. In organogenesis, new organ or whole plant is formed at the place of wound while in somatic embryogenesis, whole plant is produced from a single cell via formation of somatic embryo (Jain SM and Gupta PK, 2018) [12].

Somatic embryogenesis has become very useful method for development of important economic crops at large scale (Nic-Can GI *et al.*, 2015; Horstman A *et al.*, 2017) [15, 9]. During development of embryo, various factors like media components, phytohormones, type of explant, light *etc.* have significant effects. Somatic embryogenesis can be achieved by using different kinds of explants such as leaf, trichome, haploid cells, stomatal cells, root, cotyledons *etc.* (Wang YH. and Bhalla PL, 2004; Chung HH *et al.*, 2007; Iantcheva A *et al.*, 2005; Kim TD *et al.*, 2007; Soriano M and Li H, 2007) [30].

Grain legumes are the most important source of plant proteins and energy, and are cultivated throughout the world. But, there has been no significant increase in the production of pulses due to their low static yields and susceptibility to various fungal, viral and bacterial diseases. *Cajanus cajan* L. Millsp (Pigeon pea), belongs to family

Fabaceae, is useful grain legume crop which is good source of dietary protein. Conventional methods of breeding have not been successful due to limited genetic variations, and sexual incompatibility with wild relatives. However, the use of biotechnological techniques over conventional methods of plant propagation and improvement show promising results. (Nic-Can GI *et al.*, 2015; Horstman A *et al.*, 2017) [15, 9].

In the present investigation, effects of various phytohormones on plant regeneration via somatic embryogenesis have been studied using cotyledon segment of mature seeds as explants of *Cajanus cajan* L. Millsp.

### Materials and methods

#### 1. Explant sources

For the present study, mature cotyledons excised from soaked seeds of *Cajanus cajan* L. Millsp to use as the explant. To obtain the explant, seeds were surface sterilized with mercuric chloride (HgCl<sub>2</sub>) for 2-3 minutes. Thereafter, seeds were soaked in liquid MS media containing BAP (2.0 mg/L) for 48 hrs and cotyledons were excised after removing the seed coat.

#### 2. Culture media

Mature cotyledons were cultured on MS, B<sub>5</sub> and modified MS media (MSB<sub>5</sub>). The media were supplemented with different concentrations of various auxins, viz, IAA/IBA/NAA/2, 4-D (1.0 to 6.0 mg/L) and cytokinins, viz, BAP/kn (1.0 to 6.0 mg/L) alone as well as in various combinations. Besides auxins and cytokinins, adenine sulphate was also incorporated into the media at various levels (50 to 150 mg/L).

### 3. Culture conditions

All the cultures were incubated at 26±2°C temperature and 50-60% relative humidity under 16-hrs photoperiod using cool white fluorescent light (3000-4000 lux).

### Results & Discussion

During the present study, embryogenic callus was induced on modified MS media i.e. MSB<sub>5</sub> augmented with 2, 4-D (3.0 mg/l) BAP (5.0 mg/l) and adenine sulphate (100 mg/l). At this particular combination, nodular embryogenic callus was obtained within 2-3 weeks. These nodules denoted the embryonic initials which was developed into conspicuous globular embryos (Figure 1a-1b). Further proliferation and maturation of these somatic embryos was achieved when this embryogenic clump was sub-cultured on MSB<sub>5</sub> medium containing reduced concentrations of hormones, i.e. 2, 4-D (1.5 mg/l), BAP (2.5 mg/l) and adenine sulphate (50 mg/l). In about 20-30 days, the somatic embryos depicted typical stages of embryo development (Figure 2a-2c). Complete plantlet via somatic embryo germination was also formed (Figure 3) in the study. Germinating embryos showed well developed shoot, but meager root initiation. Therefore, these were further transferred on ½ MS media devoid of phytohormones, containing activated charcoal (5%). After 10-15 days, rooting was achieved (Figure 4). *In vitro* regenerated shoots (5-6 cm long) with well-developed roots were transferred to pots containing vermiculite and soil (1:3) and maintained at high humidity (Figure 5a-5b). However transplantation rate was low (20-25%).

For successful induction of somatic embryogenesis several factors have been found to be responsible, viz., explants and its physiological status, culture medium, growth hormones, sucrose concentration, complex and sequential treatment and environmental conditions (Wang YH and Bhalla PL, 2004; Martin *et al.*, 2001) [30, 13]. Somatic embryogenesis has been induced from different types of explants like excised embryos, and hypocotyl (Soriano M and Li H, 2013; Steward *et al.*, 1984) [23, 25]. Similarly other reports are also available on the induction of embryos from excised embryos & cotyledon (Xiao JN *et al.*, 2004) [32]. However, during the present study pre conditioned mature cotyledons proved to be the most desired explants for raising embryogenesis. Somatic embryos have been grown on a wide range of media from relatively dilute media like white's medium, (White, 1963) [31] to the most concentrated media formulation like that of MS media (Murashige and Skoog 1962) [14]; B<sub>5</sub> media (Gamborg *et al.*, 1968) [6] and SH media (Schenk and Hildebrandt., 1972) [21]. However, during the present study culture of mature cotyledons on MSB<sub>5</sub> media give optimal embryogenic response. Similarly, several reports are available on successful induction of somatic embryogenesis a wide range of plant species using MS media as such or with slight modifications (Stephan and Jayabalan., 2001, Sarasan *et al.*, 2002; Xiao JN *et al.*, 2004) [24, 32]. The role of hormones in the induction of somatic embryos is of great interest since it interacts directly with a number of factors. However in case of predetermined embryogenic cells somatic embryos have been obtained even in the absence of exogenous plant growth regulators (Vardi *et al.*, 1975; Rose RJ, 2019) [29, 19]. Whereas, in case of cultures derived from undifferentiated tissues, growth regulators in the medium appear to be essential for growth and induction of somatic embryos. Auxins have proved to be the most essential constituent for successful somatic

embryo induction in most of the plant species (Rao and Lakshmi-Sita, 1996; George and Eapen, 1994; Geovanny I *et al.*, 2016) [17, 7, 8]. Moreover the superiority of 2,4-D amongst all the auxins has also been well established (Eyer L *et al.*, 2016). Nevertheless, cytokinins have also proved to be quite important for the induction of somatic embryos (Fujimura and Komamine, 1975; Budimir and Vajcic. 1992; Eyer L *et al.*, 2016) [5, 3].

Whereas in other cases cytokinin is required together with auxin for the induction of embryogenesis (Jadhav and Hedge, 2001) [11]. Similarly during the present study (2,4-D) in combination with BAP was employed for the obtainment of somatic embryogenesis. Moreover, in some plant species, somatic embryos may be induced, proliferated and matured on the same culture medium (Su YH and Zhang XZ, 2014) [26]. However, in certain plant species change in medium at various stages of development has also been required (Geovanny I *et al.*, 2016) [8]. Similarly, during the present study nodular embryogenic callus was obtained when mature cotyledons were cultured on MSB<sub>5</sub> media along with 2, 4-D (3.0 mg/l), BAP (5.0 mg/l) and adenine sulphate (100 mg/l). At this combination initial stages of embryo formation was observed, for further development of these embryos this embryogenic callus was sub-cultured on MSB<sub>5</sub> medium supplemented with a reduced level of hormones that is 2, 4-D (1.5 mg/l), BAP (2.5 mg/l) and adenine sulphate (50 mg/l). Development of mature somatic embryos into complete plantlets generally requires the absence of auxin from the culture medium (Razdan, 1993). Similarly it was recorded in present study that when embryo germination was tried on the same medium meager roots were developed. However, their transfer to hormone free ½ MS medium containing 0.5% activated charcoal led to complete plantlet formation with well -developed shoot and roots. Similar observation recorded by Reddy and Reddy (1993) [18]. During the present study embryogenic mass was not induced on medium without sucrose. The induction percentage increased with an increase in the sucrose concentration maximum being at 3.0%. However, further increase in the sucrose concentration showed a decline in embryogenic percentage. However, higher as well as lower concentration of sucrose concentration showed a decline in embryogenic percentage. However, higher as well as lower concentration of sucrose was found to be very effective (George and Eapen, 1994) [7]. Light is another important factor, which influences somatic embryogenesis. The best response was obtained at 16-hour photoperiod. This is in consonance with Singh *et al* (2021) [22]. In some other cases, complete darkness supported embryo maturation (Ammirato, 1974) [1]

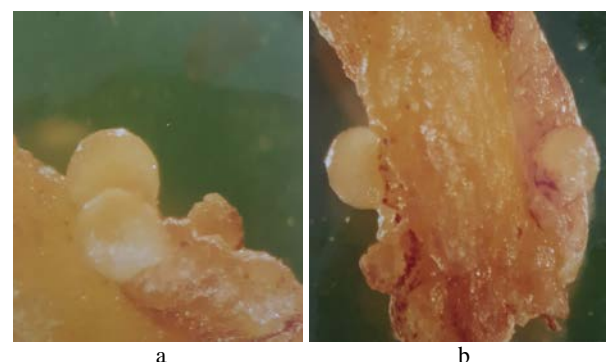


**Fig 1a-1b:** Globular embryo [MSB<sub>5</sub> + 2, 4-D (3.0 mg/L) + BAP (5.0 mg/L) + adenine sulphate (100 mg/L)].

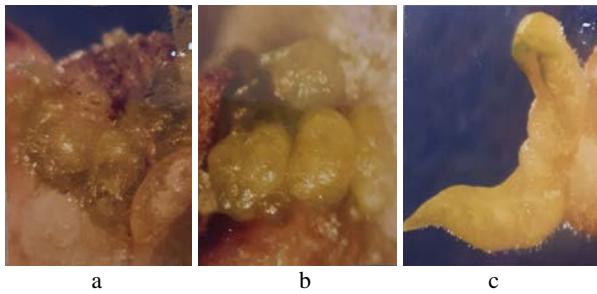


**Fig 2a-2c:** Various stages of embryo development [MSB<sub>5</sub> + 2, 4-D (1.5 mg/L) + BAP (2.5 mg/L) + adenine sulphate (50 mg/L)].



**Fig 3:** Germinated Somatic embryo with shoot differentiation.



**Fig 4:** Complete regenerate plantlet via somatic embryo showing well developed roots on ½ MS + activated charcoal (0.5%).



**Fig 5a-5b:** Acclimatization and hardening of germinated plantlets.

## References

1. Ammirato PV. The effects of abscisic acid on the development of somatic embryos from cells of caraway (*Carum carvi* L.). *Bot. Gaz*,1974:135:328-337.
2. Budimir S, Vujicic R. Benzyladenine induction of buds and somatic embryogenesis in *Picea omorika* (Pancic) Purk. *Plant Cell Tiss. Org. Cult*,1992:31:89-94.
3. Eyer L, Vain T, Parizkova B, Oklestkova J, Barbez E, Kozubikova H *et al.* 2-D and IAA Amino acid conjugates show distinct metabolism in Arabidopsis. *Plos One*,2016:11(7):e0159269.
4. Feher A. Callus, dedifferentiation, totipotency, somatic embryogenesis: What these terms mean in the era of molecular plant biology? *Front. Plant Sci*,2019:10:536.
5. Fujimura T, Komamine A. Effects of various growth regulators on the embryogenesis in a carrot cell suspension culture. *Plant Sci Lett*,1975:5:359-364
6. Gamborg OL, Miller RA, Ojima K. Nutrient requirements of suspension cultures of soybean root cells. *Exp Cell Res*,1968:50(1):151-8.
7. George L, Eapen S. Organogenesis and embryogenesis from diverse explants in pigeonpea (*Cajanus cajan* L.). *Plant Cell Reports*,1994:13:417-420. <https://doi.org/10.1007/BF00234150>
8. Geovanny I, Nic-Can, Victor M, Loyola-Vargas. The role of the auxin during somatic embryogenesis. *Somatic embryogenesis: fundamental aspects and applications*, 2016, 171-182.
9. Horstman A, Bemer M, Boutilier K. A transcriptional view on somatic embryogenesis. *Regeneration*,2017:4:201-216.
10. Ikeuchi M, Ogawa Y, Iwase A, Sugimoto K. Plant regeneration: Cellular origins and molecular mechanisms. *Development*,2016:143:1442-1451.
11. Jadhav SY, Hedge BA. Somatic embryogenesis and plant regeneration in *Goriosa*. *India J. Exp. Biol*,2001:39(9):943-946.
12. Jain SM, Gupta PK. *Stepwise Protocols for Somatic Embryogenesis in Woody Plants*; Springer International Publishing: Cham, Switzerland, 2018, 1-2.
13. Martin V, Carrillo G, Torroja C, Guerrero I. The sterol-sensing domain of Patched protein seems to control Smoothed activity through Patched vesicular trafficking. *Crr. Biol*,2001:11(8):601-607.
14. Murashige T, Skoog F. A revised medium for rapid growth and bio assays with tobacco tissue cultures. *Physiologia Plantarum*,1962:15(3):473-497.
15. Nic-Can GI, Galaz-Avalos RM, De-La-Pena C, Alcazar-Magana A, Wrobel K, Loyola-Vargas VM. Somatic embryogenesis: Identified factors that lead to embryogenic repression. A case of species of the same genus, 2015. *PLoS ONE*. 10, e0126414
16. Pulianmackal AJ, Kareem AV, Durgaprasad K, Trivedi ZB, Prasad K. Competence and regulatory interactions during regeneration in plants. *Front Plant Sci*,2014:5:1-16.
17. Rao M, Lakshmi Sita G. Direct somatic embryogenesis from immature embryos of rosewood (*Dalbergia latifolia* Roxb.). *Plant Cell Reports*,1996:15:355-359.
18. Reddy GVN, Reddy MR, Reddy NM, Das TC. Utilization of castor straw as roughage source in complete diets of growing crossbred calves. *Indian J. Anim. Sci*,1993:63(8):878-881.

19. Rose RJ. Somatic embryogenesis in the *Medicago truncatula* model: cellular and molecular mechanisms. *Frontiers in plant science*, 2019. <https://doi.org/10.3389/fpls.2019.00267>
20. Sarasan V, Cripps R, Ramsay MM, Atherton C, McMichen M, Prendergast G, Rowntree JK. Conservation in vitro of threatened plants- progress in the past decade. *In vitro cellular and developmental biology-plant*,2006;42(3):206-214.
21. Schenk RV, Hildebrandt AC. Medium and Techniques for Induction and Growth of Monocotyledonous and Dicotyledonous Plant Cell Cultures. *Canadian Journal of Botany*,1972;50:199-204. <https://doi.org/10.1139/b72-026>
22. Singh YK, Topno SE, Bahadur V, Shrivastava P. Effect of Light intensity and different levels of Nitrogen on growth, yield and photosynthetic characteristics of Giant Mustard (*Brassica juncea* var. Wong Bok). *Biological Forum- An international Journal*,2021;13(2):461-466.
23. Soriano M, Li H, Boutilier K. Microspore embryogenesis: establishment of embryo identity and pattern in culture. *Plant Reprod*.2013;26:181-196. <https://doi.org/10.1007/s00497-013-0226-7>
24. Stephan R, Jayabalan N. Propagation of *Coriandrum sativum* L. through somatic embryogenesis. *NISCAIR-CSIR, India*,2001;39(4):387-389.
25. Steward FC. Plant cell physiology: Recollections and reflections. *Proc. Indian Acad. Sci*,1984;93:231-244. <https://doi.org/10.1007/BF03053079>
26. Su YH, Zhang XS. Current topics in developmental biology, 2014.
27. Sugimoto K, Gordon SP, Meyerowitz EM. Regeneration in plants and animals: Dedifferentiation, transdifferentiation, or just differentiation? *Trends Cell Biol*,2011;21:212-218.
28. Thorpe TA. History of plant tissue culture. *Mol. Biotechnol*,2007;37:169-180.
29. Vardi A, Spiegel-Roy P, Galun E. Citrus cell culture: isolation of protoplasts, plating densities, effect of mutagens and regeneration of embryos. *Plant science letters*. Amsterdam,1975;4:231-236.
30. Wang YH, Bhalla PL. Somatic embryogenesis from leaf explants of Australian fan flower, *Scaevola aemula* R. Br. *Plant Cell Rep*,2004;22(6):408-14.
31. White PR. The cultivation of Animal & Plant Cells, 2nd edition. Ronald Press, New York, 1963.
32. Xiao JN, Huang XL, Wu YJ, Li XJ, Zhou MD, Engelmann F. Direct somatic embryogenesis induced from cotyledons of mango immature zygotic embryos. *In vitro cellular and developmental biology*,2004;40(2):196-199.

# Magicity in the nuclei with $N = 32$ & $34$

Published: 18 November 2021


Volume 242, article number 35, (2021) Cite this article



## Hyperfine Interactions



Aims and scope

Submit manuscript

R. Sharma , [A. Jain](#), [S. K. Jain](#) & [G. Saxena](#) 93 Accesses [Explore all metrics](#) →

## Abstract

Inspired by the recent experimental evidences for double magicity in  $^{52,54}\text{Ca}$ , we have employed relativistic mean-field (RMF) approach with density-dependent meson-nucleon couplings using DD-ME2 parameter for a systematic study of nuclei with neutron numbers  $N = 32$  and  $34$  with the help of ground state properties of even-even nuclei. Our extensive calculations include deformation, binding energies,  $2p$ -separation energies, radii, etc. We compare our results with the available experimental data and another parameter of RMF. Our results of potential energy surface, two proton shell gap, isotopic shift, and normalized radius demonstrate signature of double magicity in  $N = 32$  and  $34$  isotones, in particular for  $^{46,48}\text{Si}$ ,  $^{60,62}\text{Ni}$  along with what found for  $^{52,54}\text{Ca}$ .

 This is a preview of subscription content, [log in via an institution](#)  to check access.

### Access this article

[Log in via an institution](#)

### Subscribe and save

 Springer+ Basic

€32.70 /Month

Get 10 units per month

Download Article/Chapter or eBook

1 Unit = 1 Article or 1 Chapter

Cancel anytime

Subscribe now →

Buy Now

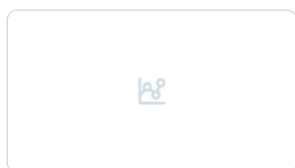
Buy article PDF 39,95 €

Price includes VAT (India)

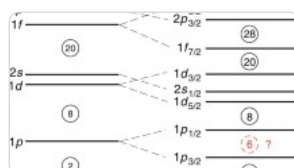
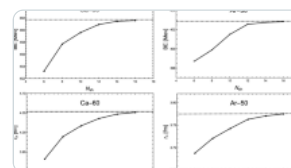
Instant access to the full article PDF.

Rent this article via [DeepDyve](#) ↗[Institutional subscriptions](#) →

## Similar content being viewed by others

**Ground-state properties of neutron magic nuclei**

Article | 01 March 2017

**Evidence for prevalent  $Z = 6$  magic number in neutron-rich carbon isotopes**Article | Open access  
23 April 2018**Neutron shell closure at  $N = 32$  and  $N = 40$  in Ar and Ca isotopes**

Article | 20 February 2020

## References

- Rosenbusch, M., Ascher, P., Atanasov, D., Barbieri, C., Beck, D., Blaum, K., Borgmann, C.H., Breitenfeldt, M., Cakirli, R.B., Cipollone, A., George, S., Herfurth, F., Kowalska, M., Kreim, S., Lunney, D., Manea, V., Navrátil, P., Neidherr, D., Schweikhard, L., Somà, V., Stanja, J., Wienholtz, E., Wolf, R.N., Zuber, K.: Probing the  $N = 32$  shell closure below the magic proton number  $Z = 20$ ., Mass measurements of the exotic isotopes  $^{52,53}\text{K}$ . *Phys. Rev. Lett.* **114**, 202501 (2015). <https://doi.org/10.1103/PhysRevLett.114.202501>  
[Article](#) [ADS](#) [Google Scholar](#)
- Michimasa, S., et al.: Magic Nature of Neutrons in  $^{54}\text{Ca}$ : First Mass Measurements of  $^{55-57}\text{Ca}$ . *Phys. Rev. Lett.* **121**, 022506 (2018). <https://doi.org/10.1103/PhysRevLett.121.022506>  
[Article](#) [ADS](#) [Google Scholar](#)
- Kumawat, M., Saxena, G., Kaushik, M., Sharma, R., Jain, S.K.: Description of nuclei with magic number  $Z(N) = 6$ . *Can. J. Phys.* **96**, 1413–1419 (2018). <https://doi.org/10.1139/cjp-2017-1013>



[Article](#) [ADS](#) [Google Scholar](#)

4. Stanoiu, M, Azaiez, F, Dombrádi, Z., et al.: N = 14 and 16 shell gaps in neutron-rich oxygen isotopes. Phys. Rev. C **69**, 034312 (2004). <https://doi.org/10.1103/PhysRevC.69.034312>

[Article](#) [ADS](#) [Google Scholar](#)

5. Brown, B.A., Richter, W.A.: Magic numbers in the neutron-rich oxygen isotopes. Phys. Rev. C **72**, 057301 (2005). <https://doi.org/10.1103/PhysRevC.72.057301>

[Article](#) [ADS](#) [Google Scholar](#)

6. Becheva, E., Blumenfeld, Y., Khan, E., et al.: N = 14 Shell Closure in  $^{22}\text{O}$  Viewed through a Neutron Sensitive Probe. Phys. Rev. Lett **96**, 012501 (2006). <https://doi.org/10.1103/PhysRevLett.96.012501>

[Article](#) [ADS](#) [Google Scholar](#)

7. Hoffman, C.R., Baumann, T., Bazin, D., et al.: Evidence for a doubly magic  $^{24}\text{O}$ . Phys. Lett. B **672**, 17 (2009). <https://doi.org/10.1016/j.physletb.2008.12.066>

[Article](#) [ADS](#) [Google Scholar](#)

8. Tshoo, K., Satou, Y., Bhang, H., et al.: N = 16 Spherical Shell Closure in  $^{24}\text{O}$ . Phys. Rev. Lett **109**, 022501 (2012). <https://doi.org/10.1103/PhysRevLett.109.022501>

[Article](#) [ADS](#) [Google Scholar](#)

9. Kanungo, R., Tanihata, I., Ozawa, A.: Observation of new neutron and proton magic numbers. Phys. Lett. B **528**, 58 (2002). [https://doi.org/10.1016/S0370-2693\(02\)01206-6](https://doi.org/10.1016/S0370-2693(02)01206-6)

[Article](#) [ADS](#) [Google Scholar](#)

10. Gade, A., Janssens, R.V.F., Bazin, D., et al.: Cross-shell excitation in two-proton knockout: Structure of  $^{52}\text{Ca}$ . Phys. Rev. C **74**(R), 021302 (2006). <https://doi.org/10.1103/PhysRevC.74.021302>

[Article](#) [ADS](#) [Google Scholar](#)

11. Wienholtz, F., Beck, D., Blaum, K., et al.: Erratum: Masses of exotic calcium isotopes pin down nuclear forces. Nature. **498**, 346 (2013). <https://doi.org/10.1038/nature12226>

[Article](#) [ADS](#) [Google Scholar](#)

12. Steppenbeck, D., Takeuchi, S., Aoi, N., et al.: Evidence for a new nuclear 'magic number' from the level structure of  $^{54}\text{Ca}$ . Nature **502**, 207 (2013). <https://doi.org/10.1038/nature12522>

13. Sharma, R., Jain, A., Kaushik, M., Jain, S.K., Saxena, G.: Structural properties of nuclei with semi-magic number  $N(Z)=40$ . *Int. J of Mod Phy E*. <https://doi.org/10.1142/S0218301321500701> (2021)
  
14. Togano, Y., Yamada, Y., Iwasa, N., et al.: Hindered Proton Collectivity in  $(^{28}_{16}\text{S}_{12})$ , Possible Magic Number at  $Z = 16$ . *Phys. Rev. Lett.* **222501**, 108 (2012). <https://doi.org/10.1103/PhysRevLett.108.22250>  
[Google Scholar](#)
  
15. Iwasaki, H., Motobayashib, T., Akiyoshic, H., et al.: Low - lying intruder  $1^-$  state in  $^{12}\text{Be}$  and the melting of the  $N = 8$  shell closure. *Phys. Lett. B* **481**, 7 (2000). [https://doi.org/10.1016/S0370-2693\(00\)01017-0](https://doi.org/10.1016/S0370-2693(00)01017-0)  
[Article](#) [ADS](#) [Google Scholar](#)
  
16. Doornenbal, P., Scheit, H., Takeuchi, S., et al.: In-Beam  $\gamma$ -Ray Spectroscopy of  $^{34,36,38}\text{Mg}$ : Merging the  $N = 20$  and  $N = 28$  Shell Quenching. *Phys. Rev. Lett* **111**, 212502 (2013). <https://doi.org/10.1103/PhysRevLett.111.212502>  
[Article](#) [ADS](#) [Google Scholar](#)
  
17. Bastin, B., Grévy, S., Sohler, D., et al.: Collapse of the  $N = 28$  Shell Closure in  $^{42}\text{Si}$ . *Phys. Rev. Lett.* **99**, 022503 (2007). <https://doi.org/10.1103/PhysRevLett.99.022503>  
[Article](#) [ADS](#) [Google Scholar](#)
  
18. Liu, J., Niu, Y.F., Long, W.H.: New magicity  $N = 32$  and  $34$  triggered by strong couplings between Dirac inversion partners. *Phys. Lett. B* **806**, 135524 (2020). <https://doi.org/10.1016/j.physletb.2020.135524>  
[Article](#) [Google Scholar](#)
  
19. Saxena, G., Kaushik, M.: Behaviour of the pf shell under the RMF+BCS description. *Chin. J. Phys.* **55**, 1149 (2017). <https://doi.org/10.1016/j.cjph.2017.03.022>  
[Article](#) [Google Scholar](#)
  
20. Leistenschneider, E., et al.: Dawning of the  $N = 32$  Shell Closure Seen through Precision Mass Measurements of Neutron-Rich Titanium Isotopes. *Phys. Rev. Lett.* **120** (06), 2503 (2018). <https://doi.org/10.1103/PhysRevLett.120.062503>  
[Article](#) [Google Scholar](#)
  
21. Lalazissis, G.A., Niksic, T., Vretenar, D., Ring, P.: New relativistic mean-field interaction with density-dependent meson-nucleon couplings. *Phys. Rev. C* **71**, 024312 (2005). <https://doi.org/10.1103/PhysRevC.71.024312>

[Article](#) [ADS](#) [Google Scholar](#)

22. Lalazissis, G.A., Karatzikos, S., Fossion, R., Pena Arteaga, D., Afanasjev, A.V., Ring, P.: The effective force NL3 revisited. Phys. Lett. B **671**, 36 (2009). <https://doi.org/10.1016/j.physletb.2008.11.070>

[Article](#) [ADS](#) [Google Scholar](#)

23. <https://www.nndc.bnl.gov/>

24. Saxena, G., Kumawat, M., Agrawal, B.K., Aggarwal, M.: A systematic study of the factors affecting central depletion in nuclei. J. Phys. G: Nucl. Part. Phys. **46**, 065105 (2019). <https://doi.org/10.1088/1361-6471/ab0853>

[Article](#) [ADS](#) [Google Scholar](#)

25. Saxena, G., Kumawat, M., Kaushik, M., Jain, S.K., Aggarwal, M.: Two-Proton Radioactivity with 2p halo in light mass nuclei  $A = 18 - 34$ . Phys. Lett. B **775**, 126 (2017). <https://doi.org/10.1016/j.physletb.2017.10.055>

[Article](#) [ADS](#) [Google Scholar](#)

26. El Adri, M., Oulne, M.: Neutron shell closure at  $N = 32$  and  $N = 40$  in Ar and Ca isotopes. Eur. Phys. J. Plus **135**, 268 (2020). <https://doi.org/10.1140/epjp/s13360-020-00277-z>

[Article](#) [Google Scholar](#)

27. Gorges, C., et al.: . Phys. Rev. Lett. **192502**, 122 (2019). <https://doi.org/10.1103/PhysRevLett.122.192502>

[Google Scholar](#)

28. Hofstadter, R., Collard, H.R.: Nuclear Radii, in Landolt-Börnstein, Group I. Vol. 2. Edited by H. Schopper, Springer, Berlin. <https://doi.org/10.1007/10201056-14>(1967)

29. Angeli, I., Marinova, K.P.: Correlations of nuclear charge radii with other nuclear observable. J. Phys. G: Nucl. Part. Phys. **42**, 055108 (2015). <https://doi.org/10.1088/0954-3899/42/5/055108>

[Article](#) [ADS](#) [Google Scholar](#)

30. Angeli, I., Marinova, K.P.: Table of experimental nuclear ground state charge radii: An update. At. Data Nucl. Data Tables **99**, 69 (2013). <https://doi.org/10.1016/j.adt.2011.12.006>

[Article](#) [ADS](#) [Google Scholar](#)

## Acknowledgements

Authors gratefully acknowledge the support provided by Science and Engineering Research Board (DST), Govt. of India under CRG/2019/001851.

## Author information

---

### Authors and Affiliations

Department of Physics, School of Basic Sciences, Manipal University Jaipur, Jaipur, 303007, Rajasthan, India

R. Sharma, A. Jain & S. K. Jain

Department of Physics, S. S. Jain Subodh P.G.(Autonomous) College, Jaipur, 302004, Rajasthan, India

R. Sharma

Department of Physics (H&S), Govt. Women Engineering College, Ajmer, 305002, Rajasthan, India

A. Jain & G. Saxena

### Corresponding author

Correspondence to [R. Sharma](#).

## Additional information

---

### Publisher's note

Springer Nature remains neutral with regard to jurisdictional claims in published maps and institutional affiliations.

These authors contributed equally to this work.

This article is part of the Topical Collection on *Proceedings of the International Conference on Hyperfine Interactions (HYPERFINE 2021), 5-10 September 2021, Brasov, Romania*

## Rights and permissions

---

[Reprints and permissions](#)

## About this article

---

### Cite this article

Sharma, R., Jain, A., Jain, S.K. *et al.* Magicity in the nuclei with  $N = 32$  &  $34$ . *Hyperfine Interact* **242**, 35 (2021). <https://doi.org/10.1007/s10751-021-01751-5>

Accepted  
22 October 2021

Published  
18 November 2021

DOI  
<https://doi.org/10.1007/s10751-021-01751-5>

### Keywords

[Relativistic mean field approach](#)

[Quadrupole deformation](#)

[Magic number](#)

[Isotopic shift](#)



# Consumer Buying Behavior of Personal Care Product: A Comparative Study of Male and Female Users

**Dr. Neelu Lamba**  
Researcher

## Abstract

In today's world, the customer's demand and the power of the retailers is tremendously growing due to competitive environment and changing business. It is vital to have a sustainable relationship with customers for the survival and success of producers. Nowadays in the market a tremendous growth is experienced by the beauty products and has become one of the leading industries in the world. In Indian scenario too, the consumption and using of cosmetic products have increased rapidly. In our country, annually 15-20% of cosmetics market is reportedly growing. Comparing to other beauty products, demand for skin whitening is driving the trend. As consumer's awareness about their appearance and beauty results in the increasing demand of cosmetic and beauty products in the market.

Manufactures are likely to be aggressive to identify consumers' needs and requirements across all categories in cosmetics. Customers purchase products based on their preferences, needs and buying power.

Keywords: Beauty products, Cosmetics, Sustainable relationship

## Introduction

The word cosmetics is derived from the Greek word *kosmetikos* which means skilled at decorating. Cosmetics colloquially known as makeup or make-up are care substances used to enhance the appearance or odour of the human body. The U.S., the Food and Drug Administration (FDA), which regulates cosmetics, defines cosmetics as intended to be applied to the human body for cleansing, beautifying, promoting attractiveness, or altering the appearance without affecting the body's structure or functions.

According to Euromonitor, the cosmetics and toiletries is divided in 11 categories which are baby care, bath and shower products, deodorants, hair care, color cosmetic, men's grooming products, oral hygiene, fragrances, skin care, depilatories and sun care. The beauty and cosmetics sector is experiencing outstanding growth. It has been one of the world's leading industries. In India the cosmetic and toiletries market has developed rapidly. Our country cosmetics market is reportedly growing at 15-20% annually. Specifically, Demand for skin whitening products by men as well as women, is driving the trend, but other beauty products are not far behind (Alexander, 2011). The growth of cosmetics and beauty products markets have surged significantly as consumers are increasingly becoming aware about appearance, beauty grooming and choice of personal care products (Hamza salimkhraim). To meet consumers' needs, manufacturers are likely to be aggressive across all categories in cosmetics. However, the concentration of new product launches will be particularly visible in dynamic categories such as skin care and emerging categories such as mouthwashes/dental rinses.

Consumers buy products according to their needs, preferences and buying power. Consumer buying behaviour depends on his perception, self-concept, social and cultural background and their age and family cycle, their attitudes, beliefs values, motivation, personality, social class and many other factors that are both internal and external. Specifically, the attitudes of consumers can have a significant effect on buying behaviour. This paper examines the influence of attitude on cosmetics buying behaviour.

The higher paying jobs and an increase in the awareness of Indian women consumers towards the cosmeceutical products and to their benefits leads to the change in the mind setup of Indian women consumers and now they are ready to pay more for their cosmeceutical products. This impact of such changes is observed more in the middle class consumers. Numbers of women, especially from the middle-class population, have more disposable income leading to a change in cosmetic and skin care products consumption.

MAJOR INDIAN COSMETIC COMPANIES:-

In India, there is a complete range of cosmetic companies. It includes regional companies, national and MNCs. Hindustan Unilever leads the companies which is followed by Godrej consumer care, Procter & Gamble, Emami, Dabur and Calvin Care.

A broad list of these companies has been given below:-

1. Hul
2. Godrej Consumer Care.
3. Emami
4. ITC.
5. Dabur.
6. Procter & Gamble.
7. Calvin Care.
8. Hankel India Ltd.
9. Marico.
10. Reckitt Benckiser (India) Ltd.
11. Colgate Palmolive Pvt. Ltd.
12. Cholyil Pvt. Ltd.
13. J.K. Helen Couties Ltd.
14. J L Morison India Ltd.
15. Modi Ravlon Ltd.

### Literature Review

Dr. Anandrajan S., Sivagami T. (2016) studied consumer purchase decision behavior towards cosmetic marketing. The aim of the study was to study consumer behavior marketing of cosmetic products. They also want to know the influence of various media in motivating the consumer on a particular brand of cosmetics. Random sampling technique was used. Sample size was 200. Direct Interview method was adopted to collect data. Simple and bi-variate tables were prepared from information collected. Percentage Analysis was used for analyzing data. It found that reduction in price and attractive promotional schemes can attract more customers. The study concluded that cosmetics are not part of luxury. Manufacturers need to identify the need before marketing the cosmetic product.

Prof. Anute N., Dr. Deshmukh A. Prof. Khandagale A. (2015) studied consumer buying behaviour towards cosmetic products. The main aim of study was to study demographic profile of consumers and to find factors affecting consumer purchase decision. They also want to know the purchase pattern for cosmetic products. They found that majority of people use domestic cosmetic brand, television is most effective media to get information of cosmetics; quality of product is considered as most important factor for consumer purchase decision.

Dr. Nagananthi T., Mahalakshmi M. (2016) Studied consumers' brand preference and buying behavior of cosmetic products at Coimbatore city. The main aim of study was to identify consumers' brand preference towards cosmetic products and to determine the relationship of brand factors with demographic data. Primary data were collected from 200 samples through convenience sampling. Chi square test and one way ANOVA were used for data analysis. They found that personal care is one of the most important reasons for purchasing cosmetics. Himalaya herbals were the most important brand among consumers. Demographic factors influence consumer to purchase the cosmetics.

Banu Rekha M., Gokila K. (2015) studied consumer awareness, attitude and preference towards herbal cosmetic products with special reference to Coimbatore city. The main aim of study was to study consumer awareness towards herbal cosmetics, to identify the factors influencing the consumers to use herbal products. Descriptive research design was used with non-probability convenience sampling with 50 respondents of Coimbatore city. Karl Pearson's co-efficient of correlation, average ranking analysis and chi-square analysis were used for data analysis. They found that family income per month and spending for herbal products have positive correlation.

Quality was ranked as most important factor that influences consumers to purchase cosmetics. They concluded the research with a note that consumers believe that herbal cosmetics are not aluxury now and should be used by consumers.

Meremadi et al. 2013 deviced a model in which they studies the factors tha are considered by the consumer before buying of the personal care product. the aim was to build a mode that can increase the impact of advertising and can save the advertiser waste efforts and money. The model resulted n finding that major factors availability price quality and packaging mattered the most. The significant contribution of these factors was also found in the studies of Sakthivel, 2000. These factors were followed by genuineness and sales promotion technique.

## **CONSUMER BUYING BEHVAIOUR**

Consumer buying behavior is a decision process as well as an attitude of the people involved in purchasing and using products. Consumers make purchase decisions for buying small as well as large products. After recognizing a need or a want, consumers begin searching for products or services that fit their requirements.

Their decision depends upon many criteria. However, consumer purchases have happened much before their actual purchase. Marketing plays an important role in this. Marketing & Advertising have a strong positive impact on buying behavior of consumers, and they directly influence consumer buying a product from a company that she/he is well aware of. In ancient days, consumers were not bothered about the attributes before buying a product. But there comes a tremendous change in the consumer buying behavior of the 21st Century.

## **CUSTOMER PURCHASING DECISSION TOWARDS**

### **COSMETICS**

Before buying a product, Consumers walk or move through a series of steps. They emphasis the product in a way that it should satisfy their needs and have good quality with low or more affordable price, and should deliver them with value added features.

Consumer buying pattern differ when comes to the product quality, price, status, features, packaging. They mostly follow the rhythm of fashion and this changing preference affects their buying pattern. To identify and predict this changing behavior, marketers spend million rupees every year for market research. Currently the marketers are facing difficulties to understand and target the consumer's behaviour because they are flourished by the different varieties, affordable price and changing trend in the market of cosmetics. Consumer's preference is changing along with time.

Five stages of consumer buying behavior

There are mainly five steps/ stages in consumer decision process

#### **1. Recognition of problem**

Recognition of a problem starts when a customer realizes a problem or need. In all phases of life, humans are considered to be the customers of one company or another. And they have requirements and needs which have to be fulfilled at each phase. These requirements may be low or high involved ones. The first step of consumer buying behavior starts when the customer realizes that he needs or wants something.

#### **2. Search for information**

Once a customer identifies a problem, the next step is to adequate enough information to solve the problem. The extent of search for information depends on the customer's level of involvement in the purchase. The major source of information which influence the consumer's buying behavior are – Advertisements, Friends, Public, commercials and experience.

#### **3. Evaluation of alternatives**

Next stage of the consumer decision process is evaluating the alternatives. In this stage the Consumer will find the alternatives. They will compare and understand what they know about the alternative products and brands with what they considered the most.



#### 4. Purchase decision

After making a decision whether or not to purchase, a consumer might move through the first decision process as it plans and intends to purchase a particular brand or product.

#### 5. Outcome

In this step, after critically analyzing each stage in the decision process, final purchase is made.

### Suggestion and Conclusion

Cosmetic products are widely used by people now a days and hence the number of players enter into this business has increased considerably. Companies try to identify the consumer's attitude towards these cosmetic products so that they position their products to the particular category of people rather spending unnecessarily on non-targeted people. This study has provided a platform for the corporate to think on different dimensions what consumers prefer, which make them in deciding on Marketing Mix of different products, like modify the product or change in product design, fixing of price that better suit the targeted audience, appropriate promotion mix namely sales promotion, advertising, publicity and personal selling, and finally change in distribution channel.

The Indian cosmeceutical Industry is considered to be one of the fastest growing industries. The reason behind that might be the increase in the disposable income of the consumers and the increase in awareness towards their looks. In our study we discussed the skin care segment and within that our focus is on three types of cosmeceutical products and these are anti-aging products, anti-wrinkle products, anti-acne products, suns creams and fairness cream products. In the Indian market these products are popular and are growing with a healthy growth rate because of this reason more and more foreign players are also entering into the Indian market for this segment. Within the cosmeceutical product segment now a day it was observed that consumers preferences are going towards those cosmeceutical products which contain herbal ingredients or are made from the natural origin. Not only females but also males are concerned with this segment.

### Bibliography

- Dr. Anandrajan, S., Sivagami, T., (2016) Consumer Purchase Decision Behavior towards Cosmetics Marketing. Vol.I. Asia Pacific Journal of Research.
- Prof. Anute, N., Dr. Deshmukh, A., Prof. Khandagale, A., (2015) Consumer Buying Behaviour towards Cosmetics Products. Vol.03 Issue 07, International Journal in Management and Social Science.
- Dr. Nagananthi, T., Mahalaxmi, M., (2016) Consumers' Preference and Buying Behavior of Cosmetic Products at Coimbatore City. Vol 04 Issue 01. Inter-continental Journal of Marketing Research Review.
- Banu Rekha, M., Gokila, K., (2015) A study on Consumer Awareness, Attitude and Preference towards Herbal Cosmetics Products with special Reference to Coimbatore City. Vol 02 No-04, Page No. 96-100, International Journal of Interdisciplinary and multidisciplinary Studies.
- Meremadi, A., Sadeh, F., Borji, N., & Naji, S. (2013). Driving Factors and Effectiveness of Sales Promotion in Shopping Malls in Iran. In Proceedings of 6th International Business and Social Science Research Conference, Novotel Hotel World Trade Centre, Dubai, UAE.